PROGRAMA DE DOCTORADO EN BIOMEDICINA

UNIVERSIDAD DE GRANADA

Tesis doctoral

•

Effects of ionizing radiation in breast cancer stem
cells: miRNAs as radio-response biomarkers

Memoria presentada por **Dña. CARMEN GRIÑÁN LISON**

para optar a la mención de Doctor Internacional por la Universidad de Granada

Granada, 2020

Si caminamos lo suficiente,
alguna vez llegaremos a alguna parte
-dijo Dorothy.

INDEX

SUMMARY

In breast cancer (BC), the presence of cancer stem cells (CSCs) has been related to relapse, metastasis, self-renew and radioresistance. Radiotherapy (RT) is an extended treatment for this tumour, but is not always effective. CSCs are thought to be directly responsible of the relapse in a tumour process after having received RT.

Ionizing Radiation (IR) enriches the fraction of cells expressing CSC markers, which also have an enhanced self-renewal capacity and tumorigenicity compared to the tumour bulk. Different tumour types and CSC markers associated with them supports this hypothesis. It has been shown that CD133 positive cells, mostly associated to brain cancer, are found in a greater proportion after receiving a fractionated radiation in both *in vitro* and *in vivo* experiments. Moreover, cells with high aldehyde dehydrogenase (ALDH1) activity increased radioresistance, whose inhibition resulted in a sensitization to IR. The mechanisms by which CSCs may be resistant to RT can be framed into four groups: repair mechanisms associated to DNA damage, redistribution of cell cycle, cells tumour repopulation, and level of intratumor hypoxia.

A microRNA (miRNA) is a small endogenous non-coding RNA molecule that regulates gene expression in transcriptional and post-transcriptional specific sequences, many of which have been shown to play important roles in a variety of biological processes, like development, differentiation, apoptosis, proliferation, and cell death. It is now clear that miRNAs contribute to carcinogenesis since their deregulation is involved in initiation and progression of cancer. They modulate the expression of their target genes by either degrading t mRNAs or inhibiting their translation through pairing of miRNA sequences to complementary bases. They also play a crucial role in the cellular response to ionizing radiation (IR).

The main aim of this work was to demonstrate how IR affects the expression of miRNAs related to stemness properties in different molecular BC subtypes. Our results showed that irradiation at 2, 4 and 6 Gy affects the phenotype, functional characteristics, pluripotency genes and *in vivo* tumorigenic capacity of different molecular subtypes of BC cells (according to ER, PR and HER-2 status) growing in monolayer and in suspension as mammospheres (BCSCs). The effect of IR over eight miRNAs (miR-210, miR-10b, miR-182, miR-142, miR-221, miR-21, miR-93, miR-15b) that play an important role in tumorigenesis, stemness and radioresistance showed a variability of expression depending on cell line subpopulation and clinicopathological features of BC patients. We conclude that clinical implementation of miRNA signature determination as a liquid biopsy for personalized and precision RT dosage regimes, could be necessary to improve prognosis, treatments and survival of BC patients due to miRNAs involvement in CSCs biology.

RESUMEN

En el cáncer de mama (BC), la presencia de células madre cancerígenas (CSC) se ha relacionado con recaídas, metástasis, auto-renovación y radio-resistencia. La radioterapia (RT) es un tratamiento ampliamente utilizado en este tumor, pero no siempre es efectivo. Así, se cree que las CSCs son directamente responsables de la recaída en un proceso tumoral después de haber recibido RT.

La radiación ionizante (IR) enriquece la fracción de células que expresan marcadores de CSCs, las cuales tienen una mayor capacidad de auto-renovación y tumorogenicidad en comparación con el resto de células cancerígenas que forman la masa del tumor. Los diferentes tipos de tumores y los marcadores de CSCs asociados con ellas respaldan esta hipótesis. De hecho, se ha demostrado que las células CD133 positivas, en su mayoría asociadas al cáncer de cerebro, se encuentran en mayor proporción después de recibir un tratamiento fraccionado con radiación tanto *in vitro* como *in vivo*. Además, las células con alta actividad de aldehído deshidrogenasa (ALDH1) tuvieron mayor radio-resistencia, cuya inhibición resultó en una sensibilización a la RT. Los mecanismos por los cuales las CSCs pueden ser resistentes a la RT se agrupan en cuatro grupos: mecanismos de reparación del daño del ADN, redistribución del ciclo celular, repoblación tumoral de las células y nivel de hipoxia intratumoral.

Los microRNA (miRNA) son pequeñas moléculas de ARN no codificantes endógenas que regulan la expresión génica en secuencias específicas transcripcionales y post-transcripcionales, muchas de las cuales han demostrado desempeñar papeles importantes en una variedad de procesos biológicos, como el desarrollo, la diferenciación, la apoptosis, la proliferación y la muerte celular. Actualmente se sabe que los miRNAs contribuyen al proceso de carcinogénesis, y que su desregulación está involucrada en el inicio y la progresión del cáncer. Éstos modulan la expresión de sus genes diana degradando su mRNA o inhibiendo su traducción mediante el

emparejamiento de secuencias de miRNA con bases complementarias en dicho RNAm, y desempeñan un papel crucial en la respuesta celular a la IR.

El objetivo principal de este trabajo fue demostrar cómo la IR afecta la expresión de miRNAs relacionados con las propiedades de células madre en diferentes subtipos moleculares de BC. Nuestros resultados mostraron que la exposición a dosis de 2, 4 y 6 Gy afecta al fenotipo, a las características funcionales, a los genes de pluripotencia y a la capacidad tumorogénica *in vivo* de diferentes subtipos moleculares de células de BC (según el estado ER, PR y HER-2) cultivadas en monocapa y en suspensión como mamosferas (BCSCs). El efecto de la IR sobre ocho miRNAs (miR-210, miR-10b, miR-182, miR-142, miR-221, miR-21, miR-93, miR-15b) que desempeñan un papel importante en la tumorogénesis, las características de células madre y la radio-resistencia, mostró una variabilidad de la expresión según la subpoblación de la línea celular estudiada y las características clinicopatológicas de los pacientes con BC. En este trabajo concluimos, que una implementación clínica mediante biopsia líquida de una determinada firma de miRNAs podría ser de gran utilidad para implementar regímenes de dosis de RT personalizados y de precisión, que mejorarían el pronóstico, los tratamientos y la supervivencia de los pacientes con BC, debido a la implicación de los miRNAs en la determinación de la biología de las CSCs.

INTRODUCTION

1. CANCER

1.1 Definition and origin

Cancer is a generic term for a large group of diseases that can affect any part of the body. Other terms used are malignant tumours and neoplasms. A defining feature of cancer is the rapid creation of abnormal cells that grow beyond their usual boundaries, invading adjoining parts of the body and spread to other organs, by the referred process of metastasis (Bray *et al.*, 2018), which is a major cause of death from cancer. Many cancers can be prevented by avoiding exposure to common risk factors, such as tobacco smoke… In addition, a significant proportion of cancers can be cured by surgery, radiotherapy or chemotherapy, especially if they are detected early (McGuire, 2016).

The hallmarks of cancer comprise six biological capabilities acquired during the development of human tumours, but, in recent times, as it has been known and studied more about this disease, new process, mechanism or cell types have been adding in these features. They include among others: sustaining proliferative signalling, evading growth suppressors, resisting cell death, enabling replicative immortality, inducing angiogenesis, activating invasion and metastasis, genome instability, tumour inflammation, reprogramming of energy metabolism and evading immune destruction (Figure 1) (Hanahan and Weinberg, 2011).
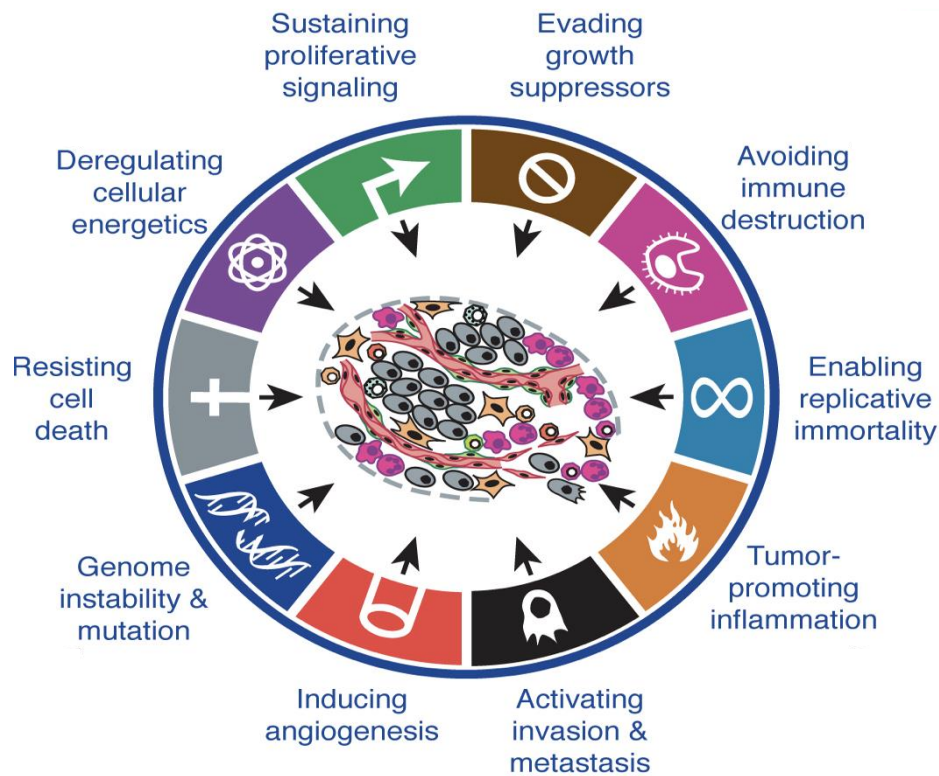
Figure 1. The hallmarks of cancer cells (Hanahan and Weinberg, 2011).

In addition to cancer cells, one of the concepts that has taken relevance in recent years is the tumour microenvironment (TME) or niche, which is another dimension of complexity and that cells construct during the different steps of tumorigenesis. This niche is formed by several cell types that contribute to tumour growth and progression. In many solid tumours exist specific microenvironments that render them more resistant to treatment with radio- and chemotherapy. Thus, the interactions of cancer cells with stromal and inflammatory cell populations make up varying components of the total tumour mass that can protect cells from the effects of treatment (Figure 2) (Hanahan and Weinberg, 2011; Marie-Egyptienne et al., 2013).
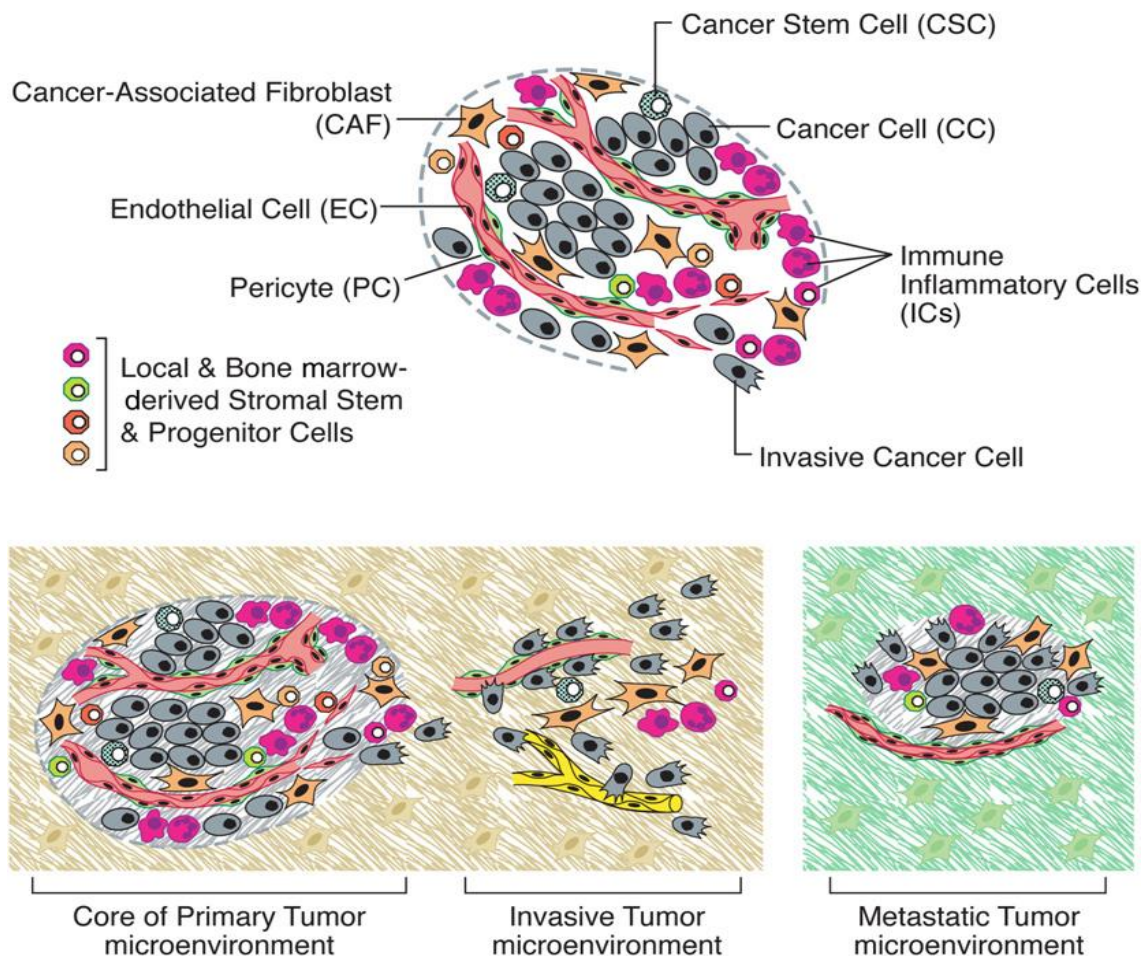
Figure 2: Image of distinct cell types within tumour and the distinctive microenvironments of tumours (Hanahan and Weinberg, 2011).

Normal cells and tissues ensure homeostasis of architecture tissue and function controlling the production and release of growth-promoting signals. Cancer cells deregulate those signals that suffer from their uncontrolled cell growth and proliferation by(Hanahan and Weinberg, 2011):

- Activating somatic mutations that trigger growth factors receptors, like B-Raf protein and the Raf to mitogen activated protein (MAP)-kinase pathway (Davies and Samuels, 2010). Similarly, mutations in the catalytic subunit of phosphoinositide 3-kinase (PI3-kinase) isoforms have been detected in an array of tumour types, which serve to hyperactivate the PI3 (Cantley, 2008).

- Disrupting negative-feedback mechanisms capable of enhancing proliferative signalling. An example are the oncogenic mutations affecting Ras genes that compromise Ras GTPase activity. Mutations that decrease GTPase activity or induce insensitivity to GAPs result in constitutive activation of signalling pathways, leading to deregulation in cell growth, inhibition of cell death, invasiveness and induction of angiogenesis. In addition, the altered state of RAS induces alterations in the expression of integrins and participates in the changes that produce cell migration (Dixit, 2010; Ling, et al. 2015).

- Evading growth suppressors by two prototypical tumour suppressors encoding the RB (retinoblastoma-associated) and TP53 proteins, which operate as central control nodes that govern the decisions of cells to proliferate or, alternatively, activate senescence and apoptotic programs. (Hanahan and Weinberg, 2011). TP53 is the most frequently mutated tumour suppressor in human cancers (Shigdar *et al.*, 2014) and is involved in cell cycle arrest and apoptosis. Cancer cells with defects in RB pathway function are thus missing the services of a critical gatekeeper of cell-cycle progression whose absence permits persistent cell proliferation (Burkhart and Sage, 2008).

- Resisting cell death by apoptosis, which serves as a natural barrier to cancer development. The central engines of apoptosis are the caspases, cascades of cysteine aspartyl proteases that implement cell death by cleaving a variety of intracellular substrates that trigger cell dissolution. The other principal death-signalling pathway involves the mitochondrion, which acts as an integrating sensor of multiple death insults by releasing cytochrome c into the cytosol where it triggers caspase activation (Evan and Vousden, 2001).

1.2 Epidemiology

Noncommunicable diseases (NCDs) are now responsible for the majority of global deaths and cancer is expected to rank as the leading cause of death and the single most important barrier to increase life expectancy in every country of the world in the 21st century (Bray *et al.*, 2018).

Cancer incidence and mortality are rapidly growing worldwide. Although there is not an only reason, but growth of the population and age are clearly related. It is estimated that there were 18.1 million new cases and 9.6 million cancer deaths worldwide in 2018. For both sexes combined, (Figures 3 and 4) lung cancer is the most commonly diagnosed cancer (11.6% of the total cases) and the leading cause of cancer death (18.4% of the total cancer deaths), closely followed by female breast cancer (BC) (11.6%), colorectal cancer (10.2%), and prostate cancer (7.1%) for incidence and colorectal cancer (9.2%), stomach cancer (8.2%), and liver cancer (8.2%) for mortality (Bray *et al.*, 2018).
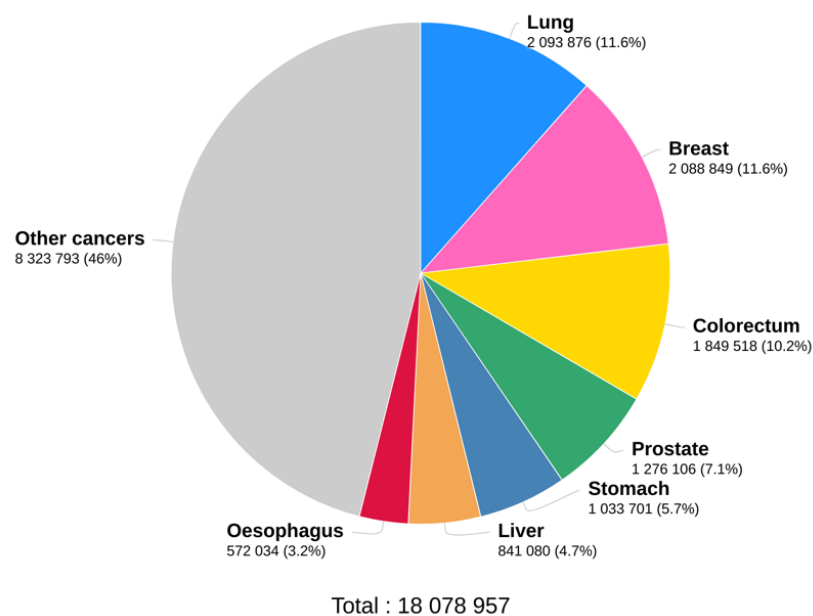
Figure 3. Pie chart present the distribution of cases for the 10 most common cancers in 2018 for both sexes. Source: GLOBOCAN 2018.
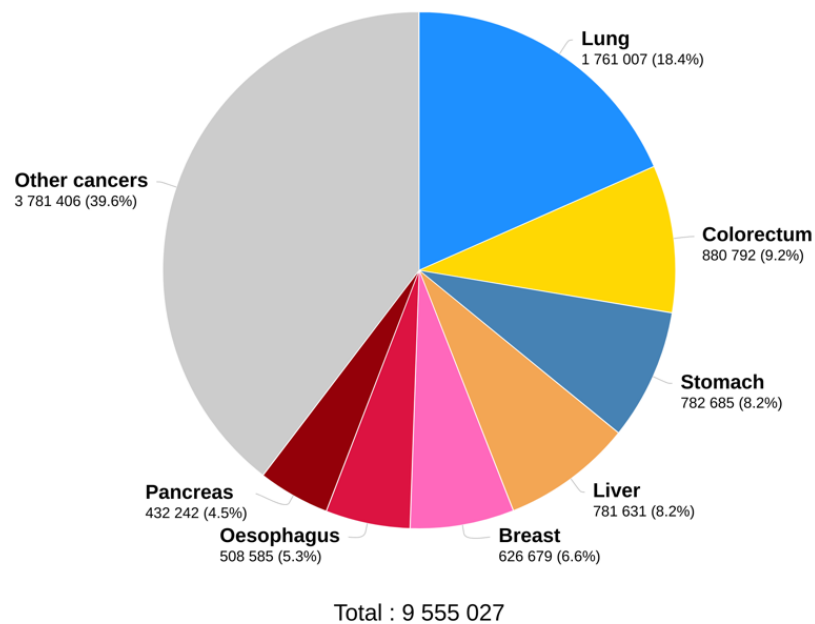
Figure 4. Pie chart present the distribution of deaths for the 10 most common cancers in 2018 for both sexes. Source: GLOBOCAN 2018.

By sex, lung cancer is the most commonly diagnosed cancer and the leading cause of cancer death in males, followed by prostate and colorectal cancer for incidence, and liver and stomach cancer for mortality (Figure 5A). Among females, BC is the most commonly diagnosed cancer and the leading cause of cancer death, followed by colorectal and lung cancer for incidence, and vice versa for mortality; whereas cervical cancer ranks fourth for both, incidence and mortality (Figure 5B). Overall, the top 10 cancer types account for over 65% of newly diagnosed cancer cases and deaths (Bray *et al.*, 2018).

A

Lung
1 368 524 (14.5%)

Other cancers
3 681 464 (38.9%)

Prostate
1 276 106 (13.5%)

Colorectum
1 026 215 (10.9%)

Oesophagus
399 699 (4.2%)

Bladder
424 082 (4.5%)

Liver
596 574 (6.3%)

Stomach
683 754 (7.2%)

Total : 9 456 418

Lung
1 184 947 (22%)

Other cancers
1 711 450 (31.8%)

Liver
548 375 (10.2%)

Pancreas
226 910 (4.2%)

Oesophagus
357 190 (6.6%)

Prostate
358 989 (6.7%)

Stomach
513 555 (9.5%)

Colorectum
484 224 (9%)

Total : 5 385 640

B

Breast
2 088 849 (24.2%)

Other cancers
3 246 828 (37.7%)

Colorectu
823 303 (9.5%

Stomach
349 947 (4.1%)

Corpus uteri
382 069 (4.4%)

Thyroid
436 344 (5.1%)

Cervix uteri
569 847 (6.6%)

Lung
725 352 (8.4%)

Total : 8 622 539

Breast
626 679 (15%)

Other cancers
1 550 997 (37.2%)

Lung
576 060 (13.8%)

Colorectum
396 568 (9.5%)

Cervix uteri
311 365 (7.5%)

Pancreas
205 332 (4.9%)

Liver
233 256 (5.6%)

Stomach
269 130 (6.5%)

Total : 4 169 387

Figure 5. Pie charts present the distribution of cases and deaths for the 10 Most Common Cancers in 2018 for males (a) and females (b) sexes. For each sex, the area of the pie chart reflects the proportion of the total number of cases or deaths. Source: GLOBOCAN 2018.

Figure 6 shows the most commonly diagnosed cancer and leading causes of cancer death at the national level in males (Figure 6A) and females (Figure 6B). The maps reveal substantial global diversity in leading cancer types, particularly for incidence in men (10 different cancer types). Prostate cancer is the most frequently diagnosed cancer in 105 countries (green), followed by lung cancer in 37 countries

(blue), and liver cancer (orange) in 13 countries. In women, BC (pink) is the most common over the world following cervix uteri (orange) (Bray *et al.*, 2018).
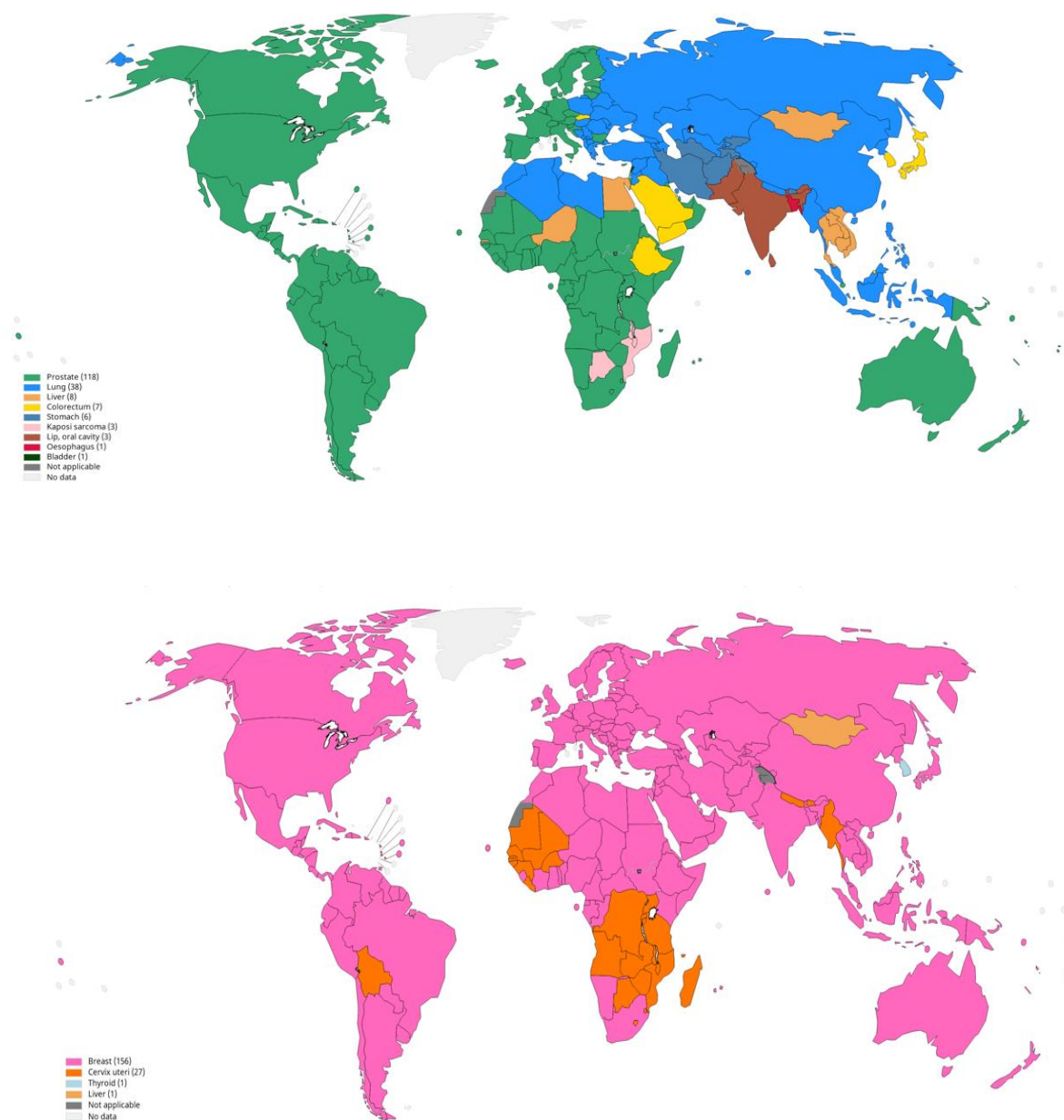
Figure 6. Global maps presenting the most common type of cancer incidence in 2018 in each country among males (a) and females (b). The numbers of countries represented in each ranking group are included in the legend. Source: GLOBOCAN 2018.

2. BREAST CANCER

Female BC is by far the most frequently diagnosed cancer and cause of cancer death among women. There were an estimated approx. 2 million new cases (24,2% of all cancers in women) and 0.6 million cancer deaths (15% of all cancer deaths in women) in 2018. The disease is the most frequently diagnosed cancer in the vast majority of the countries and is also the leading cause of cancer death in over 100 countries (Figure 7). Mortality rates vary approximately 2–5-fold worldwide, being the case fatality rate lower in countries with higher levels of human development. Mortality rates have been declining in a number of highly developed countries since the late 1980s and early 1990s, as result of a combination of improved detection and earlier diagnosis (through population-based screening) and more effective treatment regimens.
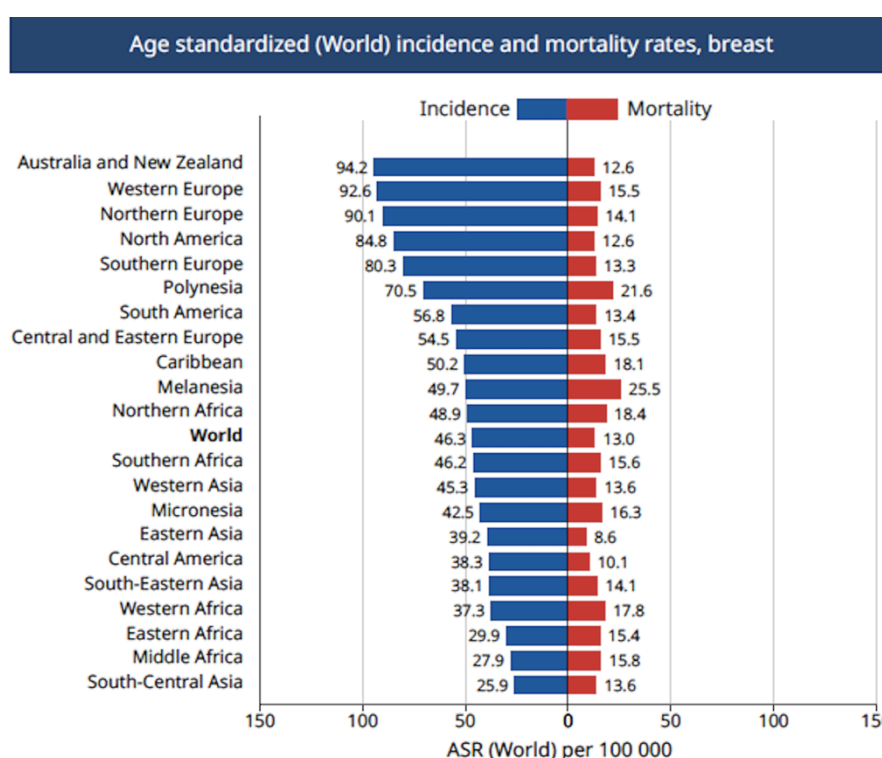
Figure 7. Bar chart of region-specific incidence and mortality age-standardized rates for BC of the female in 2018. Rates are shown in descending order of the world age-standardized rate, and the highest national age-standardized rates for incidence and mortality are superimposed. Source: GLOBOCAN 2018.

2.1 Breast cancer subtypes

The most common molecular subset of BC is defined by its ability to respond to the female hormone, the estrogen. There are four main intrinsic or molecular subtypes of BC that are based on the genes a cancer expresses (Table 1):

- **Luminal A** BC is hormone-receptor positive (estrogen-receptor and/or progesterone-receptor positive), HER2 negative, and has low levels of the protein Ki-67, which helps control how fast cancer cells grow. Luminal A cancers are low-grade, tend to grow slowly and have the best prognosis.

- **Luminal B** BC is hormone-receptor positive (estrogen-receptor and/or progesterone-receptor positive), and either HER2 positive or HER2 negative with high levels of Ki-67. Luminal B cancers generally grow slightly faster than luminal A cancers and their prognosis is slightly worse.

- **Triple-negative/basal-like** BC is hormone-receptor negative (estrogen-receptor and progesterone-receptor negative) and HER2 negative. This type of cancer is more common in women with *BRCA1* gene mutations. This type of cancer also is more common among younger and African-American women. The majority of these tumours are infiltrating ductal tumours, with a high rate of brain and lung metastases (Yersal and Barutca 2014).

- **HER2-enriched** BC is hormone-receptor negative (estrogen-receptor and progesterone-receptor negative) and HER2 positive. HER2-enriched cancers tend to grow faster than luminal cancers and can have a worse prognosis, but they are often successfully treated with targeted therapies aimed at the HER2 protein, such as trastuzumab or pertuzumab (Schnitt, 2014).

Intrinsic subtypes by gene expression profiling	Histological types	Histological grade	ER status by IHC	HER2 status by IHC/ ISH	Ki67 by IHC	Key molecular features	Predominant integrated cluster association
Luminal A	IC-NST, classic lobular, tubular, cribriform, mucinous, neuroendocrine	1–2	ER+	HER2−	Low	*PIK3CA* mutations, *MAP3K1* mutations, *ESR1* high expression, *XBP1* high expression, *GATA3* mutations, *FOXA1* mutations, quiet genomes; gain of 1q, 8q, loss of 8p, 16q	Int cluster 2, Int cluster 3, Int cluster 4, Int cluster 7, Int cluster 8
Luminal B	IC-NST, micropapillary	2–3	ER+/ −	HER2 −/+	High	*TP53* mutations, *PIK3CA* mutations, *Cyclin D1* amplification, *MDM2* amplification, *ATM* loss, enhanced genomic instability, focal amplifications (e.g. 8p12, 11q13)	Int cluster 1, Int cluster 2, Int cluster 6, Int cluster 9
HER2	IC-NST, apocrine, pleomorphic lobular	2–3	ER+/ −	HER2+	High	*HER2* amplification, *TP53* mutations, *PIK3CA* mutations, *FGFR4* high expression, *EGFR* high expression, APOBEC mutations, *Cyclin D1* amplification, high genomic instability	Int cluster 5
Basal-like	IC-NST, medullary, metaplastic, adenoid cystic, secretory	3	ER−	HER2−	High	*TP53* mutations, *RB1* loss, *BRCA1* loss, high expression of DNA repair proteins, *FOXM1* activation, high genomic instability, focal amplifications (e.g., 8q24)	Int cluster 4, Int cluster 10

+ positive, − negative, +/− mostly positive, −/+ mostly negative, *ER* oestrogen receptor, *HER2* human epidermal growth factor receptor 2, *IC-NST* invasive carcinoma no special type, *IHC* immunohistochemistry, *ISH* in situ hybridisation

Table 1. Molecular subtypes of BC. (Schnitt, 2010)

2.2 Risk factors of Breast Cancer

Recent molecular and genetic studies have emphasized that BC is a highly heterogeneous group of diseases that differ in their prognosis and response to treatment. Less than 10% of BC can be attributed to an inherited genetic mutation and it is more commonly associated with environmental, reproductive, and lifestyle factors, some of which are potentially modifiable.

- Genetic factors.

It has been described that the appearance of mutations in certain genes increases the susceptibility of BC. Among these genes we can find:

a) BRCA1 and BRCA2 tumour suppressor genes: BRCA1 is involved in the

activation of the response against DNA damage, the interaction with genes involved in its repair and in the activation of cell cycle control points; whereas BRCA2 is related to the repair of DNA damage during replication. Mutations in BRCA1 and BRCA2 are mainly associated with ER- and ER + cancers, respectively (Anderson *et al.*, 2014; Rojas and Stuckey, 2016).

b) Inherited mutations in two other genes, p53 and PTEN, are associated with familial syndromes that include a high risk of BC. P53 mutations are one of the most common alterations in breast carcinomas, reaching 30% of them. Patients with an inherited p53 mutation are estimated to be 20 times more likely to develop BC before age 45. Breast tumours in these patients tend to be estrogen, progesterone, and HER2 positive. The phosphatase and tensin homolog gene (PTEN) is a tumour suppressor gene in MAPK/mTOR pathway and those people with a PTEN mutation have an 85% estimated lifetime risk of BC (Mcpherson *et al.*, 2000; Rojas and Stuckey, 2016).

c) Exposure to X and γ radiation. According to the American Cancer Association (2013), ionizing radiation (IR) is a type of high frequency radiation that has enough energy to damage DNA. An increase in BC risk is a known delayed adverse effect of chest radiation received at a young age. The relative risk of radiation-induced BC seems to be inversely related to age of exposure. This increased risk with younger age of exposure is thought to be related to the younger breast tissue undergoing rapid cell proliferation around the time of puberty (McGuire, 2016; Rojas and Stuckey, 2016).

d) Obesity (BMI ≥30 kg/m2) is another risk factor with dual effects depending on the age of diagnosis and the status of ER. Obesity is associated with a twofold increase in the risk of BC in postmenopausal women, whereas among

premenopausal women it is associated with a reduced incidence (Figure 8). Obesity is associated with a higher number of metastatic axillary nodes and vascular space invasion than normal or underweight women. Obesity also has a stronger positive association with hormone receptor positive cancers, although it can also increase the risk of basal, triple negative and inflammatory breast
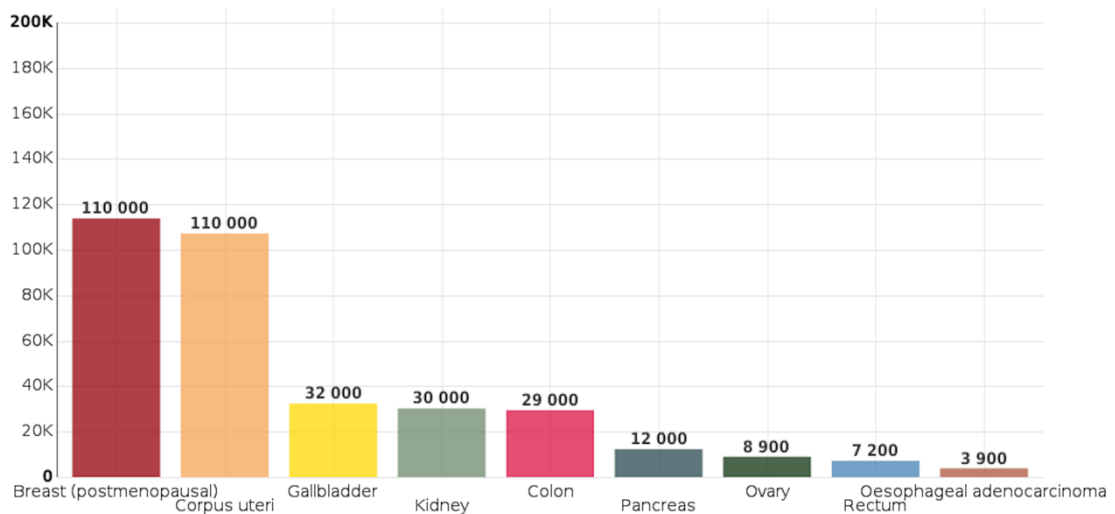
cancers (McGuire, 2016; Rojas and Stuckey, 2016).

Figure 8. Cancer cases in females (worldwide) in 2012 attributable to excess body mass index, shown by anatomical sites. Global Cancer Observatory.

e) Lifestyle, where alcohol, smoking and diet play an important role in the development of BC. Mechanisms for the role of alcohol in carcinogenesis include processes related to both formation and stimulation of BC. Acetaldehyde, benzene, and N-nitrosodimethylamine are several carcinogens produced by alcohol metabolism. Moreover, alcohol can also alter hormone levels by increasing circulating estrogen metabolites through suppression of hepatic estrogen metabolism and by enhancing the conversion of androgens to

estrogens. Tobacco and smoking have also been found to affect BC mortality. So, patients who smoke have been shown to undergo less mammographic screening, which may contribute to a higher stage disease at diagnosis. Finally, high protein intake may increase the risk of BC by increasing the amount of circulating insulin-like growth factor-1; a greater intake of carcinogenic by products with the consumption of red meat, and an increase in the intake of hormones from the exogenous hormones given to some cattle (McGuire, 2016; Rojas and Stuckey, 2016).

f) Estrogens: Breast cancer risk has also been proven to be related to prolonged exposure to estrogen and in postmenopausal women, exposure to combined hormonal therapy preparations, that is, progesterone and estrogen increases the risk of BC. An early age of menarche, nulliparity and an advanced age at first birth have been related to this risk. However, these risk factors differ in the different molecular types of BC. So, an early age of menarche (≤12 years), nulliparity and an older age at first birth are more frequent in patients with hormone receptor positive tumours. Likewise, an advanced age of menopause is associated with breast cancers positive for hormone receptors. (Anderson *et al.*, 2014; Rojas and Stuckey, 2016).

2.3 Breast cancer treatments and prevention

The treatment of BC could be established according to the stage in which it is found. The conservative surgery consists in the application of surgery to eliminate the tumour while preserving the structure of the breast, followed by radiotherapy. On the other hand, if the breast has to be preserved, neoadjuvant chemotherapy is used to

reduce the initial tumour size, such as antiestrogen therapy (for example, tamoxifen) and anti-HER2 therapy (for example, trastuzumab). Such therapy is not appropriate for approximately 15% of tumours, which are designated "triple-negative" to indicate lack of expression of ER, PR, or HER2 (Kaufmann *et al.*, 2012; McGuire, 2016).

It is also recommended the use of adjuvant radiotherapy or adjuvant hormone therapy (in the event that the tumour is hormonally dependent) if conservative surgery was performed or tumour characteristics advise. The administration of radiotherapy after conservative breast surgery not only decreases the risk of recurrence but also moderately reduces the risk of death from this type of cancer.

On the other hand, BC prevention strategies have focused on reducing its incidence in women considered to be at moderately or greatly increased risk of the disease based on calculated risks determined from prediction models, or in women with germline mutations in high-penetrance BC susceptibility genes. Selective ER modulators (SERMs) and aromatase inhibitors have demonstrated that tamoxifen and raloxifene are each associated with about a 50% reduction in the development of BC in women considered to be at moderately increased risk. Also, the potential role in prevention of various drugs that target non-endocrine signalling pathways such as metformin, cyclooxygenase 2 inhibitors, retinoids, and receptor tyrosine kinase inhibitors, among others, was associated with a reduced incidence of BC. At last, bilateral prophylactic mastectomy is a highly effective strategy to prevent the development of BC in women with BRCA mutations (Blackadar, 2016; Giuliano *et al.*, 2017).

However, the influence of modifying dietary and lifestyle factors on the prevention of BC is also under active investigation. Physical activity has been associated with a 25–30% decrease in BC risk, and research is now focused on understanding the biological mechanisms mediating this association, with the aim of determining the optimal type, dose, and timing of activity needed for maximum risk reduction (Figure 9) (McGuire, 2016).
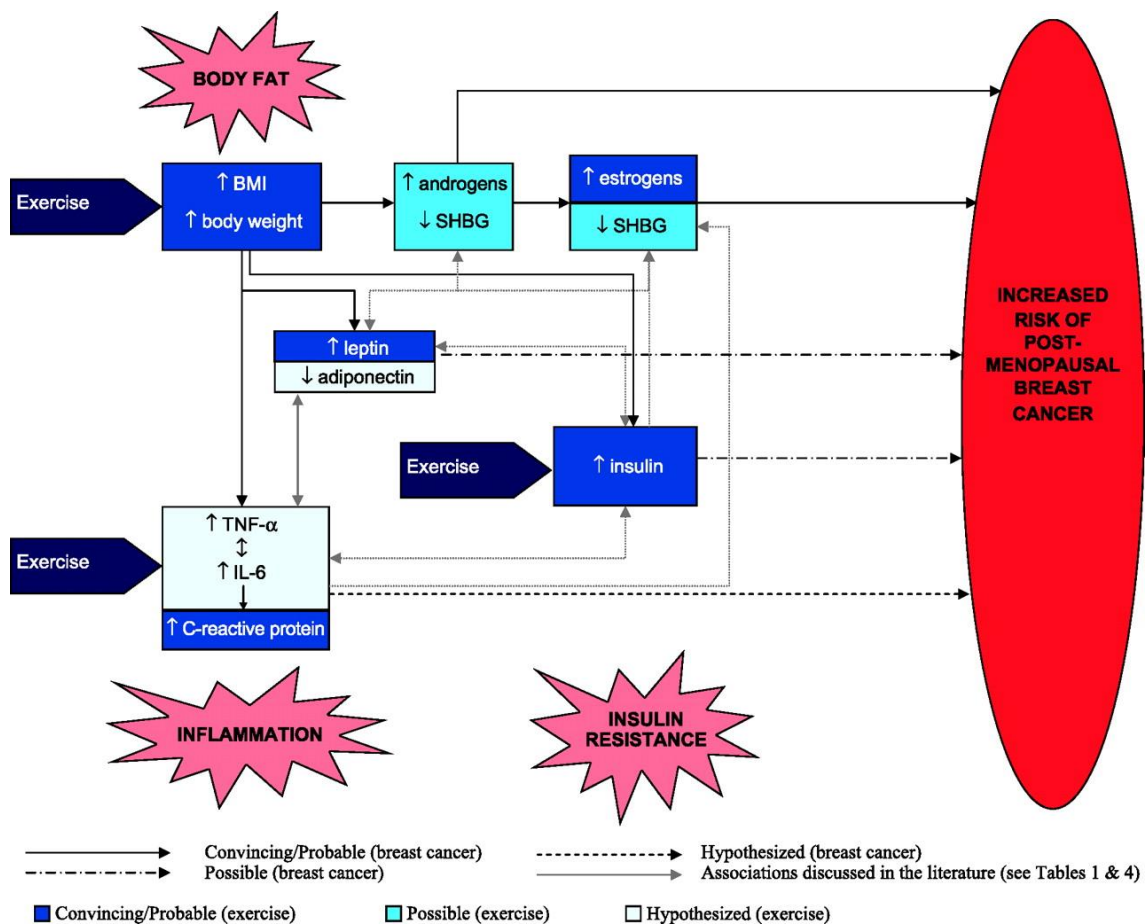
Figure 9. Biological mechanisms determining the optimal type, dose, and timing of physical activity needed for maximum reduction in breast cancer risk. IL-6, interleukin-6; SHBG, sex hormone-binding globulin; TNF-α, tumour necrosis factor α.(McGuire, 2016)

3. CANCER STEM CELLS

3.1 Definition and origin

One of the main problems facing the fight against cancer is the ability of tumours to cause relapse and metastasis, thus causing the appearance of new tumours. Tumour stem cell hypotheses are gaining more and more strength to explain this process. The stochastic cancer model postulates that one or more tissue cells acquire a mutation and through an uncontrolled division process, new genetic alterations are accumulated leading the selection of the fittest clones. According to this model, any cell of the tumour would be able to maintain and expand the tumour as well as to give rise to new tumours. Conversely, the hierarchical model of the cancer stem cell (CSC) implies the existence of a source cell in the tumours with stem cell properties, able to proliferate and maintain indefinitely the growth due to its self-renewing ability. In this model, only the population of CSC has the ability to generate and maintain tumour, unlike the other bulk tumor cells do not have that ability (Figure 10) (Al-Hajj and Clarke, 2004; Batlle and Clevers, 2017; Ghaffari, 2011).

a) Tumour cells are heterogeneous, but most cells can proliferate extensively and form new tumours

b) Tumour cells are heterogeneous and only the cancer stem cell subset (CSC; yellow) has the ability to proliferate extensively and form new tumours
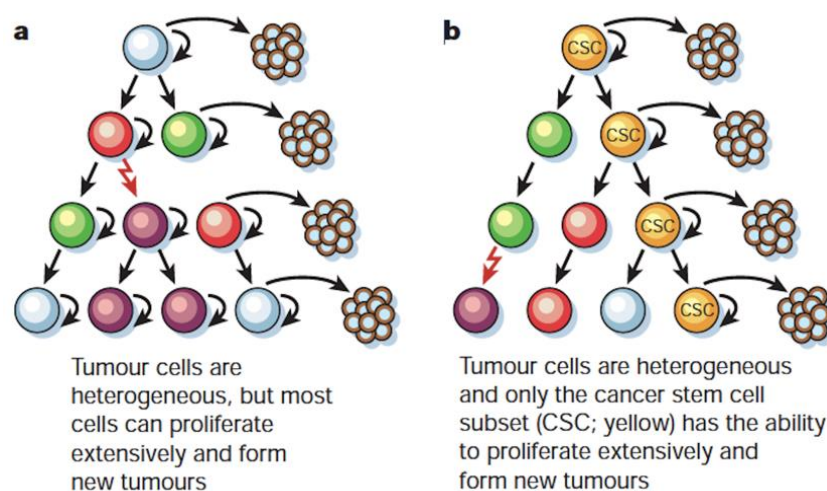
Figure 10. Two general models of heterogeneity in solid cancer cells. a) stochastic cancer model b) hierarchical cancer model (Reya *et al.*, 2001).

However, for some years, a new theory is taking hold, CSCs dynamic model, where the CSCs phenotype is flexible and conditioned by tumour TME (Figure 11). CSCs differentiate and give rise to the differentiated cell population within the tumour. Dedifferentiation of differentiated tumour cells occurs under the influence of the TME that are shaped by stromal cells. Due to, of the plasticity and the TME of the surrounding tissue-associated cells, non-stem cancerous cells located on the edges of tumour mass will be the most directly exposed to the factors derived from the TME, by the action of the secretome could revert their phenotype to a more undifferentiated state, turning into stem-like cells (CSCs) (Hernández-Camarero *et al.*, 2018; Vermeulen *et al.*, 2012).

Solid tumours mimic aberrantly developed organs and tissues and are composed of many types of cells including neoplastic cells, supporting vascular cells, inflammatory cells, and fibroblasts. The majority of cells in bulk tumours have limited self-renewal ability and are non-tumorigenic. Only a small subpopulation of cancer cells is long-lived with the ability of extensive self-renew and tumour formation. This small population is called cancer stem cells (CSCs), cancer initiating cells (CICs), or tumour stem cells (TSCs) (Al-Hajj and Clarke, 2004; Batlle and Clevers, 2017; Reya *et al.*, 2001).

The first strong *in vivo* evidence in support of the CSC concept came from classical implantation studies in human leukaemia by Bonnet and Dick in 1997. They used fluorescence-activated cell sorting (FACS) to isolate a specific cell population from acute myeloid leukaemia (AML) patients that were able to initiate AML following implantation into non-obese diabetic mice with severe combined immunodeficiency (NOD/SCID). The leukaemia-initiating cells were defined by expression of the cell

surface antigen CD34 and displayed self- renewal, differentiative and proliferative capacities similar to normal haematopoietic stem cells. The first evidence for the existence of CSCs in solid human tumours came from studies in BC (Ablett *et al.*, 2012; Al-Hajj and Clarke, 2004).

3.2 CSCs characteristics

The CSCs have the characteristics of stem cells such as the unlimited self-renewal capacity, proliferation and differentiation to different cell lines features. Among the highlights of the CSCs that make fundamental in the development of tumours can be found tumorigenic, drug resistance, radiotherapy resistance, recurrence and metastasis. (Ahmad, 2013).
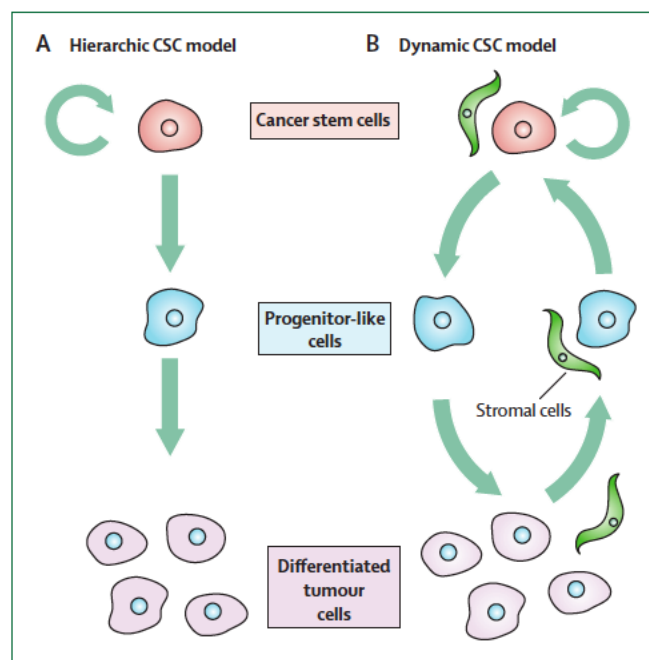
Figure 11. Scheme of the emerging dynamic CSC model. (Vermeulen *et al.*, 2012)

3.2.1 Self-renewal and pluripotency of CSCs

Self-renewal and differentiation ability in specific lineages of stem cells is regulated by environmental signals present in the niche of these cells. Normal stem cells and CSCs act via common signalling pathways that regulate self-renewal activity, including Wnt, Notch, and Sonic Hedgehog (Figure 12). Some of these routes are frequently deregulated in cancer and can play a crucial role in cancer cells with stem cell properties. Wnt/β-catenin and Notch pathways enhance self-renewal activity during leukemia stem cell propagation and also is involved in the regulation of normal and malignant mammary stem/progenitor cell populations (Reya *et al.*, 2001; Takahashi *et al.*, 2013).
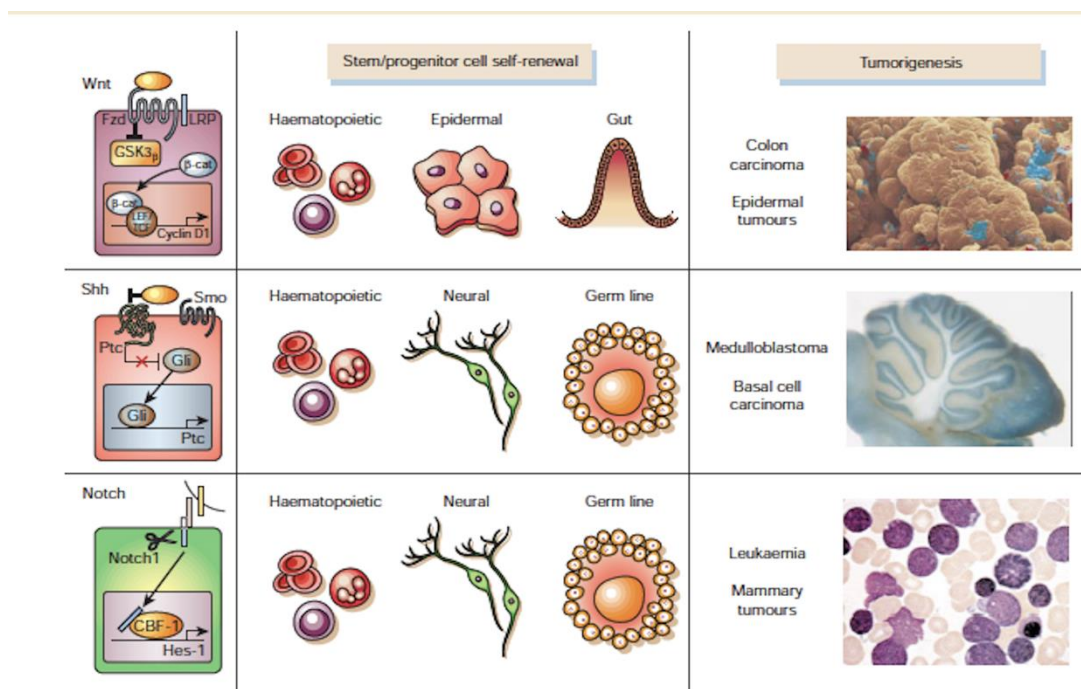
Figure 12. Signalling pathways that regulate self-renewal mechanisms during normal stem cell development and during transformation. Wnt, Shh and Notch when dysregulated, these pathways can contribute to oncogenesis. (Reya *et al.*, 2001)

3.2.2 Plasticity

Several studies have provided evidence that both CSCs and non-CSCs are plastic and capable of undergoing phenotypic transitions in response to the exposure to the right microenvironmental factors. CSCs phenotype has a high plasticity and this plasticity highly depends on the EMT. The tumor TME may play a critical role in the plasticity affecting the CSC state, from the origin of the CSCs to their metastatic potential (Hernández-Camarero *et al.*, 2018)

3.2.3 CSCs and the epithelial-to-mesenchymal transition

Epithelial-mesenchymal transition (EMT) is an essential process during embryonic development where epithelial cells convert to mesenchymal cells. During EMT, epithelial cells acquire migratory properties. It is a complex program accompanied by the loss of epithelial markers such as E-cadherin adherents proteins and the acquisition of mesenchymal markers such as vimentin and N-cadherin. EMT can be usurped by transformed cells and has been implicated in the initiation of and progression toward more invasive and metastatic state/phenotype. It is known that overexpression of EMT transcription factors not only enforces a mesenchymal-migratory phenotype, but also exacerbates the tumour-initiating potential of cell lines (Batlle and Clevers, 2017; Marie-Egyptienne *et al.*, 2013).

3.2.4 Quiescence

The property that CSCs have to maintain a quiescence state, a state in which the cell does not divide, remaining in the G_0 phase of the cell cycle allows them to survive the majority of anticancer treatments. This feature makes it possible for cancer to come

back, even decades after initial treatment, such as colon or BC (Batlle and Clevers, 2017; Reya *et al.*, 2001).

3.3 CSCs and therapeutic resistance

The residual population of chemotherapy and radiotherapy-resistant tumour cells capable of relapse the disease is enriched in CSCs. Chemotherapy and radiation resistance were initially viewed as an intrinsic property of normal stem cells and CSCs, acquired through multiple independent mechanisms such as the upregulation of drug-efflux pumps, a high DNA-repair capacity, or autophagy.

3.3.1 Enhanced of DNA repair capability

CSC can be protected from DNA damaging treatment by enhancing of DNA repair capability in a variety of different tumour entities including glioma, nasopharyngeal carcinoma, lung and breast. CSCs have significantly more Rad51 foci, less γ-H2AX foci after irradiation compared to non-CSC population and an increased expression of genes involved in DNA damage response including Nek1, Brca1, Chek1, Hus1, Ung, Xrcc5, Sfpq, and Uhrf1. In addition to the activation of DNA repair process, DNA damage induces checkpoint mechanisms including two distinct kinase signalling pathways, the ATM-Chk2 and ATR-Chk1pathways, which are activated by DSBs and single-strand DNA breaks, respectively. DNA damage checkpoint signalling inhibits cell cycle progression to allow DNA reparation (Cojoc *et al.*, 2015a).

3.3.2 Upregulation of drug-efflux pumps

As a consequence of the proliferation of CSCs, overexpression of ABC transporters that use the energy obtained from the hydrolysis of ATP to expel drugs

from cells is produced. Adenosine triphosphate-binding cassette (ABC) pumps, ABCG2 and P-glycoprotein are responsible for efflux of the fluorescent Hoechst 33342 dye, leading to the side population, which is enriched in CSCs. Moreover, the major drug resistance protein, MGMT, and anti-apoptotic genes such as FLIP, BCL-2, BCL-XL, cIAP1 and survivin were upregulated in glioma CSCs (Cojoc *et al.*, 2015a; Krause *et al.*, 2017).

3.3.3 Autophagy

CSCs use alternative sources of energy *via* activation of catabolic processes that maintain metabolic homeostasis and cell viability in the process known as autophagy. During autophagy organelles or proteins are sequestered in double-membraned autophagosomes that fuse with lysosomes to form the autolysosome. So, it has been demonstrated that CSCs have higher flux of autophagy and that is essential for progenitor cell maintenance and tumorigenicity (Cojoc *et al.*, 2015b)

3.4 Therapeutic approaches to target CSCs

Since the CSC model is highly relevant for recurrence of the cancer, a treatment based on targeting CSCs may be more effective in preventing future relapses (Ghaffari, 2011). Since CSCs are molecularly distinct from non-CSCs and bulk tumour cells, a high-throughput screening approach (HTS) was used to identify small compounds that eliminate or reduce levels of CSCs. As shown in Figure 13 the most effective treatments would consist of radiation and chemotherapy against the bulk tumour combined with direct-targeted against the CSC-specific drug, a challenging task due to potential toxic

side effects on the normal stem cell compartment (Cojoc *et al.*, 2015b; Krause *et al.*, 2017)
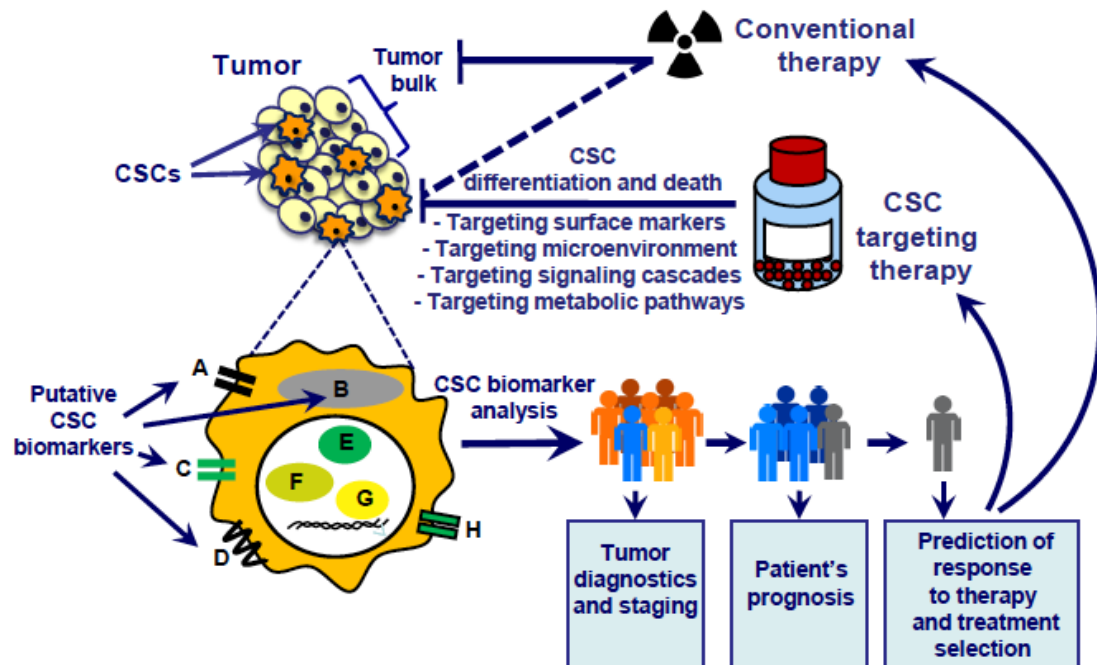
Figure 13. Scheme of possible therapeutic targets and treatments in cancer (Cojoc *et al.*, 2015a)

3.6 Breast Cancer Stem Cells

3.6.1 Isolation and characterization

Al-Hajj and colleagues (Al-Hajj and Clarke, 2004) prospectively isolated a tumorigenic population of cells from primary human BC using FACS based on the ESA$^+$/ CD44$^+$/CD24^{-low}/lineage$^-$ phenotype (Ablett *et al.*, 2012). The CD44+/CD24- phenotype has been used extensively to identify and isolate cancer cells with increased tumorigenicity. In addition to cell surface markers, other expression-based methods of CSC enrichment have been developed. Aldehyde dehydrogenase1 (ALDH1) activity

has been identified as a method of enriching for normal human breast stem and CSCs. Furthermore, by combining ALDH1 activity with CD44^{high}CD24$^-$ expression, the CSC fraction was refined further compared to either method alone. Interestingly, the ALDH$^-$/CD44^{high}/CD24$^-$ population was not enriched for CSCs demonstrating that the CD44^{high}CD24$^-$ population retains significant heterogeneity (Ginestier *et al.*, 2007; Owens and Naylor, 2013; Rabinovich *et al.*, 2018).

Due to the intra and inter-tumour heterogeneity in cancer, it is possible that CSCs from different tumours have distinct expression profiles. Thus, isolating CSCs by function and detailing their expression profiles may prove extremely valuable where traditional markers fail. A range of experimental procedures that have been developed for their isolation and characterization includes the following: a side population technique based on the overexpression of ATP binding molecules such as ATP-binding cassette half transporter (ABCG2)/breast cancer-resistant protein 1 (BCRP1); sphere-forming assays in suspension culture conditions in the presence of growth factors such as basic fibroblast growth factors or epidermal growth factors and in vitro mammospheres formation by BC cells enriched with stem cells (Gangopadhyay *et al.*, 2013).

4. IONIZING RADIATION

Radiotherapy (RT) has remained one of the most effective treatments for cancer, with around half of all patients receiving radiation therapy at some point during their management (Delaney *et al.*, 2005). Ionizing radiation (IR) damages cells by producing intermediate ions and free radicals that cause DNA double-strand breaks (DSBs), the

most common injury from IR, when cells fail to repair this damage carry on to cell death.

The majority of cancer patients are treated with IR, alone or in combination with chemotherapy, surgery and immunotherapy. Currently, RT has become the standard treatment of early stage BC, where a total dose of 60 - 66 Gy given in 30-33 fractions administered over 6 weeks is used. The standard fractionation schedule is the delivery of 1.8–2.0 Gy per day, five days per week. Post-operative RT given to the breast and regional lymph nodes increases control by up to 20% and improves long-term survival. The radiobiological rationale in support of standard fractionation is the sparing of normal tissues with smaller daily doses of radiation without compromise in tumour control. Fractionated treatment regimens increase damage to the tumour; it may reoxygenate the tumour cells and re-distribute their cell into more sensitive cycle phases (Lee *et al.*, 2017).

More recent data has helped to establish hypofractionated whole breast irradiation (HF-WBI), which consists of a 3-4-week regimen, as a new standard of care for the vast majority of women with early-stage BC undergoing breast-conserving surgery. In the post-mastectomy setting, there are some data to support the use of a hypofractionated regimen, with additional ongoing trials investigating this question (Ohri and Haffty, 2020).

4.1 IR promote CSCs phenotype

Exposure to IR causes damages to various cellular organelles and components in particular DNA, mitochondria and cellular membrane. Nuclear DNA is the primary target of IR; radiation causes DNA damage (genotoxic stress) by direct DNA ionization

or indirectly *via* the free radicals generated from the radiolysis of water. IR exposure produces sequential molecular events that culminate either in the repair of the damage or sustaining genomic instability or cell death. At the level of tissues, organs and the total body, the consequence of irradiation may be recovery or to induce the manifestation of early and delayed injuries such as acute and late tissue reactions, radiation sickness, sterility, hereditary effects and cancer (Lomax *et al.*, 2013).

The therapeutic effects of IR are traditionally associated with DSBs that are the most lethal form of damage to tumour cells. ROS have been shown to play an important role in mediating the biological effects of IR and, then, it can increase ROS production both by inducing extracellular water radiolysis and by causing intracellular metabolic changes or damage to mitochondria. Although IR is used as a standard treatment for a variety of malignant tumours, paradoxically also promotes tumour recurrence and metastasis.

IR is known to induce EMT *in vitro* stemness and metabolic alterations in cancer cells. Metabolic alterations are involved in tumour progression, and include growth, invasion, metastasis, and the acquisition of the CSC phenotype, thereby contributing to tumour recurrence and distant metastasis. IR activates cancer-associated fibroblasts (CAFs) to promote the release of growth factors, including transforming growth factor-β (TGF-β), and extracellular matrix (ECM) modulators, including matrix metalloproteinase (MMP) that degrade the ECM, facilitating tumour invasion and metastasis (Artacho-Cordón *et al.*, 2012; Steer *et al.*, 2019).

Although IR activates an antitumor immune response, this signalling is frequently suppressed by tumour escape mechanisms such as cell death and by suppressive immune cells (Kim *et al.*, 2015; Lee *et al.*, 2017; Zhou *et al.*, 2011) (Figure

14). Radiation *in vivo* enriches the fraction of cells expressing CSC markers, which also have an enhanced self-renewal capacity and tumorigenicity compared to the tumour bulk. In addition, sorted CSC cells from different types of tumours survive such treatments in culture much better than unsorted or negative cells (Garvalov and Acker, 2011).
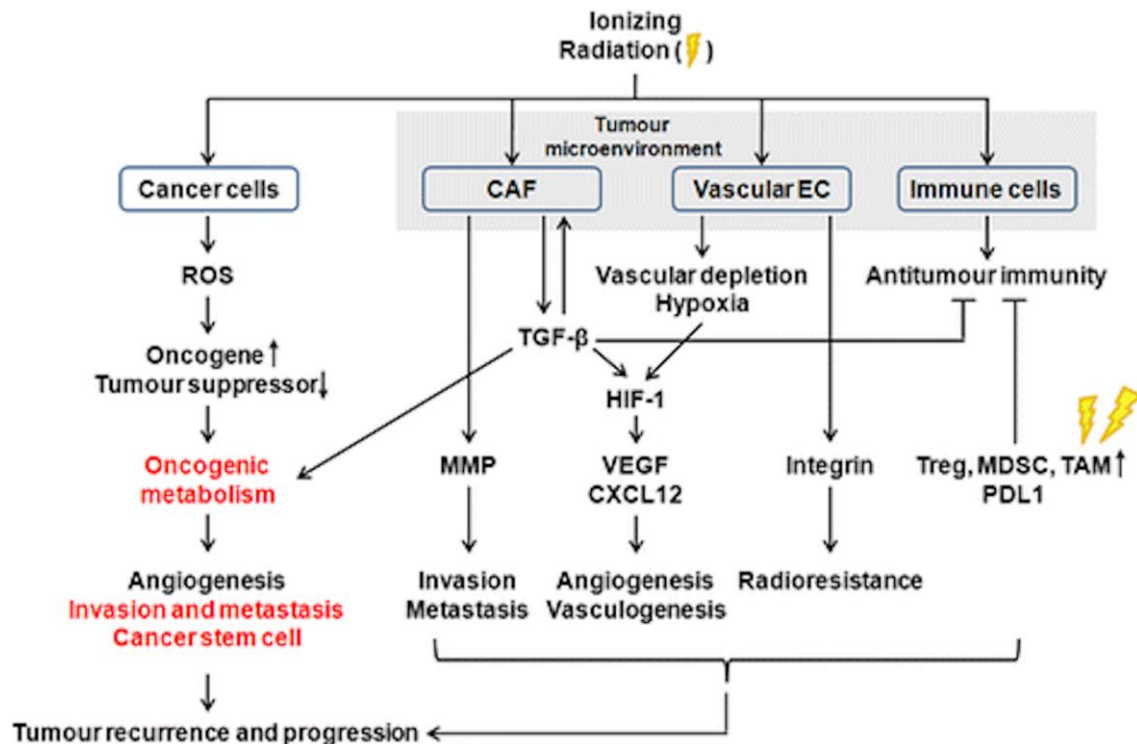
Figure 14. IR-induced side effects on cancer cells and the tumour TME (Lee *et al.*, 2017).

There are numerous studies on different tumour types, and CSC markers associated with them, supporting this hypothesis. It has been shown that CD133 positive cells, mostly associated to brain cancer, are found in a greater proportion after receiving a fractionated radiation both *in vitro* and *in vivo* (Lee *et al.*, 2017). The population characterized as CD44$^+$/ CD24-^{low} is resistant to fractionated radiation treatment, keeping intact its capacity for self-renew and being more aggressive and better able to reproduce the tumour and initiate metastasis (Lagadec *et al.*, 2013; Phillips *et al.*, 2006). Cells with high ALDH1 character a subpopulation with increased radioresistance,

whose inhibition resulted in a sensitization to the same (Croker and Allan, 2012; Ghisolfi *et al.*, 2012). It is possible that if radiation recruits CSCs into the proliferating pool, their intrinsic radiosensitivity may alter, which would give a therapeutic advantage to fractionated as opposed to single-dose radiotherapy (Brunner *et al.*, 2012).

4.2 Radioresistance and CSCs

The CSC is thought to be directly responsible of the relapse in a tumour process after having received RT. The mechanisms by which CSCs may be resistant to RT can be framed into four groups: systems repair of DNA damage, redistribution of the cell cycle, cells tumour repopulation, and level of intratumor hypoxia in the TME (Figure 15).
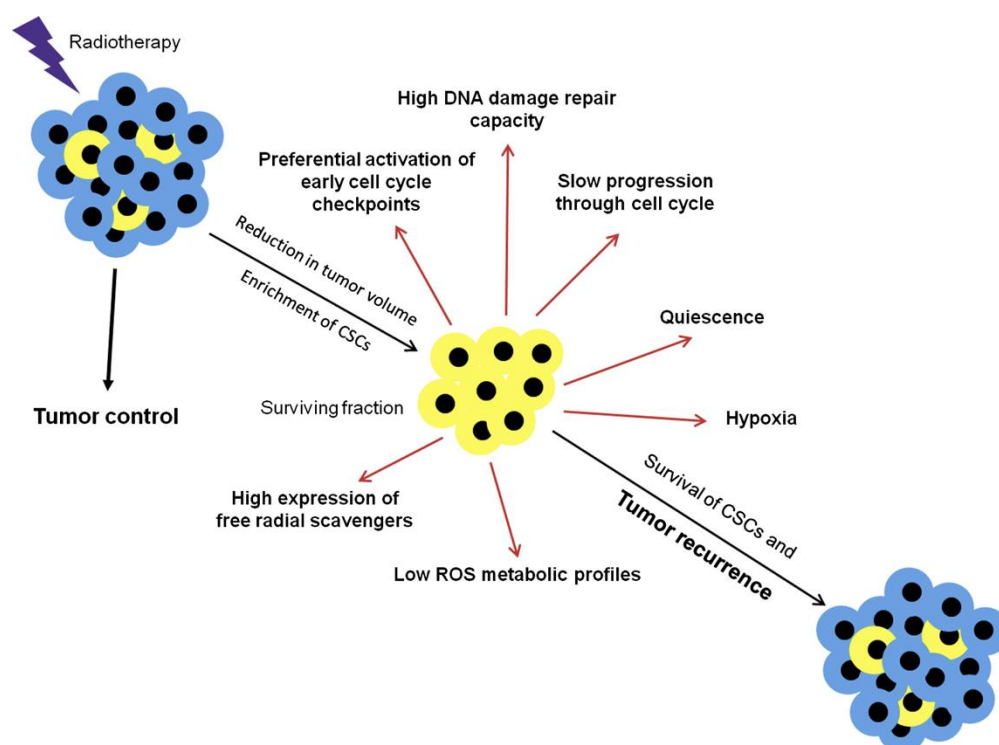
Figure 15. CSCs evade radiation-induced cell death through the activation of survival pathways (Marie-Egyptienne et al, 2013).

4.2.1 Cell cycle phase

Treatment of cells with radiation IR causes delays in the movement of cells through the phases of the cell cycle. This occurs through the activation of DNA damage checkpoints, which are specific point in the cell cycle at which progression of the cell into the next phase can be blocked or slowed. The DNA damage response (DDR) activates four distinct checkpoints in response to irradiation that take place at different point within the cell cycle. These checkpoints are G_1/S, S, early G_2 and late G_2. In a large proportion of tumour cells, one or more of these checkpoints are disable due to genetic changes and other alterations that occur during tumorigenesis. When functional, the checkpoints block further proliferation of these cells and can thus actively suppress cancer development. Alteration in genes that influence checkpoint activation will result in the failure to delay cell-cycle progression in response to irradiation. ATM is the apical kinase thought to be regulating, through phosphorylation of hundreds of substrates, the global cellular responses initiated by DSBs, including the coordination of DSB repair events and the activation of cell cycle checkpoints. Radiation-dose-dependent functional synergisms between ATM, ATR and DNA-PKCs have also been described in checkpoint control (Bower *et al.*, 2017; Chao *et al.*, 2017; Matsuoka *et al.*, 2007; Mladenov *et al.*, 2019; Paull, 2015; Shiloh and Ziv, 2013).

The presence or absence of checkpoints will affect the redistribution of cells in the cell cycle after irradiation. Cells in mitosis/G_2 are more sensitive to radiation and those found in late S phase more radioresistant. Since not only radioinduced damage varies during the course of the cell cycle but also DNA repair capacity changes, this may indirectly affect the sensitivity of cells to subsequent doses of radiation. Thus, radiation exposure induces a redistribution of the cell in the cycle resulting in an accumulation of cell in S phase. So, if the radiation dose administered in the appropriate

moment may act on the most sensitive stage, i.e. G_2/M, would make the treatment most effective.

Radiation induced activation of the DNA damage checkpoint-Chk1 signalling in stem-cell enriched subset within NSCLC led to cell cycle arrest, more efficient DNA damage repair and a higher cell survival rate. ATR-Chk1 and ATM-Chk2 signalling pathways are preferentially activated in CD133+ progenitor cells, but not in CD133− cells in response to radiation-induced genotoxic stress, and CD133+ cells repair DNA more effectively than CD133- tumour cells (Bao *et al.*, 2006).

4.2.2 High ability to repair DNA

More evidence suggesting increased DNA damage repair capacity in CSCs came from the observation of γ-H2AX induction in BCSCs. γ-H2AX is the phosphorylated form of H2AX which is the gene encoding the histone H2A variant, H2AX. Starting within a few minutes of DSB formation, H2AX becomes phosphorylated. γ-H2AX is the sensitive surrogate of DNA DSBs, which can be quantified after radiation. It has been demonstrated by several groups that CSCs have lower γ-H2AX foci after radiation in human breast CSCs (BCSCs). In addition to ATM, two other kinases have been shown to phosphorylate H2AX at the sites of DSBs: DNA-dependent protein kinase catalytic subunit (DNA-PKcs) and AT-related (ATR) protein (Falck *et al.*, 2005).

Among different control points altered in the repair process allowing survival are the activation of ataxia telangiectasia mutated (ATM) in CD44^{+}/CD24$^{-/low}$ cells (Yin 2011), the enrichment of polycomb group protein BMI1 in CD133 positive cells (S. Y. Kim *et al.*, 2012; Rich, 2007) or the activation of the checkpoint kinases 1/2, which also leads to a survival of CD133 positive cells (Bao *et al.*, 2006).

Wnt/β-catenin signalling pathway is a network of proteins essential in embryogenesis, stem cell maintenance and survival. This pathway has also been shown to be important in CSCs and their responses to DNA damages. One transcriptional target of β-catenin is survivin which can promote survival in response to apoptotic stimuli. Survivin has been linked to radiation resistance and it has been demonstrated that suppression of this target with inhibitor may sensitize the radiation effects and induce more apoptosis (Chumsri and Shah, 2013; Cojoc *et al.*, 2015b).

4.1.3 Hypoxia and microenvironment

Hypoxia is a fundamental pathophysiological phenomenon strongly associated with the development and aggressiveness of various solid malignancies and also implicated in radioresistance (Brunner *et al.*, 2012). Since hypoxic cells are resistant to radiation, their presence in tumours are critical in determining the response of tumours to treatment with large doses of radiation.

The oxygen is a key requirement for any biological process, so that the concentration thereof is controlled with great precision. An imbalance that results in a hyperoxia induces formation of reactive oxygen species (ROS) that can go causing cell death, and hypoxia can trigger the activation of pro-apoptotic pathways and pro-angiogenic (Brunner *et al.*, 2012). In the case of the ROS, a study based on CD44 $^+$/ CD24$^{-/low}$ cells growing in suspension showed a higher level of ROS compared to monolayer culture. After receiving a radiation dose an increase thereof in monolayer culture was shown but not in the suspension, which suggests that a large removal control of ROS lead to cell death avoidance caused by radiation (Phillips *et al.*, 2006). Cellular responses to hypoxia are commonly regulated by the hypoxia inducible factor (HIF). The higher level of HIF in the tumour can be correlated with the level of oxygen

and it has been shown to correlate with the radiation resistance (Liu and Wang, 2015). There are two isoforms, HIF1a and HIF2a with differential expression in CD133 glioma cells, while HIF2a significantly was present in the CD133 positive population HIF1a was detected in the complete pool of cells, but was stabilized under conditions of hypoxia, and HIF2a overexpression way further related with poor prognosis (Li, 2009).

As tumour develop, the requirement for oxygen increases, leading to regions of hypoxia. Hypoxia causes activation of HIFs, which enable to cells to adapt to the low-oxygen environment. Hypoxic culture conditions (1% O_2) induced an increase in the ALDH1$^+$ proportion in BC cell lines. Cancer cell phenotype and expression profiles are altered under hypoxia conditions. So, a subfraction of the phenotypically adapted cancer cells may indeed show stemness characteristics as defined by functional and/or surrogate biomarkers combined with enhanced survival capacity. Treatment strategies to overcome hypoxia-driven radioresistance have thus always aimed at enhanced killing of this cancer cell population. (Brunner *et al.*, 2012; Ejtehadifar *et al.*, 2015) (Figure 16).
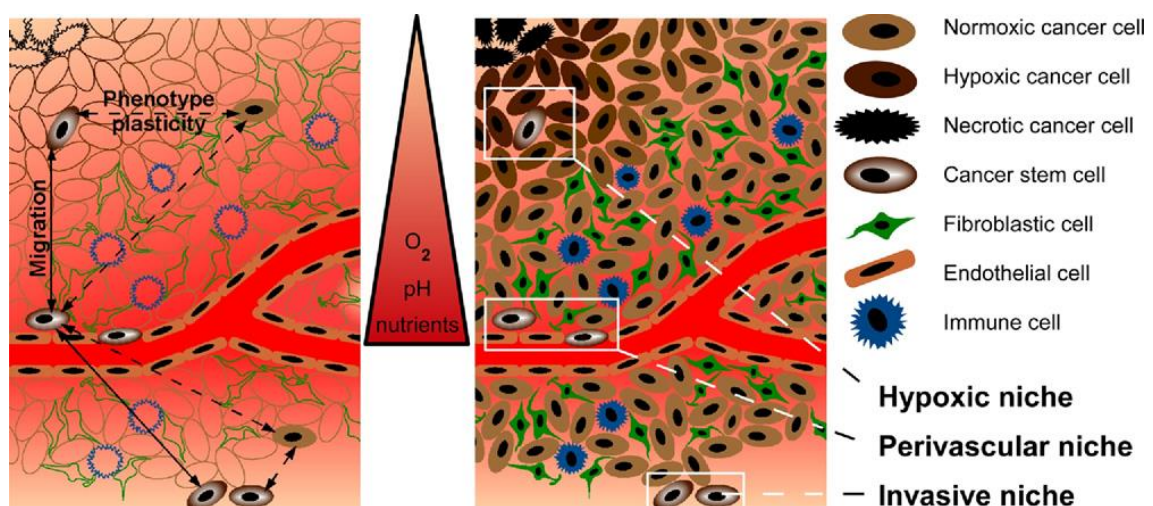
Figure 16. The central role of TME. Three different niches are hypothesized in tumour tissue, in particular based on work in brain cancer models: A hypoxic niche, a perivascular niche, and a niche at the invasion front (right panel). (Brunner *et al.*, 2012)

4.1.4 Activation of developmental pathways

Resistance to anti-cancer treatment and accelerated repopulation of CSC after or during treatment might be also attributed to the activation of signalling pathways which are essential for adult tissue homeostasis and embryonic development such as canonical wingless-type MMTV integration site family (WNT), Notch signalling and Hedgehog pathways. Repopulation of tumours may be one of the most common reasons for the failure of conventional fractionated courses of radiation therapy. Notch pathway by radiation might be part of the acute response to IR transcriptional activator, thereby initiating the transcription of gene products that promote progression into the S-phase of the cell cycle. In BC, IR induces the expression of Notch receptor ligands on the surface of nontumorigenic cells and activation of Notch signalling in CSCs than redistribute quiescent CSCs into the cell cycle (Figure 17). Another developmental pathway activated in response to radiation is the TGF-β pathway, which is thought to be an antiproliferative pathway that controls tissue homeostasis. TGF-β is produced by the mass of the nontumorigenic, radiosensitive cancer cells and activated by radiation. (Brunner *et al.*, 2012; Cojoc *et al.*, 2015b; Vlashi and Pajonk, 2015).
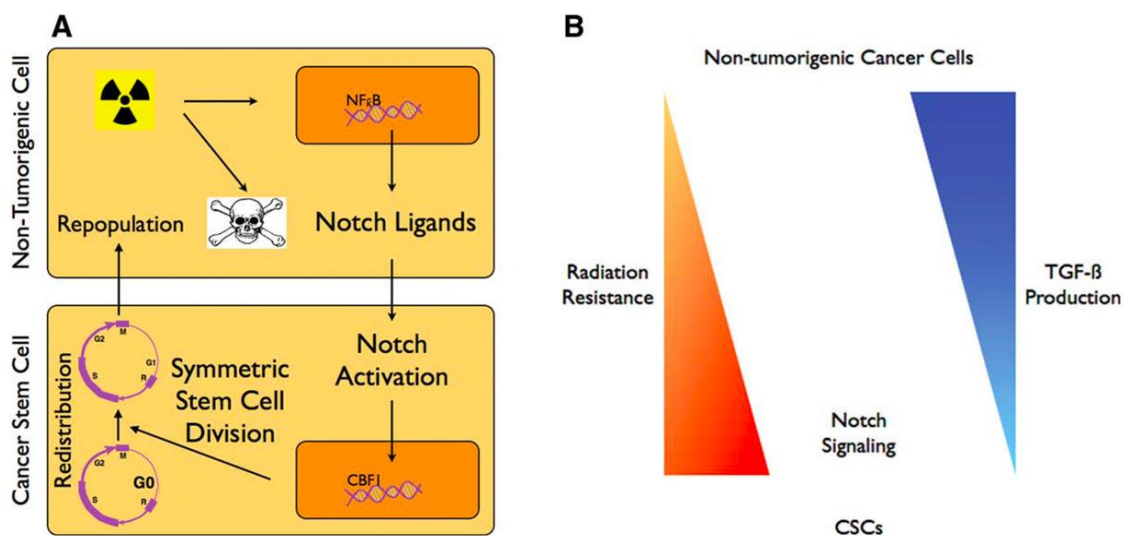
Figure 17. Radiation-induced redistribution and accelerated repopulation employs the developmental Notch pathway. (Cojoc *et al.*, 2015a)

5. MICRORNAS

5.1 miRNAs definition and biogenesis

A microRNA (miRNA) is a small endogenous non-coding RNA molecule that regulates gene expression in transcriptional and post-transcriptional specific sequences. In 1993, Victor Ambros and colleagues discovered miRNAs studying the gene of the protein lin-14 in. *Caenorhabditis elegans* development. Subsequent studies revealed that the 21 nucleotides transcript is complementary to the 3' untranslated region (3'UTR) of lin-14 and, most interestingly, negatively regulates the expression of lin-14. Initially, these findings were not appreciated by the scientific community, because it was believed to be a rare process occurring only in *C.elegans*. However, in 2000, another such 22 nucleotides non-coding RNA named as let-7, was identified in *C.elegans*. The discovery of two miRNAs, lin-4 and let-7, in *C.elegans* suggested that miRNAs are important regulators of embryonic development and stem cell functions in mammals (Garofalo and Croce, 2015; Rosalind C. Lee and Ambrost, 1993; Virginie *et al.*, 2013).

Biogenesis of miRNAs is a complex process (Figure 18). miRNAs are transcribed for the most part by RNA polymerase II as long primary transcripts characterized by hairpin structures (pri-miRNA), and are processed in the nucleus by RNase III Drosha into 70–100 nucleotide long precursor miRNAs (pre-miRNAs) in combination with cofactors such as DGCR8, an evolutionarily conserved protein that interacts with proline rich peptides through its WW domain (Feinbaum *et al.*, 2004; Virginie *et al.*, 2013).

Pre-miRNAs are then exported to the cytoplasm by the nuclear export factor

Exportin 5 and the Ran-GTP cofactor, where they are cleaved by another RNase III type enzyme, Dicer, to generate a ~22 nt RNA duplex. One strand of the miRNA duplex is usually selected as a mature miRNA, and is assembled into an RNA induced silencing complex (RISC), while the other strand is degraded. (Abba *et al.*, 2014). The RISC complex interacts with the Argonuate proteins and they collectively act to silence target mRNAs.

The mechanism of mRNA silencing is dependent on the degree of complementarity. In the case of completely aligned miRNA/mRNA pairs, degradation occurs as a consequence of endonucleolytic cleavage resulting from the proteins bound to RISC. However, in the case of most animals, perfect complementarity rarely exists, and as such the target mRNA cannot be degraded by this mechanism. Consequently, these imperfect miRNA/mRNA pairs are either translationally repressed or silenced independent of the above-mentioned mechanism. The complementarity to the messenger RNA within positions 1–8 of the microRNA is the most crucial parameter for regulation, and binding sites on the mRNA are located in most instances on the 3' untranslated region (UTR) (Figure 18) (Shah and Chen, 2014)

Figure 18: miRNAs
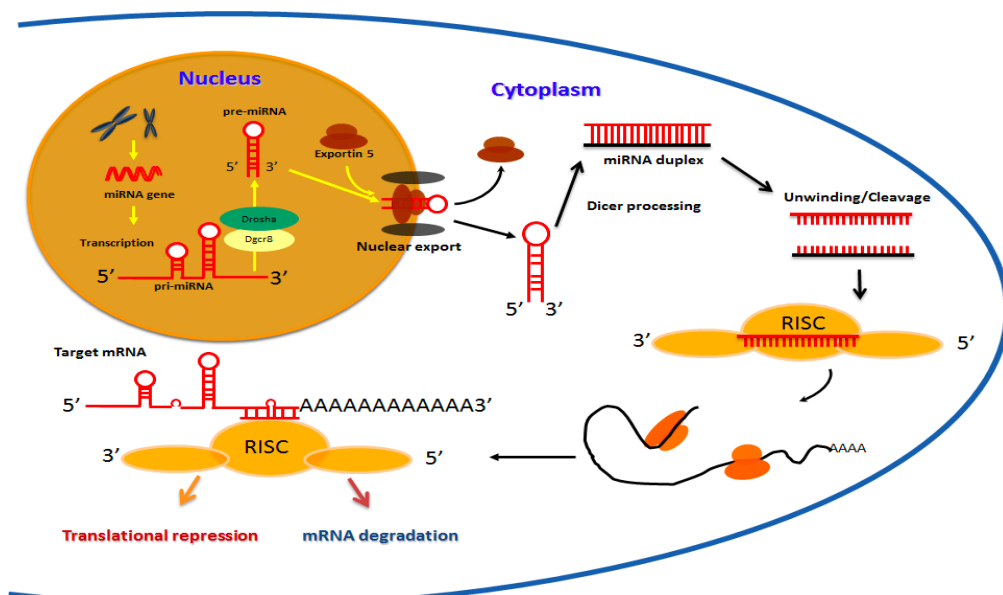
biogenesis (Abba et al, 2014).

6.2 miRNAS and BCSCs

Thousands of miRNAs have been identified many of which have been shown to play important roles in a variety of biological processes, like development, differentiation, apoptosis, proliferation, and cell death. It is now clear, that miRNAs together with other non-coding RNAs (long non-coding RNAs, small nucleolar RNAs and ultraconserved regions) contribute to carcinogenesis. A miRNA deregulation is involved in initiation and progression of cancer. They modulate the expression of their target genes by either degrading their target mRNA or inhibiting their translation through pairing of miRNA sequences to complementary bases on the target mRNA. Recently, abnormalities in non-coding RNAs have been reported to be fundamental in the regulation of CSC properties such as asymmetric cell division, tumorigenicity and drug resistance (R. u Takahashi *et al.*, 2013). There are many studies where miRNAs related with BCSCs are described and mainly, grouped according function (oncogene or suppressor tumour) (Garofalo and Croce, 2015; Schwarzenbacher *et al.*, 2013; Shah and Chen, 2014; Shimono *et al.*, 2015) (Table 2 and Table 3).

MiRNAs	Known target MiRNAs	Function
Let-7 family	RAS, HMGA2	Inhibit cell proliferation and mammosphere formation
MiR-125	HER2, HuR, ETS1, Cyclin, MEGF9	Inhibit cell proliferation and invasion
MiR-205	ZEB1/2	Reduces EMT and metastasis
MiR-200 family	ZEB1/2	Reduces EMT and metastasis
MiR-206	Cyclin D2	Inhibit cell proliferation and invasion
MiR-34a	Bcl2, SIRT1	Inhibit migration, metastasis and invasion
MiR-335	SOX4, TNC	Inhibits metastasis
MiR-342	HER2	Increases cell proliferation
MiR-15a/16	HER2	Increases cell proliferation
MiR-302	RAD52 and AKT1	Affects DNA repair
MiR-31	RhoaA, ITGA5, RDX	Reduces invasion and metastasis
MiR-519c	HIF-1a	Inhibits angiogenesis

Table 2. List of some suppressor miRNAs studies in (Shah and Chen, 2014)

MiRNAs	Known target MiRNAs	Function
Let-10b	HOXD10	Promotes cell proliferation, metastasis and angiogenesis
MiR-126	IGFBP2, MERTK, PITPNC1	Promotes angiogenesis
MiR-155	SOCS1, TP53INP1, FOXO3, RhoA	Promotes cell proliferation
MiR-21	PTEN, TPM1, PDCD4, Maspin	Promotes cell proliferation
MiR-375	RASD1	Epigenetic modification of tumour suppressor genes
MiR-221/22	TRPS1	Induce metastasis
MiR-373	CD44	Induce metastasis
MiR-520c	CD44	Induce metastasis
MiR-9	SOCS5, E-cadherin	Induce metastasis
MiR-632	DNAJB6	Induce metastasis
MiR-196b	HOXD10	Promotes angiogenesis
MiR-7	HOXB3	Epigenetic modification of tumour suppressor genes
MiR-218	HOXB3	Epigenetic modification of tumour suppressor genes
MiR-203	SOCS3	Promotes cell proliferation

Table 3. shows the main tumour oncoge microRNAs involved in breast cancer development.

In conclusion, the use of miRNAs as biomarkers in clinical practice is a potentially powerful tool for non-invasive analysis. A more detailed understanding of the role of miRNAs in CSC biology may improve cancer treatments and possibly lead to the clinical application of miRNAs in cancer diagnosis, prognosis and treatment. (Garofalo and Croce, 2015; Schwarzenbacher *et al.*, 2013).

6.3 miRNAS and radioresistance

RT, through ionizing radiations aims to cure tumours, determining damages by the production of free radicals at various levels in the neoplastic cell. miRNAs participate in processes involved in radioresistance; for example, miR-24 and miR-428 participate in cellular response to IR that simultaneously activates a number of signalling pathways mediating the DDR. Therefore, miRNAs are deeply involved in the regulation of this processes (Korpela *et al.*, 2015; Metheetrairut and Slack, 2013a; Tessitore *et al.*, 2014).

There are several avenues by which the heterogenous hypoxic intratumour landscapes can protect cancer cells from irradiation. The hypoxic environment can

influence radiosensitivity through activation of the hypoxia-inducible factor-1 (HIF-1) pathway and transcription of HIF-1-responsive genes. miR-210 induces hypoxia and can stabilise the HIF-1 complex and enhance radioresistance in vitro.

Other example is that miR-dependent alterations in key survival signalling pathways are also common ways cancer cells circumvent irradiation-induced growth arrest and death. For example, miR-21 and miR-95 promote phosphatidylinositol 3 kinase-AKT-pathway-mediated survival by suppressing its direct and indirect negative regulators PTEN and SGPP1, respectively (Halimi *et al.*, 2012; Korpela *et al.*, 2015).

Finally, as shown in Figure 19 miRNAs could be useful for monitoring and understanding professional and accidental exposures to IR and may lead to novel therapeutic strategies employing miR mimics or antagomirs (Cellini *et al.*, 2014; Korpela *et al.*, 2015).
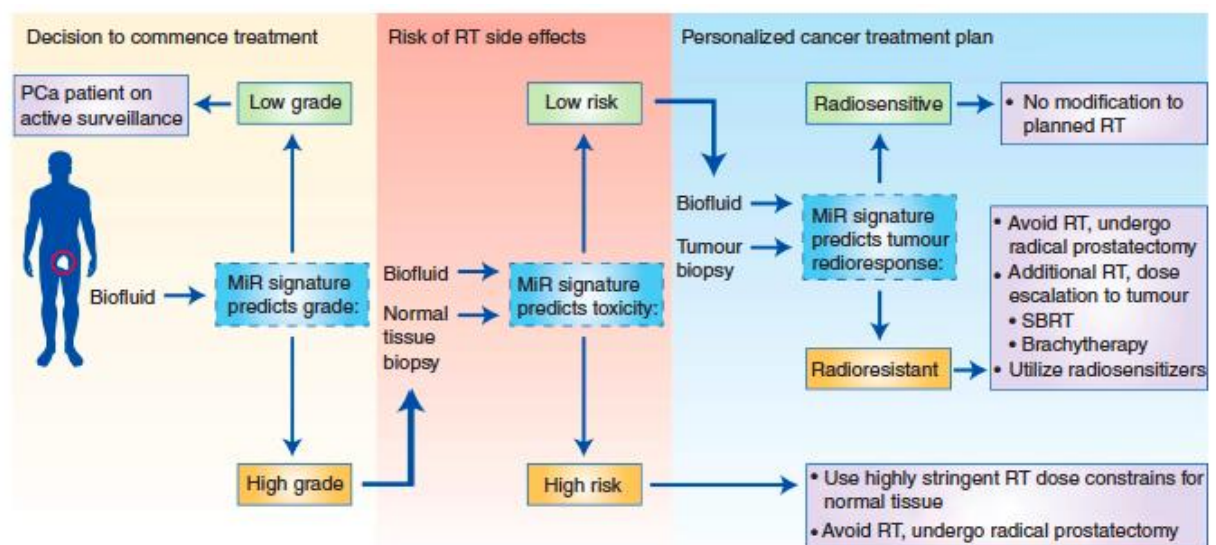

Figure 21. The potential utility for miR-predictive signatures in personalising the management of cancer and radiotherapy treatment (Korpela *et al.*, 2015).

HYPOTHESIS

CSCs have been found to exhibit a number of genetic and cellular adaptations that confer resistance to RT. They include among others, efficient DNA repair (most importantly), the role of the CSC TME and hypoxia, and the apoptosis resistance to RT. Cells repair sub-lethal damage between irradiation fractions and, therefore, a failure of radiation treatment might be attributed to the incomplete eradication of CSC subpopulations. Furthermore, it has been well established that miRNAs play a crucial role in the cellular response to IR. A review of scientific literature has demonstrated that expression of miRNAs is different in CSCs and non-CSCs, playing radiation an important role in this expression. The differential expression of miRNAs in CSCs may promote greater tumorigenic potential, pluripotency and radioresistance of CSCs. The determination of these miRNA signatures is important since alterations in miRNA expression profiles could provide predictive information about sensitivity or resistance of breast tumours to RT. In this sense miRNAs could be use as therapeutic targets and biomarkers of response to radiotherapy in patients with breast cancer.

Our hypothesis is based on the following evidences:

1. BCSCs subpopulations confer radioresistance to this physical agent because of: i) their higher DNA damage repair rate, ii) their lower levels of reactive oxygen species (ROS) and iii) their reduced apoptotic rate.

2. miRNAs are key players in the regulation of metastasis, DNA damage, apoptosis, hypoxia and radioresistance.

3. BCSCs that are not eliminated by radiation would stimulate the recurrence, invasion and metastasis processes. Since radiation enriches the fraction of CSCs subpopulation, this physical agent may modulate specific miRNAs of these cells involved in radio-response.

OBJECTIVES

The **main objectives** of this work were (Figure 22):

1. To evaluate effect of IR on stemness properties, proliferation rates, apoptosis and gene expression profiling on established BC cell lines cultured as monolayer and as mammospheres.

2. To study and analyse the expression of specific miRNAs related to metastasis, hypoxia and DNA damage response in BCSCs after receiving radiation doses versus a sham-irradiated control cells.

3. To monitor the effect of IR on tumour growth orthotopic inoculation of irradiated triple negative BCSCs.

4. To analyse specifics miRNAS of CSCs and their modulation by IR in BC patients' serum treated with RT to assess the potential application for miRNA signatures as predictive biomarkers in both RT outcome and disease prognosis.
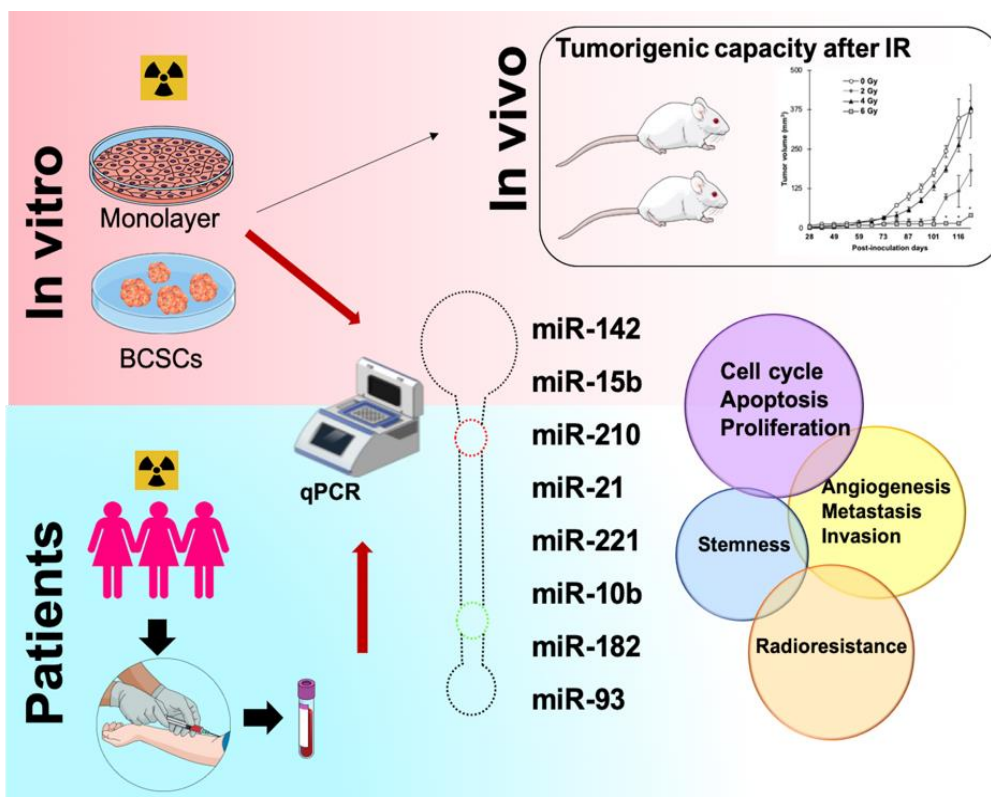
Figure 22: Graphical abstract of the main objectives in this study

MATERIAL AND METHODS

1. CELL CULTURE

1.1 Cell lines

We used three established cell lines derived from three different human breast adenocarcinomas: MCF-7 (reference ATCC HTB-22), an $ER^+/PR^+/HER2^+$ breast cancer cell line; MDA-MB-231 (reference ATCC HTB-26), a triple- negative ($ER^-/PR^-/HER2^-$) breast cancer cell line and SKBR-3 (ATCC HTB-30), a $HER2^+$ breast cancer cell line. American Type Culture Collection (ATCC).

1.2 Culture conditions

Cell culture was performed under sterile conditions, in a laminar flow hood (Micro-V, Telstar, Spain). Cells were maintained in Dulbecco's Modified Eagle Medium (DMEM; Sigma-Aldrich, St Louis, MO, USA) supplemented with 10% fetal bovine serum (FBS) (BioWhittaker, Lonza, Basel, Switzerland) and with 1% of a solution of penicillin / streptomycin (10,000 U / ml penicillin G and 10 mg / ml streptomycin, Sigma-Aldrich, St Louis, MO, USA). All cells were grown at 37°C with 5% CO2 and 90% humidity (Steri-Cult CO2 Incubator, Thermo Electron Corporation, Waltham, MA, USA). Media were changed every 48-72 hours and cultured cells with a maximum of 80-90% confluence were passed. For that, culture medium was removed, cells were washed with phosphate buffered saline (PBS) (Lonza, Basel, Switzerland) and detached enzymatically using 1 mL trypsin-EDTA (Sigma-Aldrich, St Louis, MO, USA); after 3-5 minutes of incubation at 37°C DMEM was added to the culture flask and cell suspension recovered in sterile 30 mL tubes (BD Falcon) and spinning down at 1500 revolutions per minute (rpm) for 5 minutes (Centrifuge 5810R, Eppendorf Corp., Hamburg, Germany). Pellet cells were resuspended in culture media pre-warmed at

37ºC and reseeded into 75 or 25 cm2 culture flasks. All cell lines were tested for authentication using the short-tandem repeat profiling and were passaged for less than 5 months, and routinely assayed for mycoplasma contamination.

1.3 Cell count

To determine the number of cells contained in a cell suspension, the Neubauer chamber, was used. Cell counting was performed by diluting the cell suspension 1:1 with a 0.4% trypan blue solution (Sigma-Aldrich, St Louis, MO, USA) and loading 10 µL of this cell suspension into the Neubauer chamber with the glass cover placed on the top. Trypan blue solution was used to determine live cells within the cell suspension since these cells has an intact cytoplasmic membrane and therefore are not stained with this dye. Live cells were counted in 4 of the 9 square subdivisions; cells that appeared in each quadrant of the chamber were counted, the number obtained was divided by four, and multiplied by 10,000 and finally the dilution factor (X2) was applied to obtained the number of cells per millilitre. To know the final cells that we have in the solution we multiplicate the formula results per the total volume.

1.4 Cell cryopreservation

In order to maintain the cell lines, they were frozen. For that, culture medium was removed, cells were washed twice with PBS and incubated with 0.25% trypsin-EDTA at 37°C in 5% CO_2 and 90% humidity for 5 minutes. Then, trypsin-EDTA were inactivated and cell suspension was collected into sterile 30 mL tubes. Cells were centrifuged at 1500 rpm for 5 minutes, resuspended in freezing medium containing 93% FBS and 7% Dimethyl Sulfoxide (DMSO) (Sigma- Aldrich, St Louis, MO, USA) and placed into cryotubes (Nunc, Thermo Fisher Scientific, Waltham, MA, USA) in a total volume of 1 mL. Cryovials containing the cells were placed into an isopropanol cryo-

freezing container (Sigma-Aldrich, St Louis, MO, USA) at -80ºC for short periods; in case of long periods time they were transferred into a liquid nitrogen tank at -180ºC for their permanent storage.

1.5 Cell recovery

Cell lines stored at -80 ° C or in liquid nitrogen were thawed at 37 ºC in a water bath and immediately resuspended in sterile in fresh culture medium and centrifuged at 1500 rpm for 5 min to remove DMSO residues (two washes). Cells pellets were resuspended in culture media and seeded into a 25 cm^2 culture flask.

2. ISOLATION OF CANCER STEM CELLS

CSCs from breast were isolated using the ALDEFLUOR kit assay (StemCell Technologies, Vancouver, Canada) by fluorescence-activated cell sorting in FACS ARIA III (BD Biosciences) according to manufacturer's instructions. ALDEFLUOR is a reagent kit that is used to identify human cells that express high levels of the enzyme aldehyde dehydrogenase (ALDH1). BODIPY-aminoacetaldehyde (BAAA), the activated ALDEFLUOR reagent, is a fluorescent non-toxic substrate for ALDH1, which freely diffuses into viable cells. In the presence of ALDH1, BAAA is converted into BODIPY-aminoacate (BAA), which is retained inside the cells and is measured or isolated using a flow cytometer. A specific inhibitor of ALDH1, diethylaminobenzaldehyde (DEAB), is used to control for background fluorescence. To perform the assay, 1×10^6 cells of each condition were resuspended in 1 mL ALDEFLUOR assay buffer, that contains a transport inhibitor, which prevents efflux of the BAA from the cells. Then, 5 µL of BAAA was added to the cell suspension, 500 µL were transferred into control tube where 5µL of the DEAB-ALDH1 inhibitor was

added. Tubes were incubated for 30 minutes at 37°C in the dark. Then, cells were spin down at 1500 rpm 5 minutes at 4ºC, resuspended in cold buffer and isolated by flow cytometry.

For the maintenance of ALDH1+ mammospheres, spheres medium was used: DMEM/F12 (Sigma-Aldrich, St Louis, MO, USA), supplemented with 1X B27 (Gibco, Big Cavin, OK, USA), 1 µg/ml hydrocortisone, 4ng/ml heparin, 10 µg/ml insulin, 10 ng/ml EGF, 20 ng/ml of FGF, and 1% of a solution of penicillin/streptomycin (10,000 U/ml penicillin G and 10 mg/ml streptomycin, Sigma-Aldrich, St Louis, MO, USA) in ultra-low attachment plates (Corning Inc., Corning, NY, USA).

3. CELL RADIATION PROTOCOL

Attached cells and ALDH1+ mammospheres suspension were irradiated by the X-ray equipment Yxlon Smart Maxishot 200-E at room temperature, under a constant current of 4.5 mA and power of 200 kW at different doses of 2 Gray (Gy), 4 Gy and 6 Gy, and cultured for 24h. Sham-irradiated cells were used as control (0 Gy). For the field size of 15cm x 8 cm, the focal distance was 15cm and for 11.3cm x 7cm field size, focal distance was 25cm. Traceable dosimetry was performed following protocol TRS.398.

4. CHARACTERIZATION OF CANCER STEM CELLS

4.1 Flow cytometry analyses

Cell surface marker levels of CSCs were determined with human antibodies anti CD44-phycoerithrin (PE) and anti CD24-allophycocyanin (APC) (Miltenyi Biotec,

Auburn, CA, USA) such as ALDEFLUOR kit assay- fluorescein isothiocyanate (FITC) (StemCell Technologies, Vancouver, Canada) to detect enzyme ALDH1 activity was performed to completed characterization. Samples were analyzed on a FACS CANTO II (BD Biosciences) and data obtained were analyzed with FACS DIVA software. The brightly fluorescent PE, APC and FITC were detected in the red (564-606 nm), blue (650-670 nm) and green (520-540 nm) fluorescence channels respectively.

Firstly, cells were washed with PBS and then resuspended in 100 µL of blocking buffer, prepared by diluting 1% bovine serum albumin (BSA) (Sigma-Aldrich, St Louis, MO, USA) and 2mM EDTA in PBS; in case of ALDH1, cells were resuspended in ALDEFLUOR assay buffer. After that, cells were spin down and 6 µL of anti- human antibodies or 5 µL of ALDH1 were added to the cell suspension for breast cancer cell lines in the different conditions.

Incubation with CD44 and CD24 antibodies was performed for 10 minutes at 4°C in the dark; incubation with ALDH1 was 30 minutes at 37°C in the dark. Then, cells were centrifuged at 4°C and resuspended in cold PBS.

4.2 Secondary sphere-forming assay

For the secondary mammosphere-forming assay, cells from primary ALDH1+ mammospheres irradiated 24h before at 2, 4 and 6 Gy were collected by centrifugation, then dissociated with trypsin-EDTA and mechanically disrupted with a pipette. Cells from sham-irradiated 0 Gy primary ALDH1+ mammospheres were used as control. From 1000 to 2000 single cells (depending on the cell line plating efficiency) were plated and resuspended in spheres culture medium (DMEM:F12 containing 1% penicillin – streptomycin (P/S), 1X B27 (Gibco), 1X insulin transferrin selenium (ITS) (Gibco), 1 µg/mL Hydrocortisone, 4 ng/mL Heparin, 10 ng/mL EGF and 20 ng/mL

FGF (Sigma-Aldrich, St Louis, MO, USA)),in ultra-low adherence 24-wells plates (Corning Inc., Corning, NY, USA) and cultured at 37°C in an humidified incubator with 5% CO2. Spheres were counted after 5 days by fluorescence microscopy and representative images were taken. (Leica DM5500 B and Leica CW4000 software Leica, Solms, Germany).

4.3 Soft agar assay

For colonies formation, ALDH1+ mammospheres sham-irradiated 0 Gy and irradiated at 2, 4 and 6 Gy were disaggregate and seeded in 1mL 0.4% cell agar base layer (1×10^4 cells), which was on top of 1 mL 0.8% base agar layer in 6-well culture plates after 24h.

To prepare these solutions, 1.6% agar (Sigma- Aldrich, St Louis, MO, USA) diluted in PBS was mixed 1:1 with DMEM supplemented with 20% FBS and 2% P/S. 0.8% base layer was left to solidify by incubating for 2 h at room temperature. Then, to obtain a final concentration of 0.4% agar with cells, they were resuspended in 1 mL of a solution composed of 0.8% agar diluted in PBS mixed 1:1 with DMEM supplemented with 20% FBS and 2% P/S.

Cells were then incubated for further 28 days at 37°C and 5% CO_2, adding 200 μL of medium DMEM supplemented with 10% FBS and 1% P/S every 2 days. Cell colony formation was then counted using a Leica DM5500 B fluorescence microscope equipped with Leica CW4000 software after staining with 1 mg/ml iodonitrotetrazolium chloride (Sigma-Aldrich, St Louis, MO, USA) in PBS overnight at 37˚C.

5. PROLIFERATION ASSAYS

2, 4, 6 Gy and sham-irradiated monolayer cells of three breast cancer cell lines were seeded in 96-well plates in a concentration on 3000 cells/well in DMEM medium supplemented with 10% FBS for 5 days. Cells were incubated with MTT every day and the fluorescence were measured at 570 nm on a Microplate reader MB-580, (Heales, Shenzhen, China).

2, 4, 6 Gy and sham-irradiated ALDH1+ mammospheres of each breast cancer cell line were seeded in a concentration of 3000 cells/well in 96-well ultralow attachment plates (Corning Inc., Corning, NY, USA) in 100 µl sphere forming medium during 5 days. Every day, 10 µl of CCK-8 Cell Proliferation Assay and Citotoxicity Asssay, WST-8 (Dojindo laboratories, Kumamoto, Japan) was added to each well and incubated at 37°C for 1-4 h. Plates were read at 450 nm on a Microplate reader MB-580 (Heales, Shenzhen, China).

6. APOPTOSIS

Cell death was analysed by eBiosciencie TM Annexin V-FITC Apoptosis detection kit (Invitrogen., Carlsbad, CA, USA) and propidium iodide staining solution (PI) was used according to the manufacturer's instructions. In short, cell subpopulations treated with different Gray doses were harvested, washed, and suspended in Annexin V and Binding Buffer (1 mL 10X Binding Buffer + 9 mL dH20). The Annexin V-FITC (2.5 µg/mL) and PI solution (20 µg/mL) were added to 1-5 x 10^6 cells/mL in 100 µL of Binding Buffer and incubated for 15 min at room temperature in the dark. After that, cells were washed and then resuspended in Binding Buffer. Apoptosis was measured 24

h after irradiation using flow cytometry (BD FACS Canto II flow cytometer, Becton Dickinson) and data obtained were analysed with FACS DIVA software.

7. *IN VIVO* TUMOUR ORTHOTROPIC XENOGRAFT ASSAY

For orthotopic assays, MDA-MB-231 monolayer at 80% confluence and ALDH1+ mamospheres were irradiated at 2, 4, 6 Gy and a control sham-irradiated was also used. 24 hours after irradiation 3000 cells of each condition were injected in 0.05 mL matrigel (Corning, Inc., Corning, NY, USA) and 0.05 mL culture medium into one inguinal mammary fat pad of eight-week-old NOD scid mice gamma (NOD.Cg-Prkdcscid Il2rgtm1Wjl/SzJ, NSG). Groups of five mice were used per dose of radiation, in each cell subpopulation which means a total of 30 mice. Tumour growth was assessed twice weekly using a digital calliper and the tumour volume was calculated by the formula $V=\text{length}^2 \times \text{width} \times \pi/6$. The mice were euthanized 120 days after injection and the tumours removed for analysis. A tumour was obtained from each mouse.

Animal experimentation was performed according to the protocols reviewed and approved by the Institutional Animal Care and Use Committee of the University of Granada (PI730/13). Detailed in Supplementary data.

8. HISTOLOGICAL ANALYSIS

Tumours of different conditions were fixed in 4% paraformaldehyde in 0.1 M PBS at 4ºC for 24h, washed in 0.1M PBS and dipped in paraffin in an automatic tissue

processor (TP1020, Leica, Germany). Paraffin blocks were cut into 4mm sections for later staining. Sections were deparaffinized with xylene and hydrated with decreasing alcohol concentrations (absolute to 75%), and stained with haematoxylin-eosin. Later, sections were dehydrated with increasing alcohol concentrations (75% to absolute), were cleared with xylene. The stained slides were mounted on coverslips with mounting medium. Observation samples with and digital image acquisition was carried out with an inverted microscope (Nikon H550s).

9. IMMUNOFLUORESCENCE ANALYSIS

For intracellular staining, paraffin blocks were permeabilized with 0.1 % Triton X-100 for 15 min, blocked for 1 h at room temperature with 5 % BSA, 5 % FBS in PBS and incubated with the primary antibody overnight at 4 °C. Primary antibodies used were: Vimentin Cruz Biotechnology. Next day, samples were washed thrice with PBS and incubated with the secondary antibodies (Alexa) for 1h at room temperature, after washing thrice with PBS and mounted with DAPI-containing mounting medium. Images were taken by confocal microscopy (Nikon Eclipse Ti-E A1, USA) and analysed using NIS-Elements software. Its immunofluorescence intensity was qualified using Image J software.

10. FUNCTIONAL ANNOTATION OF MIRNAS

We data mined relevant existing literature about the eight selected miRNAs in PubMed (https://www.ncbi.nlm.nih.gov/pubmed/) through the Entrez Direct (Kans, 2010) unix access to NCBI's suite of databases. The search was narrowed down to the

last 10 years. The articles retrieved were manually inspected and miRNAs functions were categorized according to known Cancer Hallmarks (Hanahan and Weinberg, 2011), radioresistance, and stemness. The obtained data were completed using pathway ((Fabregat *et al.*, 2017; Minoru Kanehisa and Susumu Goto, 2000), and Gene Ontology (Carbon *et al.*, 2017) annotation for the studied miRNAs. The resulting data were analysed using clustering, an unsupervised learning technique common for statistical data analysis, to group the obtained functional data into a specific group with similar properties and/or features. Analysis were performed using the Cluster Analysis Basics and Extensions for the R language (Maechler M, Rousseeuw P, Struyf A, Hubert M, 2018).

11. GENE EXPRESSION

11.1 RNA isolation

Total RNA from different conditions of the three breast cancer cell lines was extracted from duplicate 80% confluent cultures in monolayer culture and for ALDH1+ mammospheres cultures the RNA extraction was after 5 days. All extractions were executed 24 hours after irradiation doses.

Total RNA was obtained using trizol, Tri-Reagent following the instructions of the manufacturer (Sigma-Aldrich, St Louis, MO, USA). For this, we transfer cell suspension to a tube and centrifuge at 1500 rpm for 5 minutes to pellet cells. Carefully supernatant was decanted. Then 1 mL of trizol was added to the pellet and maintained at room temperature for 15 minutes. 200 µl of chloroform was added to the sample and the cells were vortexing. Subsequently, they were left 10 min at room temperature.

After this they were centrifuged 15 min at 12000 g at 4 ° C. The aqueous phase containing the RNA was transferred to a nuclease-free tube (Eppendorf Corp., Hamburg, Germany). To precipitate the RNA, 500 µl of isopropanol was added. The sample was vortexing and incubated at room temperature for 10 min. Then, the sample was centrifuged at 12000 g at 4 ° C for 10 min. Isopropanol was discarded and 1 ml of 75% ethanol was added. After vortexing, the sample was centrifuged at 12000 g for 5 min at 4 ° C, the ethanol was discarded and the sample was left at room temperature for the rest of the ethanol to evaporate and finally, 20-50 µL of water was added.

11.2 RNA Quantification

For quantification of RNA, we proceeded to the reading of the absorbance at 260 and 280 nm using a NanoDrop (NanoDrop ™ 2000/2000c Spectrophotometers, Thermo Scientific ™). The OD260/OD280 relationship allowed us to calculate the purity of nucleic acids, whereas an optimal range of values between 1.8 and 2. RNA concentration was calculated considering an OD unit at 260 nm corresponds to a concentration of 40 mg/ml nucleic acid. The purified RNA samples were placed at 80°C for long-term storage.

11.3 Reverse transcription

cDNA was synthesized by reverse transcription of total RNA for mRNA using the Reverse Transcription System (Promega, Madison, WI). The RNA was incubated at 70 ° C for 10 min and then kept on ice. The volume of each reaction was adjusted to 20

µl in each nuclease-free Eppendorf tube. For each reaction 1 µg of the extracted RNA was used and 4 µl of MgCl2, 2 µl of 10x buffer, 2 µl of the dNTPs mixture, 0.5 µl of the RNAs inhibitor, 15 U of the AMV enzyme and 0.5 were added µg of Oligo (dT) primers.

For miRNAs, miRCURY LNA TM Synthesis kit II (Exiqon, Vedbaek, Denmark) was used. For each reaction 4µL of 5x Reaction buffer, 2 µL enzyme mix and 4.5 µL of nuclease-free water mix was added and 2.5 µL of RNA extracted. The reaction was mixed pipetting all the reagents. The reverse transcriptase reaction was performed in a thermocycler (DOPPIO Thermal Cycler, VWR). The reaction tubes were heated at 42 ° C for 60 min and then the temperature rose to 95 ° C for 5 min. Finally, samples were kept on ice for 5 min, and the cDNA was stored at -20 ° C.

11.4 Quantitative real time RT-PCR

qRT-PCR assay was done using SYBR Green PCR Master Mix (Promega, Madison, WI) for mRNAs and miRCURY LNA TM EXILENT SYBR Green (Exiqon, Vedbaek, Denmark) for miRNAs. Each experiment was done in duplicate and reactions were performed in triplicate. The comparative threshold cycle (Ct) method was used to calculate the amplification factor as specified by the manufacturer ABI 7500 (Applied Biosystems, Inc.). The process steps for qPCR was 95℃, 10 min to polymerase activation/denaturation, 40 amplification cycles at 95℃, 10 seconds and 60℃ 1 min. Mel-curve 30 min to 60

For mRNAs, human GAPDH was used as an internal standard to normalize and hsa-miR-24-3p, RNU6 and hsa-miR-425-5p for miRNAs. The amount of target and endogenous reference were determined from a standard curve for each experimental sample. Primer sequences are listed in Table 4 (mRNAs) and Table 5 (miRNAs).

Table 4: Primer sequences used to qRT-PCR for mRNAs

Gene	Primer Sequence	
NANOG	Forward	5´ TCCTGAACCTCAGCTACAAAC 3´
	Reverse	5´ GCGTCACACCATTGCTATTC 3´
SOX2	Forward	5´ GGAGCTTTGCAGGAAGTTTG 3´
	Reverse	5´ GGAAAGTTGGGATCGAACAA 3´
OCT4	Forward	5´ CACCATCTGTCGCTTCGAGG 3´
	Reverse	5´ AGGGTCTCCGATTGCATATCT 3´
E-CADHERIN	Forward	5´ AATTCCTGCCATTCTGGGGA 3´
	Reverse	5´ TCTTCTCCGCCTCCTTCTTC 3´
N-CADHERIN	Forward	5´ TGAGCCTGAAGCCAACCTTA 3´
	Reverse	5´ AGGTCCCCTGGAGTTTTCTG 3´
VIMENTIN	Forward	5´ AGCTAACCAACGACAAAGCC 3´
	Reverse	5´ TCCACTTTGCGTTCAAGGTC 3´

Table 5. Primer sequences used to qRT-PCR for miRNAs

miRNA	Mature sequence
hsa-miR-210-3p	CUGUGCGUGUGACAGCGGCUGA
hsa-miR-10b-5p	UACCCUGUAGAACCGAAUUUGUG
hsa-miR-182-3p	UGGUUCUAGACUUGCCAACUA
hsa-miR-142-3p	UGUAGUGUUUCCUACUUUAUGGA
hsa-miR-221-3p	AGCUACAUUGUCUGCUGGGUUUC
hsa-miR-21-3p	CAACACCAGUCGAUGGGCUGU
hsa-miR-93-5p	CAAAGUGCUGUUCGUGCAGGUAG
hsa-miR-15b-5p	UAGCAGCACAUCAUGGUUUACA
hsa-miR-24-3p	UGGCUCAGUUCAGCAGGAACAG
hsa-miR-425-5p	AAUGACACGAUCACUCCCGUUGA

12. PATIENTS

Blood serum samples obtained from 20 women with BC were collected and analysed for miRNA detection using q-PCR. These patients were treated with either

hypofractionated RT (16 fractions, 2.65Gy/fraction) or conventional RT (25 fractions, 2Gy/fraction). Three blood samples were collected from each patient at different times of the treatment, obtaining a total of 60 samples. First samples were taken approximately 1 week before the start of the RT; second samples were taken during the RT (depending on RT regimen received, 8 or 11 days after the start of the treatment); and third samples were taken on the last day of treatment. This study was approved by the corresponding ethical committee associated with grants PI-730 and PIE16-00045. Written informed consent was obtained from all the patients involved in this study.

13. STATISTICAL ANALYSIS

All statistical tests were performed with the statistical Package for the IBM-SPSS Statistics Ver.21.0. Variables with normal distribution were expressed as mean ± SEM. For quantitative variables, when two groups when compared, we used t-Student test (parametric) in a case of normality, or U Mann-Whitney test (non-parametric) for non-normal. For comparisons between multiple means, non-parametric tests of Kruskal-Wallis were used. Differences were considered statistically significant at $p<0.05$ level. Data charts were carried out using Microsoft® Excel and R Statistical Computing Environment 3.4.

RESULTS

1. EFFECT OF IONIZING RADIATION IN STEMNESS PROPERTIES

1.1 Breast CSCs surface markers increase after specific IR

The three BC cell lines grown in monolayer or ALDH1+ mammospheres were treated with 2, 4 or 6 Gy and twenty-four hours later, cells were characterized using specific BCSCs surface markers (ALDH1 activity and CD44^{+}/CD24$^{-/low}$ expression) and results were compared with sham-irradiated control cells (0 Gy).

In MDA-MB-231 monolayer, ALDH1 expression was similar at different IR doses, while CD44^{+}/CD24$^{-/low}$ expression was significantly higher at 2 Gy (*p<0.05). ALDH1 activity in mammospheres significantly decreased in all doses showing 4 Gy and 6 Gy a significant lower ALDH1 activity (##p<0.01) in comparison to 2 Gy (*p<0.05); however, CD44^{+}/CD24$^{-/low}$ expression was higher in all IR doses being more significant in 4 Gy and 6 Gy (Figure 23).
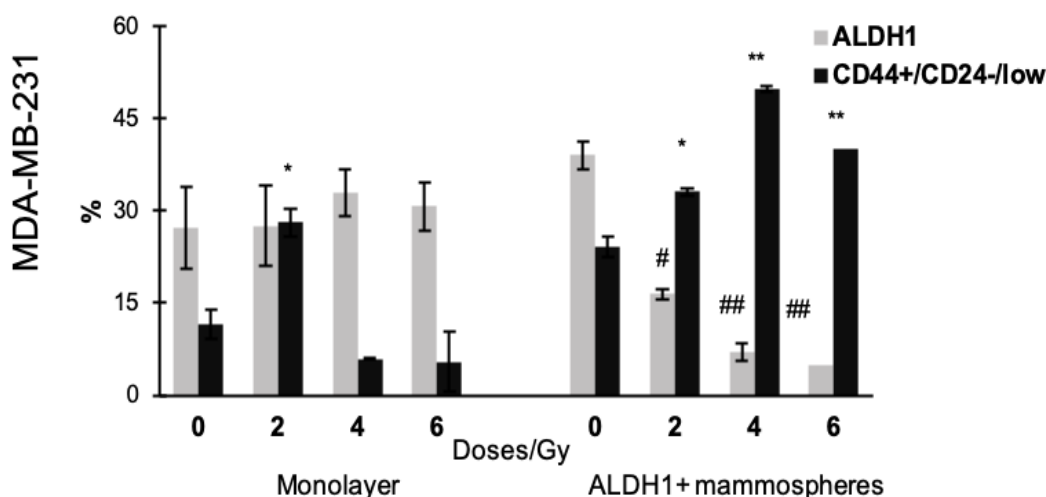

Figure 23: Variation in percentage of ALDH1 and CD44^{+}/CD24$^{-/low}$ surface markers in comparison to control non-treated cells (0 Gy) determined in both monolayer and mammospheres cultures of MDA-MB-231 cancer cell line measured by flow cytometry. Data are graphed as mean ± SEM (#p < 0.05 or ##p <0.01 for ALDH1 expression) (**p<0.01; *p<0.05).

In MCF7 (Figure 24) monolayer cells, ALDH1 activity and CD44$^+$/CD24$^{-/low}$ expression were significantly decreased at 4 Gy and 6 Gy doses (#p<0.05) (*p<0.05), and increased at 2 Gy. On the other hand, ALDH1+mammospheres showed lower ALDH1 activity (##p<0.01) in all different IR doses, and in CD44$^+$/CD24$^{-/low}$ expression we also observed similar behaviour that in monolayer, showing a significantly decreased (*p<0.05) at 4 Gy and 6 Gy doses.
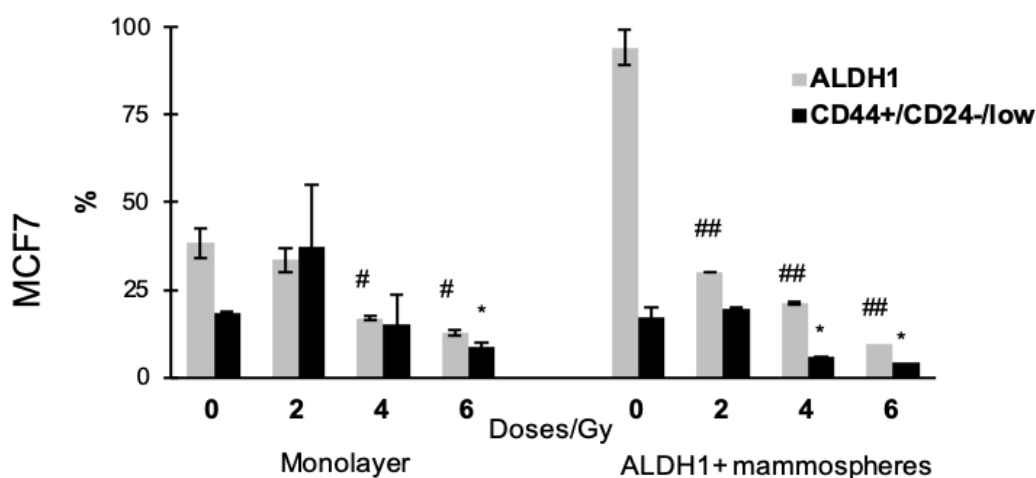
Figure 24: Variation in percentage of ALDH1 and CD44$^+$/CD24$^{-/low}$ in comparison to control non-treated cells (0 Gy) determined in both monolayer and mammospheres cultures of MCF7 cancer cell line measured by flow cytometry. Data are graphed as mean ± SEM *(#p < 0.05 or ##p <0.01 for ALDH1 expression) (*p<0.05)*.

Figure 25 shows an important decrease of ALDH1 activity in both subpopulations of the SKBR3 cell line for all IR doses used, being very significative (##p<0.01) for 4 Gy and 6 Gy. In monolayer CD44$^+$/CD24$^{-/low}$ expression was lower than control cells in all different IR doses being more significant for 6 Gy (*p<0.05). Moreover, a significant decrease of CD44$^+$/CD24$^{-/low}$ expression was observed after irradiation at 2 and 6 Gy in ALDH1+ mammospheres. These data suggest that the stemness phenotype is differentially modulated depending on IR doses and molecular profile.
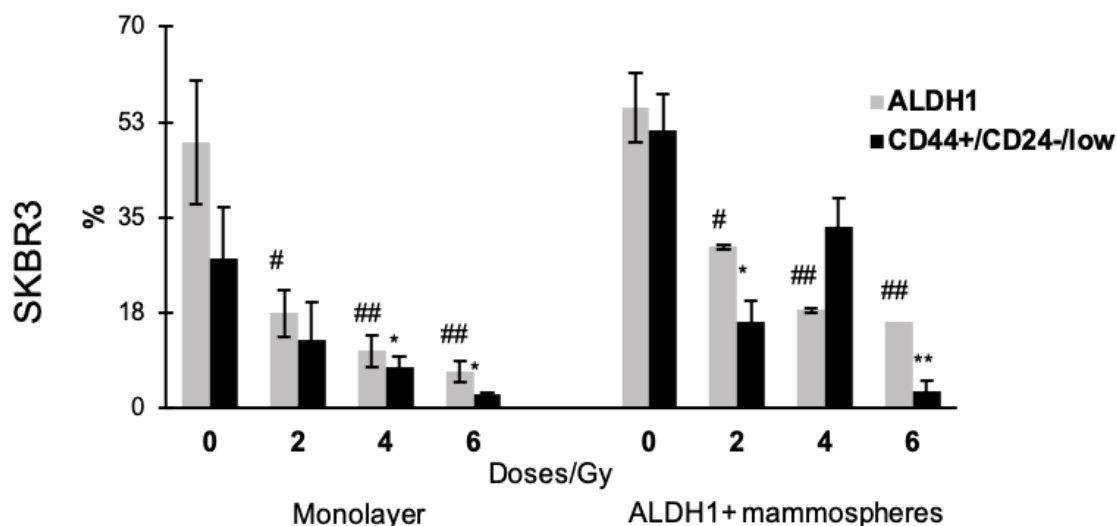
Figure 25: Variation of percentage of ALDH1 and CD44$^+$/CD24$^{-/low}$ in comparison to control non-treated cells (0 Gy) determined in both monolayer and mammospheres cultures of SKBR3 cancer cell line measured by flow cytometry. Data are graphed as mean ± SEM (#p < 0.05 or ##p <0.01 for ALDH1 expression) (*p<0.05).

In general terms, the expression level of ALDH1 decreased with IR dose in the cell lines in both culture models. In contrast, the expression of CD44$^+$/CD24$^{-/low}$ increased with IR doses in MDA-MB-231 triple negative BC.

1.2. Effects of IR on self-renewal ability and clonogenicity in ALDH1+ mammospheres

To study the effect of IR doses on BCSC functional characteristics, both mammosphere formation and clonogenicity capacity of ALDH1+ mammospheres were analysed.

As is shown in Figures 26 and 27, the mammosphere number was higher at 4 Gy (**p<0.01) in MDA-MB-231 cell line, and at 2 Gy in MCF7 cell line, compared to respective controls. In contrast, SKBR3 showed a minor mammosphere formation ability for all different IR doses. Interestingly, a statistically significant inhibition of

secondary mammosphere formation was found at 6 Gy in MDA-MB-231 (**p<0.01),

MCF7 (*p<0.05) and SKBR3 (*p<0.05) cell lines.

Figure 26: Secondary spheres number for each cell line after IR (**p<0.01 *p<0.05*)

Figure 27: Representative images of MDA-MB 231, MCF7 and SKBR3 ADLH1+
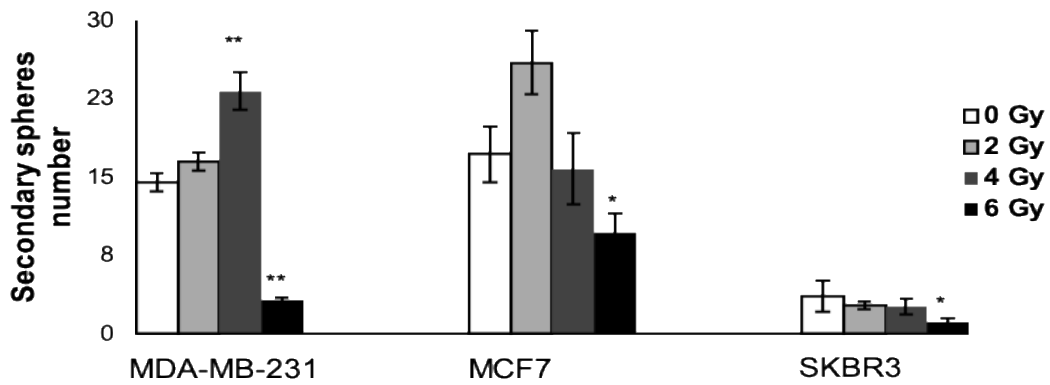
mammospheres formed after different IR doses. Scale bar = 100 μm.
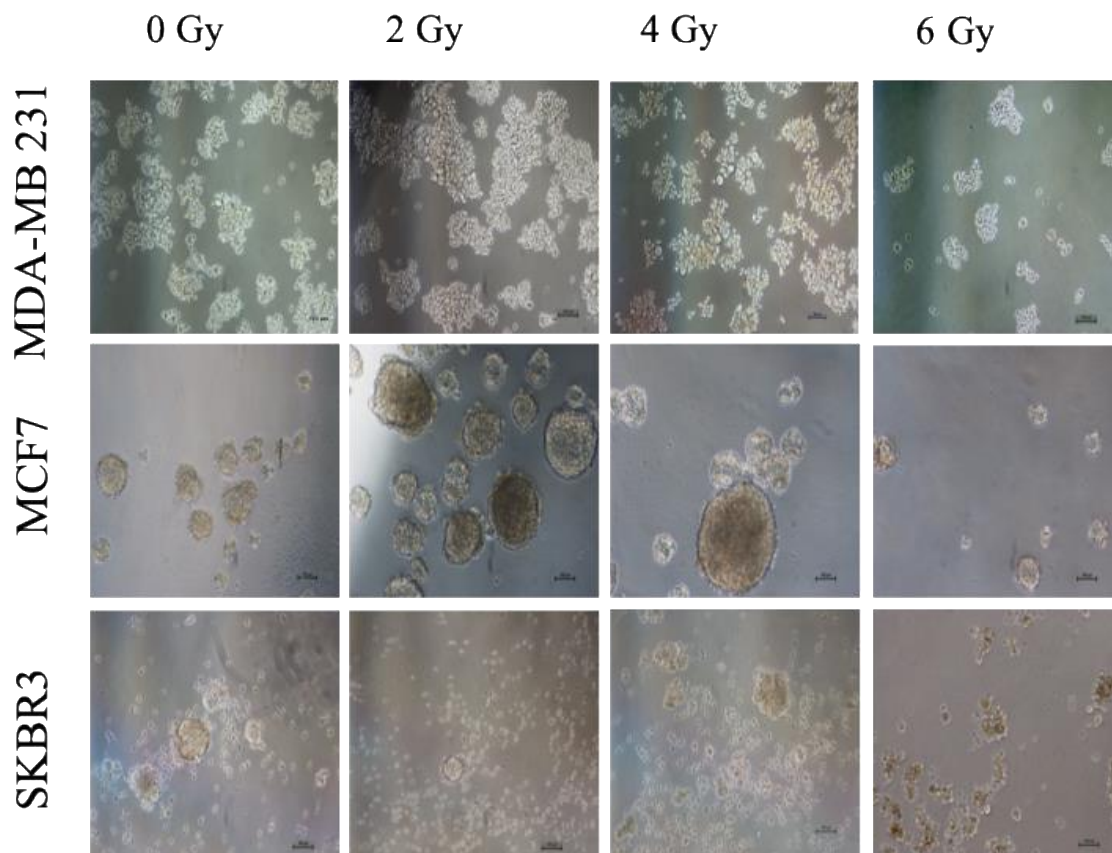
In concordance with these results, 6 Gy irradiated cells showed a lower capacity to form colonies in soft agar in comparison to 0 Gy cells (*p<0.05). Also, 4 Gy significantly decreased clonogenicity in Her2+ BC cells (*p<0.05) (Figures 28 and 29).
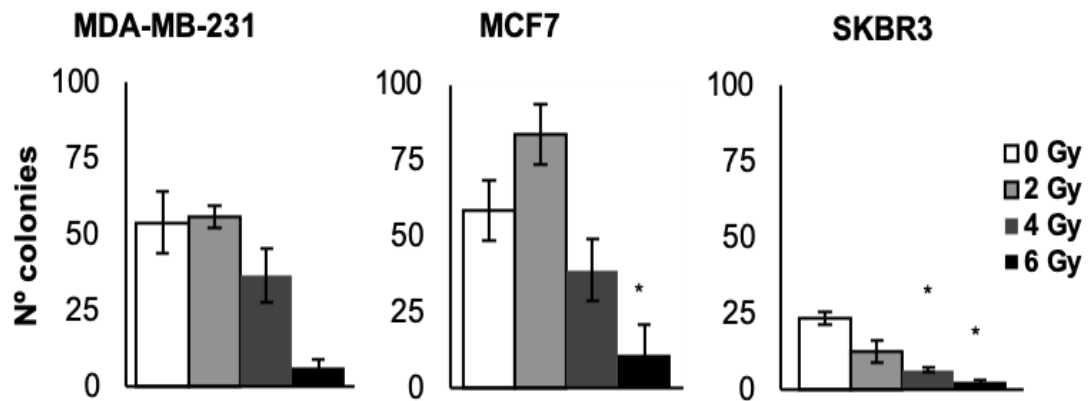
Figure 28: Colony-forming ability of BC cell lines after IR. Data are graphed as mean ± SEM (*p<0.05*).
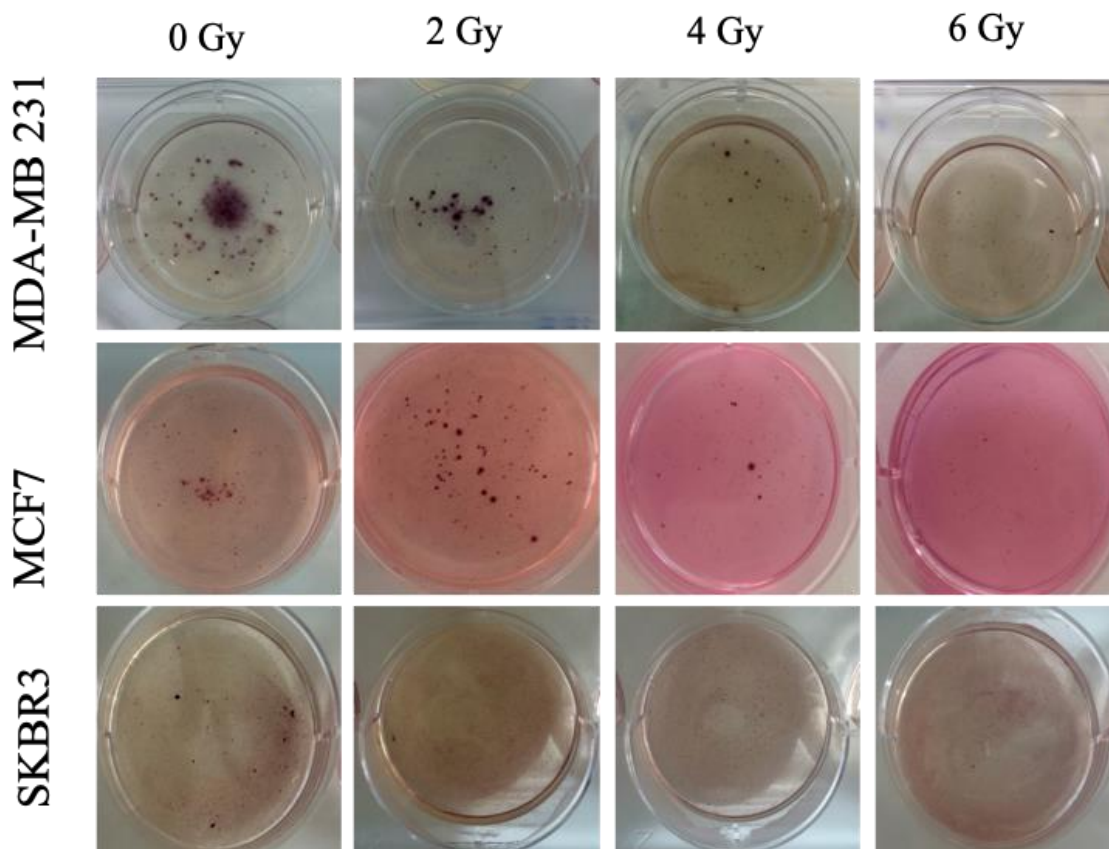
Figure 29: Representative images of colonies formed in MDA-MB 231, MCF7 and SKBR3 ADLH1+ cells after different IR doses.

These data suggest that in MDA-MB-231 and MCF7 cell lines 2 Gy was the most efficient dose in maintaining stemness properties; however, SKBR3 cell line lost the majority of these properties after receiving IR.

2. EFFECTS OF IONIZING RADIATION IN PROLIFERATION RATES

We compared the proliferation rate in monolayer and ALDH1+ mammospheres subpopulation between the three BC cell lines after treatment with different IR doses during a period of four days (Figure 30).

In MDA-MB-231 cells cultured in monolayer we observed that sham-irradiated (0 Gy) cells had a major growth rate in comparison to the different IR doses (2, 4 and 6 Gy), whose behaviour showed higher to lower growth as we increased the IR doses respectively. However, in ALDH1+ mammospheres not differences in the proliferation were observed between IR doses and they had a very low growth rates when compared to monolayer ones.

MCF7 cell line monolayer showed a great increase in proliferation at 0 and 4 Gy doses after 24 hours, but finally, measures performed at 96 hours showed that cells of 0 Gy group grew more compared to the other IR dose groups. In ALDH1+ BCSCs, we observed that cell proliferation rates were very low for all radiation doses in comparison to cells cultured as monolayers.

Finally, in SKBR3 cell line growth as monolayer 2 Gy induced an increase in proliferation respect to the other groups, being 6 Gy the dosage that decreased the proliferation rate up to the day 4. Similarly, to the rest of cancer cell lines ALDH1+

mammospheres displayed a low growth rate compared to monolayer cells, showing no differences between the IR doses.

In general, proliferation assay demonstrated that ALDH1+ mammospheres cultures had a lower growth rate than monolayer cultures, and that IR has not influence on cell growth in the three BC cell lines analysed. However, in monolayer cultures each molecular subtype of BC showed differences for certain IR doses.
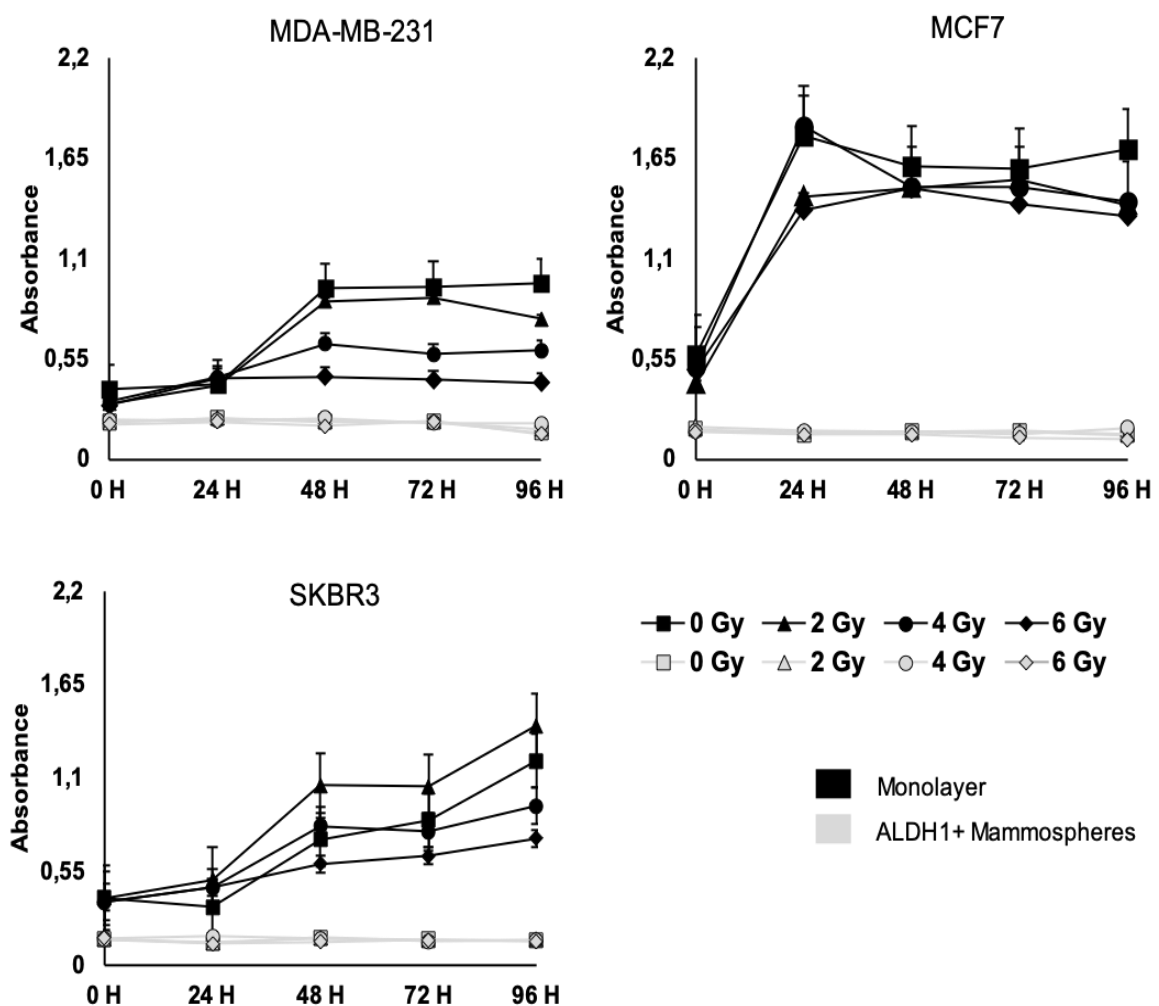
Figure 30: Proliferation rates of MDA-MB 231, MCF7 and SKBR3 for both monolayer and ALDH1+ mammospheres cell cultures after treatment with different doses of IR during 4 days. Data are graphed as mean ± SEM.

3. APOPTOSIS

To study inherent radioresistance of the generated cell subtypes we measured apoptotic rates after 24 h of irradiation in monolayer and ALDH1+ mammospheres subpopulations.

MDA-MB-231 monolayer cell cultures showed high levels of apoptosis at 2, 4 and 6 Gy than control non-treated cells, being this increase statistically significant for 6 Gy (68,85%). On the other hand, in BCSCs apoptosis levels were lower (minor 20%) for all IR doses (Figure 31, Table 6).

Table 6: Percentage of apoptosis in MDA-MB-231 cell line after IR.

IR doses	% Apoptosis MDA-MB-231	
	Monolayer	**ALDH1+ mammospheres**
0 Gy	45,5	8,4
2 Gy	74,05	6,95
4 Gy	57,45	9,3
6 Gy	68,85	13,4
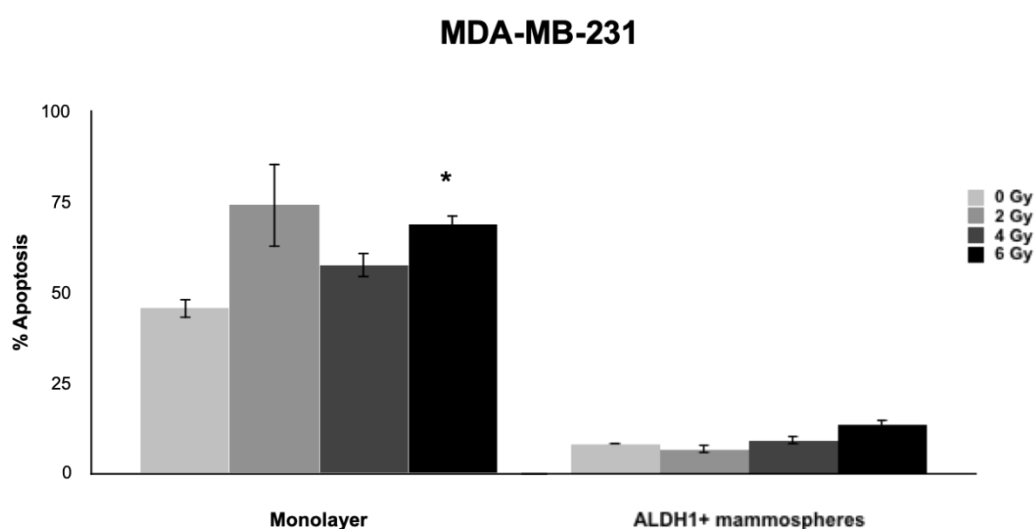
Figure 31: Values of apoptosis (%) at 0, 2, 4 and 6 Gy measured 24 h after treatment in MDA-MB-231 cell line grown as monolayer and in ALDH+1 mammospheres subpopulation cultures. Values are expressed as the mean ± SEM; * $p < 0.01$.

In MCF7 monolayer, 4 and 6 Gy IR doses showed high percentage of apoptosis (89,8 and 91,25% respectively) both were very significant $p<0.0001$ when we compared with control. ALDH1+ mammospheres apoptosis was lower than monolayer, only mammospheres irradiated at 2 Gy had a higher apoptosis and significant respect control non-irradiated (Figure 32, Table 7).

Table 7: Percentage of apoptosis in MCF7 cell line after IR.

IR doses	% Apoptosis MCF7	
	Monolayer	**ALDH1+ mammospheres**
0 Gy	4,25	11,15
2 Gy	24,4	16,15
4 Gy	89,8	12,6
6 Gy	91,25	13,65
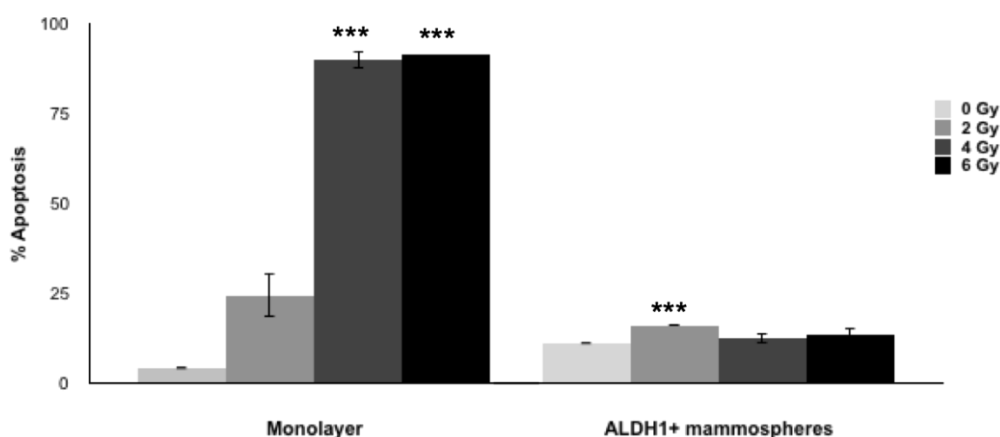
Figure 32: Values of apoptosis (%) at 0, 2, 4 and 6 Gy measured 24 h after treatment in MCF7 cell line grown as monolayer and in ALDH+1 mammospheres subpopulation cultures. Values are expressed as the mean ± SEM; *** $p < 0.0001$.

In SKBR3 cell line (Figure 33, Table 8), we observed a very different result in monolayer than the other two BC cell lines studied. So, 2 and 6 Gy induced high

apoptosis levels but any irradiated group exceeded 16 % of apoptosis. Similarly, ALDH1+ mammospheres apoptosis were lower, and only BCSCs irradiated at 2 Gy and 4 Gy displayed a percentage of apoptosis higher than 20 %, with significant *p-values* *0.0001* and *0.001* respectively.

Table 8: Percentage of apoptosis assay in SKBR3 cell line after IR.

| IR doses	% Apoptosis SKBR3	
	Monolayer	**ALDH1+ mammospheres**
0 Gy	7,15	4,15
2 Gy	16,1	38,45
4 Gy	6,05	23,65
6 Gy	11,15	19,25
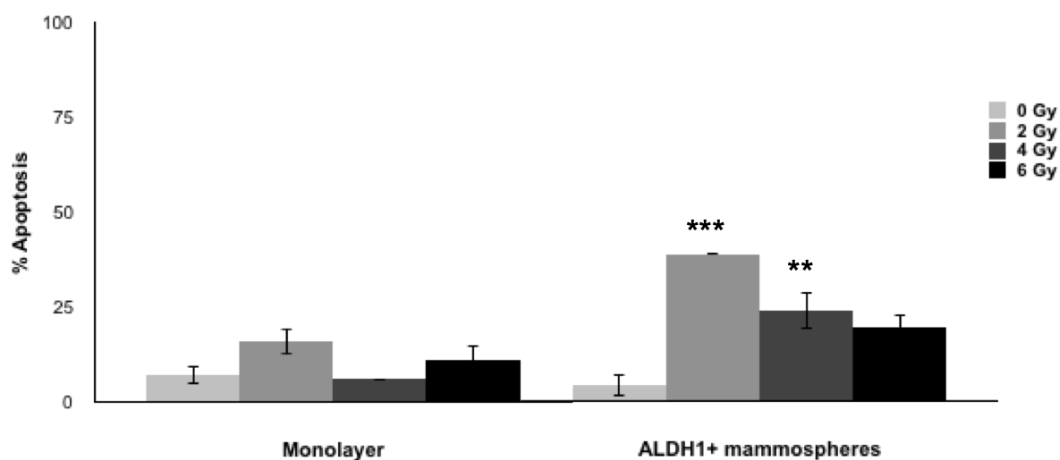
Figure 33: Values of apoptosis (%) at 0, 2, 4 and 6 Gy measured 24 h after treatment in SKB3 cell line grown as monolayer and in ALDH+1 mammospheres subpopulation cultures. Values are expressed as the mean ± SEM; ** $p < 0.001$ and *** $p < 0.0001$.

In general, our results showed that BCSCs subpopulation in MDA-MB-231 and MCF7 were more radioresistant (low levels of radio-induced apoptosis) than in monolayer (high rate of radio-induced apoptosis); however, SKBR3 BCSCs, were more radiosensitive than monolayer culture (high rate of radio-induced apoptosis).

4. EXPRESSION OF PLURIPOTENCY AND EMT-RELATED GENES IN BC CELL LINES AFTER IONIZING RADIATION

Real time RT-PCR analysis was used to quantify the effect of IR in the expression of specific transcription factors that promote stemness properties and those related to EMT process.

Triple negative MDA-MB-231 cells cultured in monolayer (Figure 34) and treated with 2 Gy and 6 Gy showed a significant lower expression of *NANOG* (**$p<0.01$). Similarly, all irradiation doses decreased *OCT4* expression, being significant for 4 Gy and 6 Gy (*$p<0.05$), and only 2 Gy was able to decrease *SOX2* expression (**$p<0.01$). In contrast, 4 Gy was the unique dosage that significantly increased *NANOG* (*$p<0.05$) expression. In ALDH1+ mammospheres, 6 Gy significantly incremented *SOX2* and *OCT4* expression (*$p<0.05$). Regarding to EMT, we observed that *VIMENTIN* decreased in all radiation doses in monolayer cells being statistically significant for 2 and 6 Gy (*$p<0.05$), while in mammospheres occurred a significant increment of expression for 2 Gy and 4 Gy respectively (*$p<0.05$ and **$p<0.01$). In monolayer, *E-CADHERIN* and *N-CADHERIN* expression increased for 2 Gy (**$p<0.01$ and *$p<0.05$); however, this expression significantly decreased with 6 Gy (*$p<0.05$) for both genes and with 4 Gy (*$p<0.05$) for *N-CADHERIN*. In, ALDH1+ mammospheres, occurred similar behaviour than in monolayer for *N-CADHERIN*; however, *E-CADHERIN* decreased with all doses being more significant for 6 Gy (*$p<0.05$).

MDA-MB 231
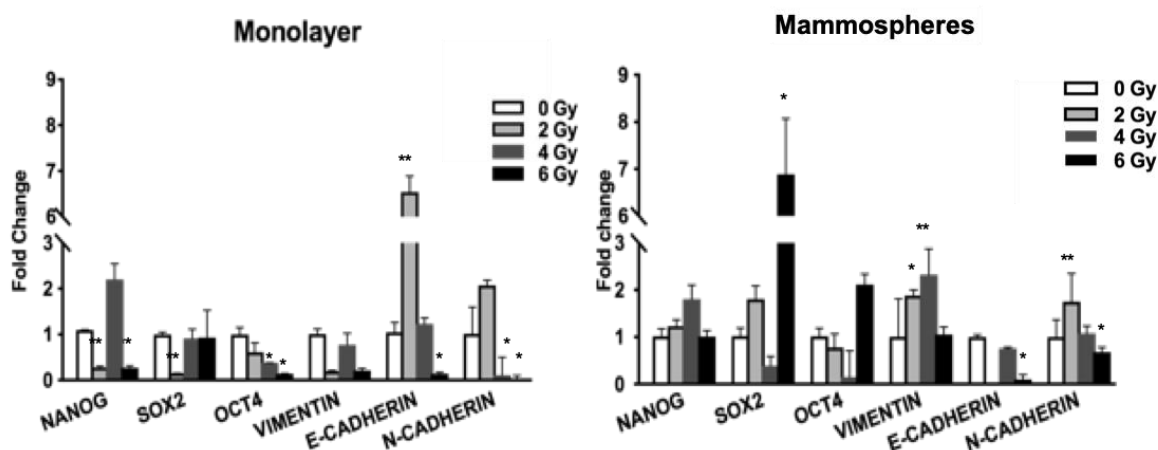
Figure 34: qRT-PCR analysis of pluripotency and EMT-related genes in monolayer and mammospheres after treatment with 0 Gy, 2 Gy, 4 Gy and 6 Gy in MDA-MB-231. The statistical comparison was 0 Gy versus 2, 4 and 6 Gy respectively. Data are normalized to 1 for 0 Gy using GAPDH as internal control, and graphed as mean ± SEM *p < 0.05* and **p < 0.01*.

Hormone receptors positive MCF7 cells grown in monolayer displayed lower expression (*p<0.05) for *NANOG* and *SOX2* after the exposition to 2 Gy and 4 Gy, but 6 Gy significantly increased the expression of both *NANOG* and *OCT4* (*p<0.05) genes and, also, 4 Gy was able to augment *OCT4* expression (*p<0.05). Similarly, in ALDH1+ mammospheres the expression of *NANOG* and *SOX2* decreased for 2 Gy and 4 Gy; however, conversely to cells grown in monolayer, *OCT4* expression significantly increased with 2 Gy and decreased with 4 Gy and 6 Gy (*p<0.05) (Figure 35). In the case of EMT-related genes, for monolayer cultures *VIMENTIN* was overexpressed at 2 Gy and 4 Gy and downregulated at 6 Gy (**p<0.01); *E-CADHERIN* and *N-CADHERIN* showed a higher increment for 4 (*p<0.05) and 6 Gy and decreased for 2 Gy; however, in ALDH1+ mammospheres *E-CADHERIN* was non-detected, *VIMENTIN* was downregulated with 2 Gy and 4 Gy (*p<0.05) and *N-CADHERIN* significantly (*p<0.05) decreased for every dose of radiation (Figure 35).
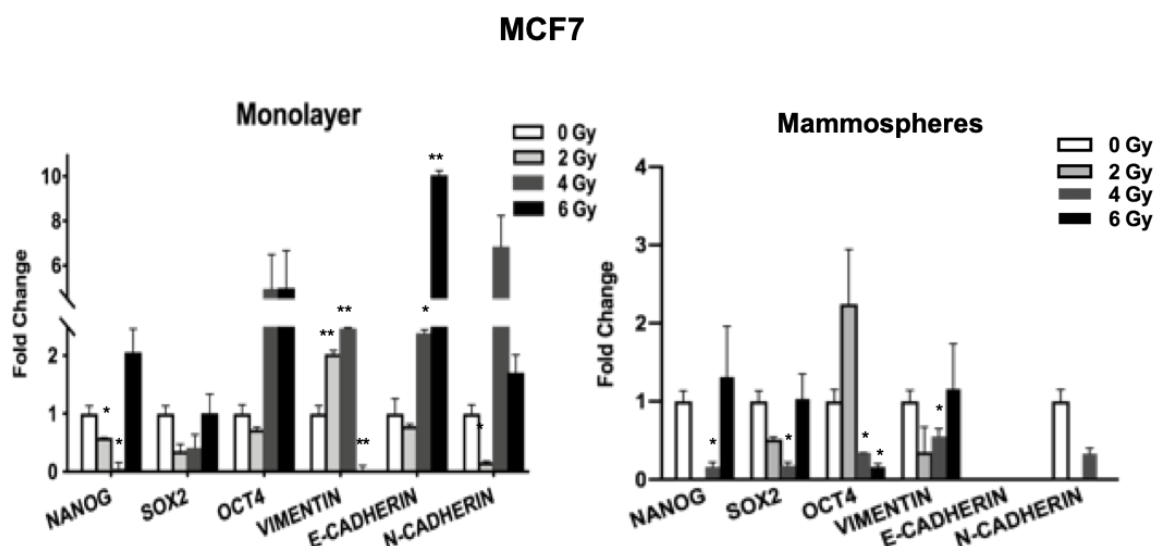
Figure 35: qRT-PCR analysis of pluripotency and EMT-related genes in monolayer and mammospheres after treatment with 0 Gy, 2 Gy, 4 Gy and 6 Gy in MCF7. The statistical comparison was 0 Gy versus 2, 4 and 6 Gy. Data are normalized to 1 for 0 Gy using GAPDH as internal control, and graphed as mean ± SEM *$p < 0.05$ and **$p < 0.01$.

Finally, HER2+ SKBR3 cells grown in monolayer showed higher expression for *NANOG* and *SOX2* after the treatment with 4Gy (**$p<0.01$), *OCT4* expression increased in all doses used (*$p<0.05$) and only 2 Gy reduced expression level of *NANOG* (**$p<0.01$) (Figure 36). However, in ALDH1+ mammospheres gene expression was lower compared to monolayer, being significantly for *OCT4* at 2 Gy (**$p<0.01$) and increasing for *NANOG* (*$p<0.05$) (Figure 36). Regarding to EMT-genes in monolayer cultures, *N-CADHERIN* displayed lower expression than control in all doses and *E-CADHERIN* for 4 Gy and 6 Gy; however, only *VIMENTIN* showed higher expression for 4 and 6 Gy (*$p<0.05$). In contrast, in ALDH1+ mammospheres *VIMENTIN* expression significantly decreased (**$p<0.01$) for 2 Gy and 4 Gy, *E-CADHERIN* decreased for all dosed and *N-CADHERIN* increased (**$p<0.01$) for 2 Gy and decreased for 6 Gy (**$p<0.01$).
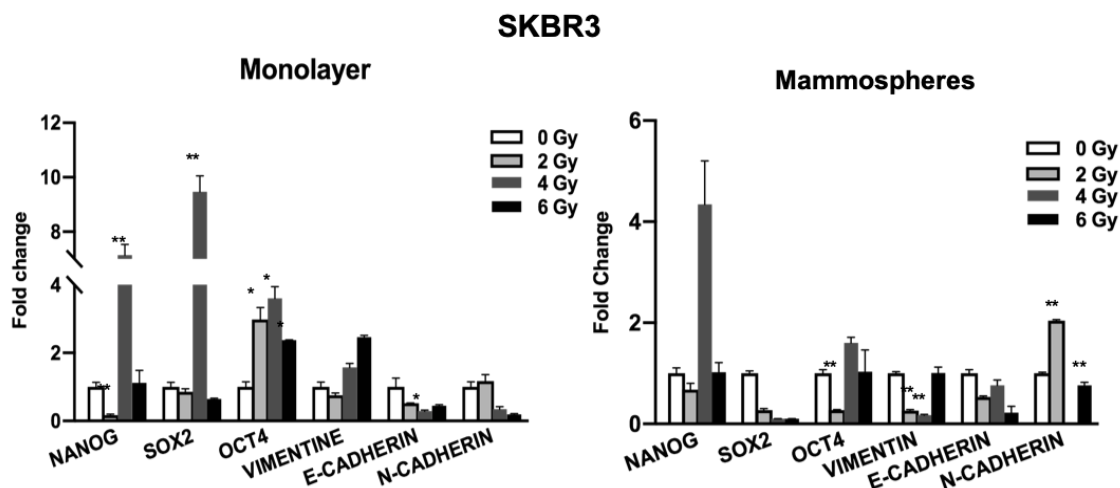
Figure 36: qRT-PCR analysis of pluripotency and EMT-related genes in monolayer and mammospheres after treatment with 0 Gy, 2 Gy, 4 Gy and 6 Gy in SKBR3. The statistical comparison was 0 Gy versus 2, 4 and 6 Gy. Data are normalized to 1 for 0 Gy using GAPDH as internal control, and graphed as mean ± SEM *p < 0.05* and **p < 0.01*.

5. *IN VIVO* ANALYSIS OF TUMORIGENIC CAPACITY OF BREAST CANCER CELL LINE MDA-MB-231 AFTER IRRADIATION

Triple negative MDA-MB-231 irradiated cells (2, 4 and 6 Gy) grown in monolayer and ALDH1+ mammospheres were orthotopically injected into the mammary gland of female NSG mice and were compared with sham-irradiated cells (0 Gy).

As it is shown in Figures 37 and 38, tumours generated by non-treated cells grown in monolayer displayed higher volume than those generated after inoculation of irradiated cells, and tumours emerged 28 days after the injection. In contrast, 6 Gy irradiated cells developed the tumour 58 days after the injection and the evolution of tumour size showed a dose-dependent reduced growth being 6 Gy the dose that significantly (**p<0.01) inhibited tumorigenicity (90%).
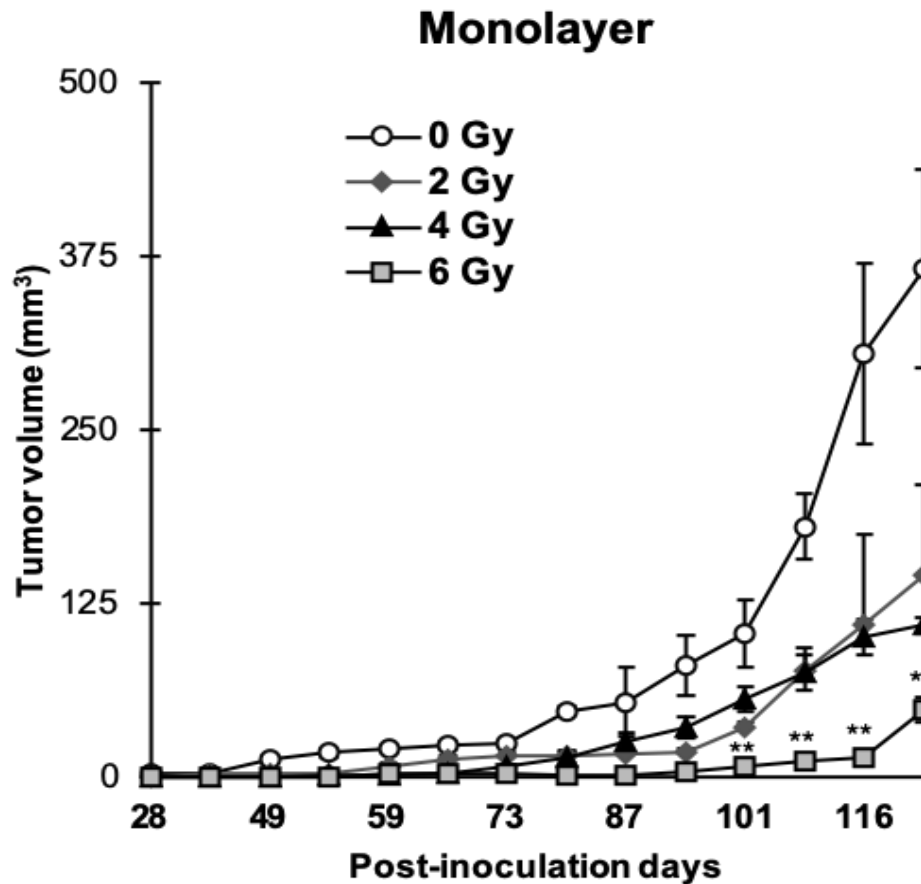
Monolayer

Figure 37: Tumour volume of orthotopic xenograft mammary gland tumours developed in NSG mice after inoculation of cell cultured as monolayers and irradiated at 0 Gy, 2 Gy, 4 Gy and 6 Gy, respectively. Data are shown as mean ± SEM. Statistical Student's test analysis comparing IR doses vs 0 Gy *(**p <0.01; *p <0.05)*.

In the case of ALDH1+ mammospheres, tumours appeared 28 days after the injection in all groups. 0 Gy and 4 Gy showed an increased growth rate although no differences were found between them. However, treatments with 2 Gy and 6 Gy significantly decreased tumour growth, being 6 Gy the dosage that generated significantly lower volume tumours (*p<0.05) (Figures 37 and 38). These results could suggest that 6 Gy is a dose that negatively affects tumour growth inhibiting BCSCs tumorigenic *in vivo* ability.

ALDH1+ mammospheres
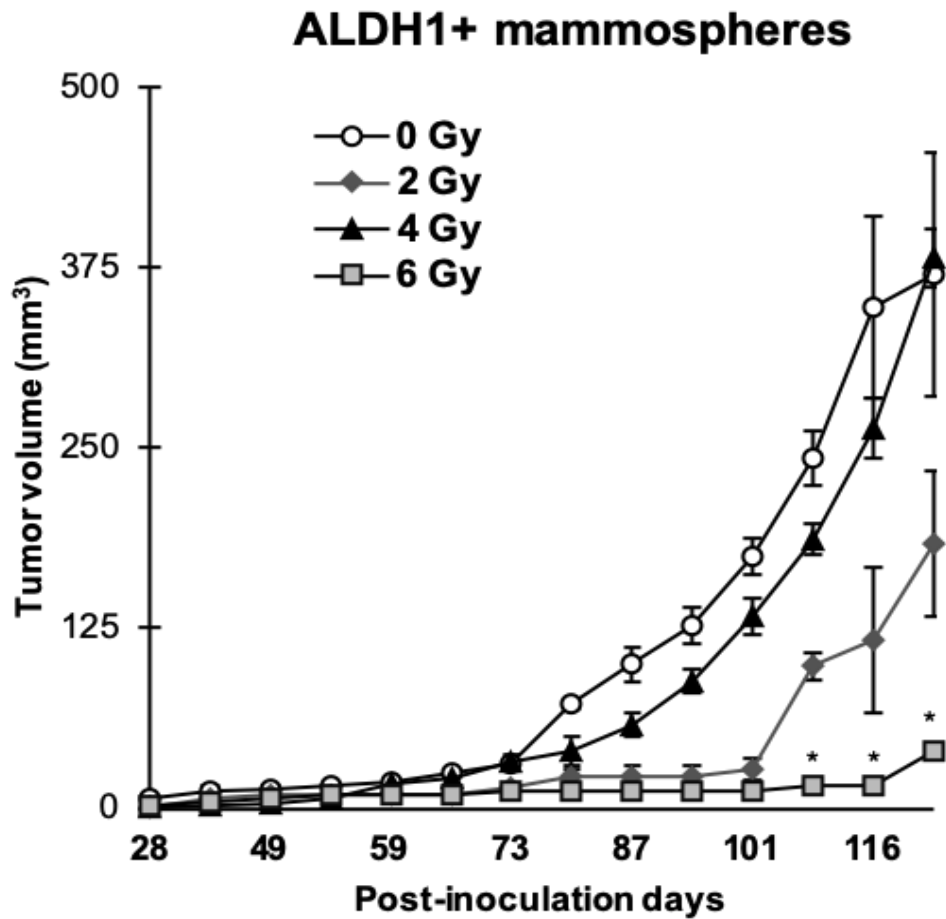
Figure 38: Tumour volume of orthotopic xenograft mammary gland tumours developed in NSG mice after inoculation of ALDH1+ cells grown as mammopheres and irradiated at 0 Gy, 2 Gy, 4 Gy and 6 Gy, respectively. Data are shown as mean ± SEM. Statistical Student's test analysis comparing IR doses vs 0 Gy *(**p <0.01; *p <0.05)*.
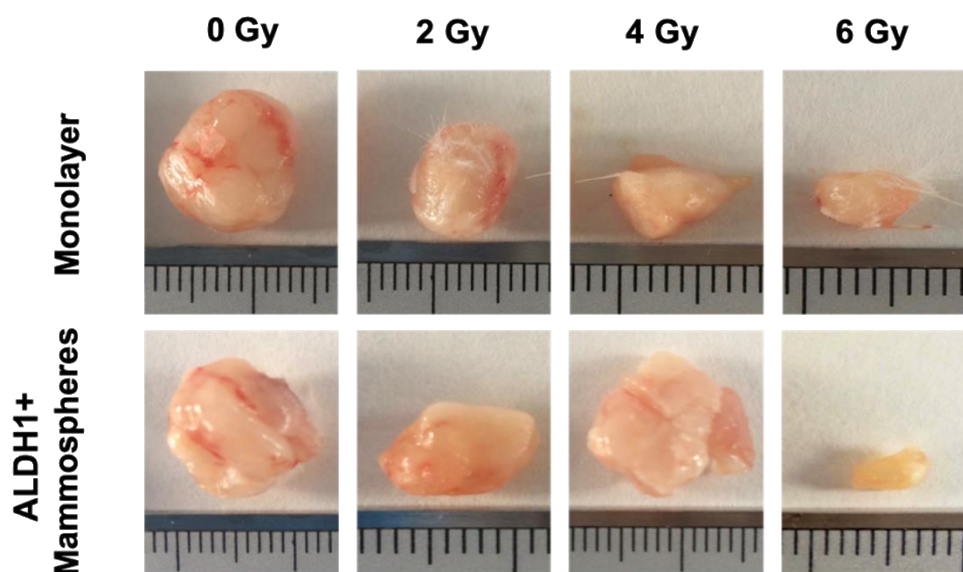
Figure 39: Size of tumours developed in NSG mice after inoculation of cell irradiated at 0 Gy, 2 Gy, 4 Gy and 6 Gy in orthotopic xenograft mammary glands.

After 123 days, animals were sacrificed and tumours extirpated for further analysis. Histological H&E staining of tumours (Figure 40) showed lower cellularity in
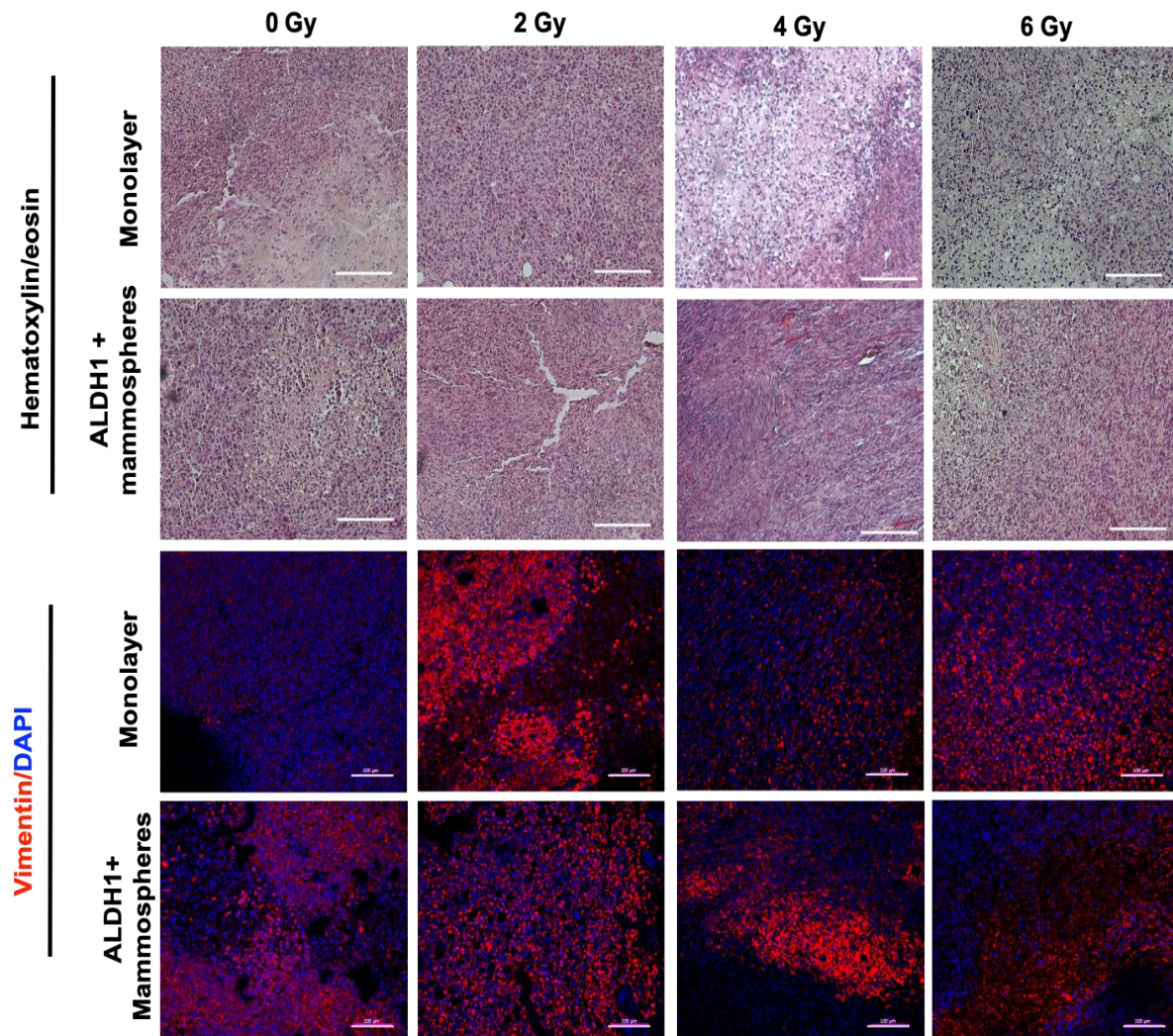
tumours generated with cells previously treated with 6 Gy.

Figure 40. A) Representative images of haematoxylin/eosin staining in MDA-MB-231 TNBC irradiated cells obtained from mice tumours. Original magnification: 20X. Scale bar = 100 μm. B) Representative immunofluorescence images for *vimentin* of xenograft tumours generated by injection of cells grown in monolayer and as mammospheres previously treated with 0, 2, 4 and 6 Gy. Samples were obtained after 123 days of inoculation. Original magnification: 20x. Scale bar = 100 μm

Tissue sections from tumours induced with both populations and after treatment with different doses of IR were immunostained to detect the expression of the vimentin EMT marker. Results showed significantly higher level of this marker in monolayer cells irradiated at 2 Gy (*p<0.05) compared to untreated control tumours (0 Gy). In contrast, in ALDH1+ mammospheres group, untreated, 2 Gy and 4 Gy irradiated cells showed a high expression of vimentin; however, cells irradiated at 6 Gy displayed a
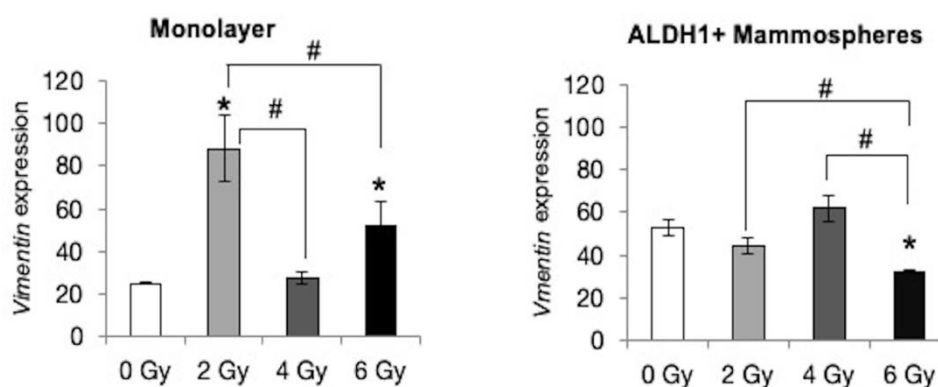
significant decrease in this EMT marker, even with a lesser level than in 6 Gy monolayer treated-cells (*p<0.05) (Figure 41).

Figure 41: Quantification of the fluorescence intensities. The average fluorescence intensities were calculated from three parallel immunofluorescence images. Data represents means ± SD (n = 3), *p < 0.05 (#p < 0.05 for comparison between doses).

6. EFFECTS OF IONIZING RADIATION ON SELECTED miRNAS.

To study the effect of IR on miRNA expression we selected the following miRNAs implicated in functions according to known Cancer Hallmarks (Hanahan and Weinberg, 2011), radioresistance, and stemness (Figure 42): *hsa*-miR-21-3p, *hsa*-miR-210-3p, *hsa*-miR-221-3p, *hsa*-miR-15b-5p, *hsa*-miR-182-5p, *hsa*-miR-10b-5p, *hsa*-miR-142-3p and *hsa*-miR-93-5p. These miRNAs were differently expressed depending on the tumour cell line studied. In general, MDA-MB-231 and MCF7 cells showed a

greater miRNA expression in mammospheres than SKBR3 cell line (Figures 43-45; tables 9-14).
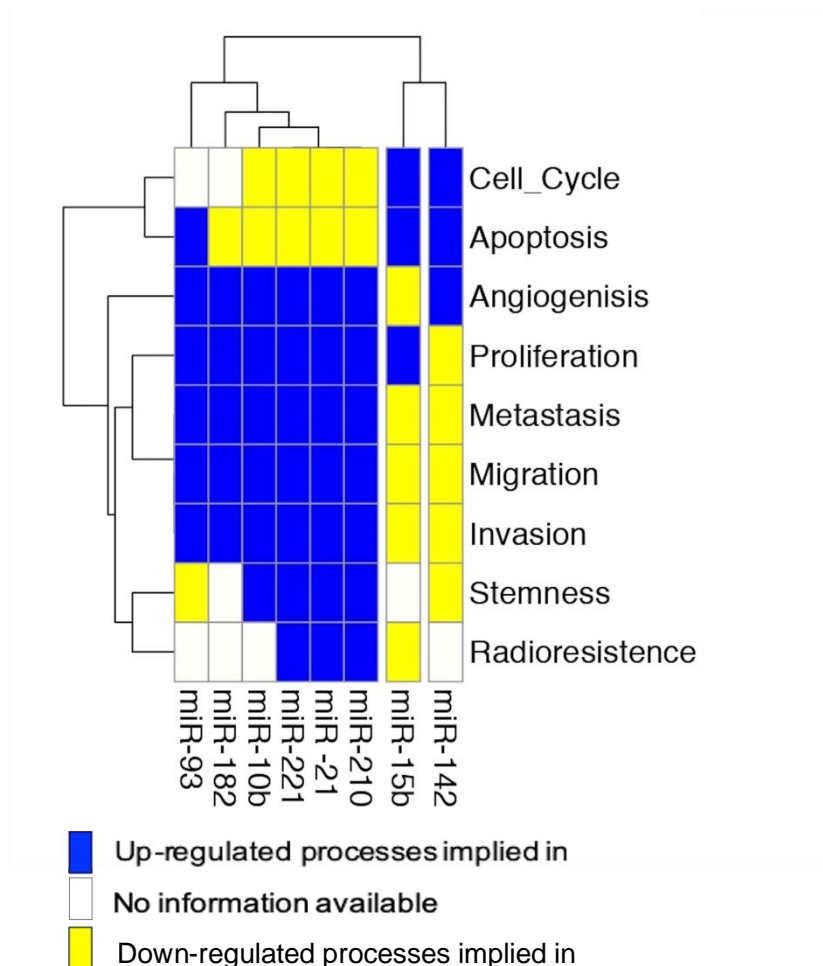
Figure 42: Heatmap with the biological functions where miRNAs are implicated according to the specialized literature using datamining techniques.

In MDA-MB-231 mammospheres treated with 4 Gy, miR-21, miR-221, miR-15b, miR-182, miR-10b and miR-142 were overexpressed in comparison to 2 and 6 Gy. For mammospheres all miRNAs showed significant differences in comparison to sham-irradiated control cells *(#p<0.05 or ##p<0.01)* (Figure 43, Table 9 and 10). Also, we could observe that miR-93 and miR-210 displayed lower expression for all IR doses. On the other hand, monolayer cultures showed a similar expression, and only miR-142,

miR-210, miR-221 displayed lower expression in all the different doses. At 2 Gy, miR-21 and miR-182 expression was higher than the other doses in monolayer cells cultures.
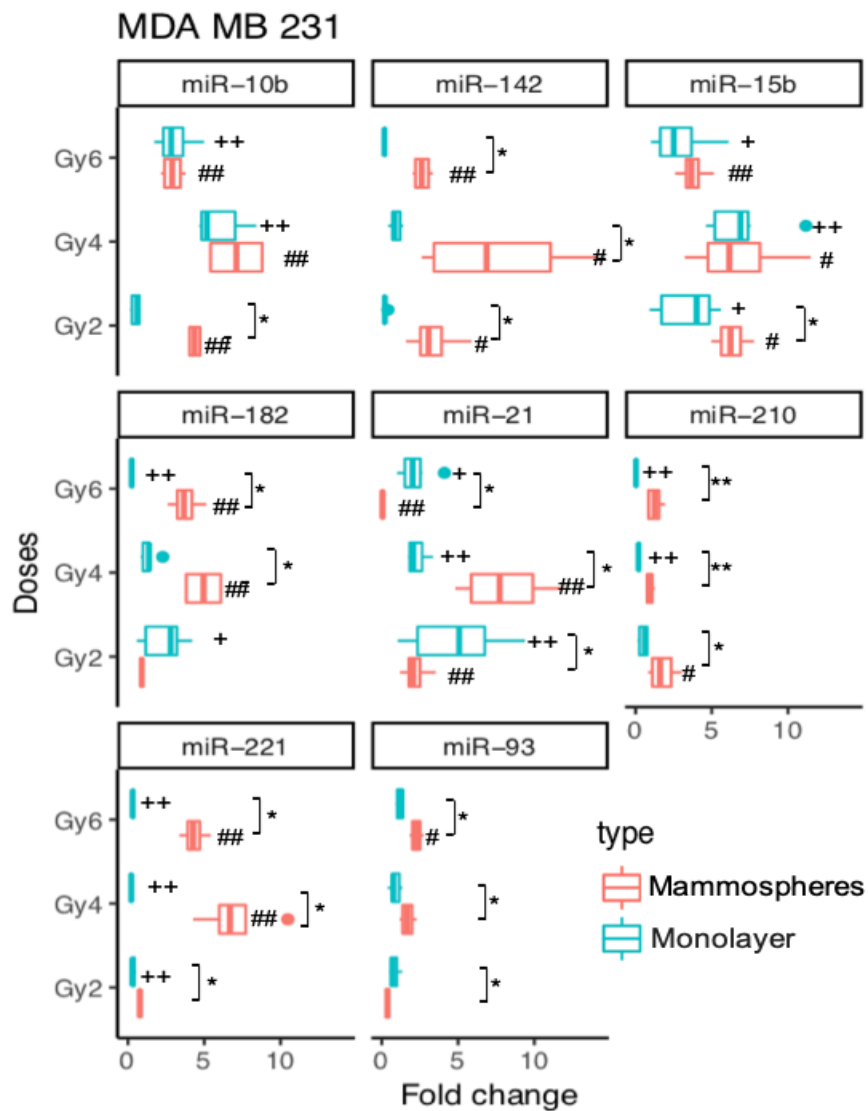
Figure 43: Differential expression of miRNAs in MDA-MB-231 cells grown in monolayer and as mammospheres. U-Mann-Whitney and Kruskal-Wallis non-parametric tests were used for comparison between two or more groups, respectively. Significant differences were indicated differently as + or # when the IR doses are compared with the non-irradiated control monolayer and mammospheres cultures respectively; and * when monolayer and mammospheres subpopulations were compared. The value of p ($^{*/+/\#}$ for $p < 0.05$; $^{**/++/\#\#}$ for $p < 0.01$).

Table 9: Fold changes and p-values corresponding to Figure 43. U-Mann-Whitney non-parametric test were used for comparison between doses.

		MDA-MB-231					
		Monolayer			**Mammospheres ALDH1+**		
		2 Gy	**4 Gy**	**6 Gy**	**2 Gy**	**4 Gy**	**6 Gy**
miR-93	Fold	0,83	0,87	1,21	0,37	1,70	2,28
	p-value	0,26	0,34	0,86	**0,03**	0,14	**0,01**
miR-10b	Fold	0,52	5,97	3,07	4,39	7,12	2,94
	p-value	0,08	**0,00**	**0,00**	**0,00**	**0,00**	**0,00**
miR-15b	Fold	3,43	6,96	2,92	2,92	6,76	3,78
	p-value	**0,01**	**0,00**	**0,04**	**0,00**	**0,02**	**0,00**
miR-142	Fold	0,22	1,36	0,19	3,40	7,64	2,66
	p-value	0,07	0,36	0,06	**0,04**	**0,05**	**0,00**
miR-182	Fold	2,40	1,18	0,26	0,91	4,96	1,91
	p-value	**0,03**	0,44	**0,00**	0,39	**0,00**	**0,00**
miR-21	Fold	4,89	2,30	2,20	2,22	8,05	0,05
	p-value	**0,00**	**0,00**	**0,05**	**0,05**	**0,00**	**0,00**
miR-221	Fold	0,34	0,21	0,32	0,78	7,03	4,28
	p-value	**0,00**	**0,00**	**0,00**	0,09	**0,00**	**0,00**
miR-210	Fold	0,53	0,22	0,04	1,76	0,95	1,26
	p-value	0,05	**0,00**	**0,00**	**0,04**	0,56	0,38

Table 10: *p-values* comparing monolayer and ALDH1+ mammospsheres fold changes in MDA-MB-231.

	MDA-MB-231		
	2 Gy	**4 Gy**	**6 Gy**
miR-93	**0,01**	**0,03**	**0,01**
miR-10b	**0,01**	0,09	0,83
miR-15b	**0,03**	1,00	0,39
miR-142	**0,01**	**0,01**	**0,01**
miR-182	0,39	**0,01**	**0,01**
miR-21	0,29	**0,01**	**0,01**
miR-221	**0,01**	**0,01**	**0,01**
miR-210	**0,01**	**0,00**	**0,00**

In MCF7 mammospheres, miR-21, miR-142, miR-182, and miR-210 were up-regulated in comparison to monolayer cell cultures for the majority of doses, especially for 4 and 6 Gy (Figure 44, Tables 11 and 12). In contrast, for miR-10b and miR-93 a lower expression was found in mammospheres than in monolayer at 4 and 6 Gy where a significant dose dependent miRNA expression miR-15b and miR-221 showed a low expression in both culture conditions.
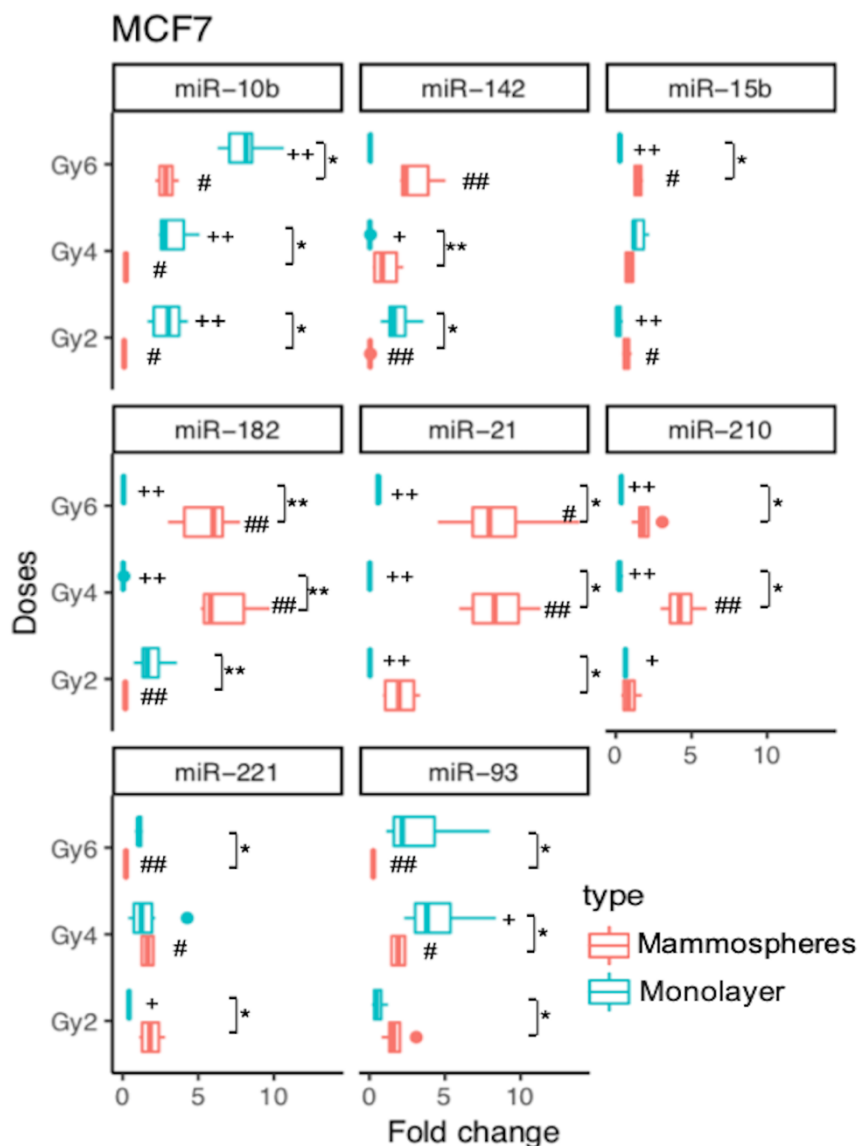
Figure 44: Differential expression of miRNAs in MCF7 cells grown in monolayer and as mammospheres. U-Mann-Whitney and Kruskal-Wallis non-parametric tests were used for comparison between two or more groups, respectively. Significant differences were indicated differently as + or # when the IR doses are compared with the non-irradiated control in monolayer and mammospheres cultures respectively; and [*] when monolayer and mammospheres subpopulations were compared. The value of p ([*/+/#] for $p < 0.05$; [**/++/##] for $p < 0.01$).

Table 11: Fold changes and p-values corresponding to Figure 44. U-Mann-Whitney non-parametric test were used for comparison between doses.

		MCF7					
		Monolayer			**Mammospheres ALDH1+**		
		2 Gy	**4 Gy**	**6 Gy**	**2 Gy**	**4 Gy**	**6 Gy**
miR-93	Fold	0,58	4,48	3,31	1,76	1,91	0,25
	p-value	0,11	**0,01**	0,09	0,17	**0,01**	**0,00**
miR-10b	Fold	2,95	3,32	8,11	0,10	0,22	2,88
	p-value	**0,00**	**0,00**	**0,00**	**0,01**	**0,01**	**0,01**
miR-15b	Fold	0,18	1,48	0,26	0,70	0,90	1,46
	p-value	**0,00**	0,06	**0,00**	**0,02**	0,06	**0,01**
miR-142	Fold	1,91	0,03	3,05	0,05	1,08	2,85
	p-value	0,49	**0,01**	0,15	**0,00**	0,84	**0,00**
miR-182	Fold	1,96	0,03	0,08	0,18	6,75	5,50
	p-value	0,08	**0,00**	**0,00**	**0,00**	**0,00**	**0,00**
miR-21	Fold	0,04	0,02	0,57	2,04	8,45	8,57
	p-value	**0,00**	**0,00**	**0,00**	0,26	**0,00**	**0,01**
miR-221	Fold	0,43	1,64	1,09	1,87	1,65	0,22
	p-value	**0,01**	0,43	0,87	0,07	**0,03**	**0,00**
miR-210	Fold	0,63	0,25	0,36	0,92	4,34	1,91
	p-value	**0,02**	**0,00**	**0,00**	0,65	**0,00**	0,18

Table 12: *p-values* comparing monolayer and ALDH1+ mammospsheres fold changes in MCF7.

	MCF7		
	2 Gy	**4 Gy**	**6 Gy**
miR-93	**0,03**	**0,03**	**0,01**
miR-10b	**0,01**	**0,01**	**0,01**
miR-15b	0,07	0,06	**0,01**
miR-142	**0,01**	**0,00**	0,06
miR-182	**0,00**	**0,00**	**0,00**
miR-21	**0,01**	**0,01**	**0,01**
miR-221	**0,01**	0,67	**0,01**
miR-210	0,67	**0,01**	**0,01**

In contrast, SKBR3 cells (Figure 45, Tables 13 and 14) cultured as mammospheres showed a low expression of most miRNAs and for all irradiation doses, except for miR-93 where there was an increased expression at 2 and 4 Gy, both in monolayer and mammospheres cell cultures. On the other hand, in cells grown in monolayer miR-21, miR-142, miR-221, miR-210 and miR-15b tended to increase more for 4 Gy and 6 Gy.
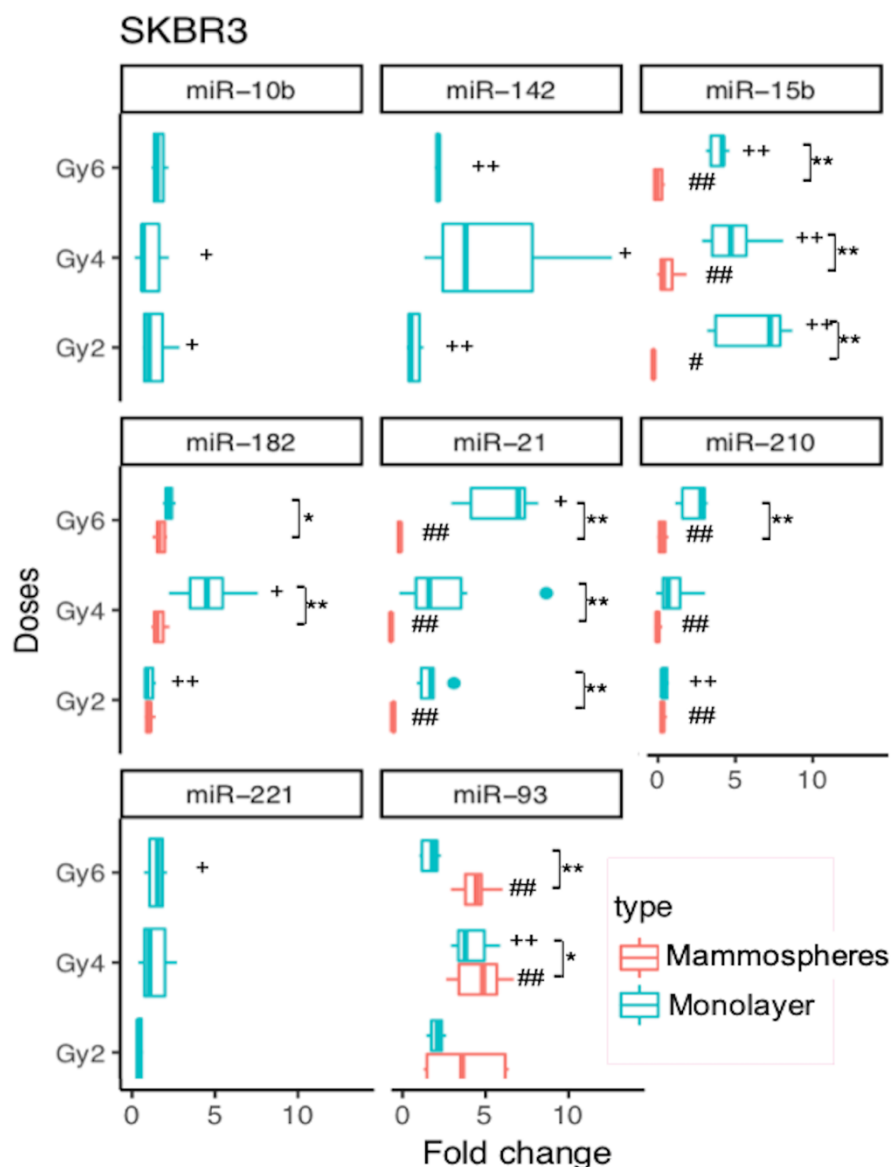

Figure 45: Differential expression of miRNAs in SKBR3 cells grown in monolayer and as mammospheres. U-Mann-Whitney and Kruskal-Wallis non-parametric tests were used for comparison between two or more groups, respectively. Significant differences were indicated differently as + or # when the IR doses are compared with the non-irradiated control in

monolayer and mammospheres cultures respectively; and * when monolayer and mammospheres subpopulations were compared. The value of p ($^{*/+/\#}$ for $p < 0.05$; $^{**/++/\#\#}$ for $p < 0.01$).

Table 13: Fold changes and p-values corresponding to Figure 45. U-Mann-Whitney non-parametric test were used for comparison between doses.

		SKBR3					
		Monolayer			**Mammospheres ALDH1+**		
		2 Gy	**4 Gy**	**6 Gy**	**2 Gy**	**4 Gy**	**6 Gy**
miR-93	Fold	1,21	2,13	1,06	0,31	2,34	2,25
	p-value	0,11	**0,00**	0,80	0,06	**0,00**	**0,00**
miR-10b	Fold	0,59	0,48	0,73			
	p-value	**0,03**	**0,03**	0,11			
miR-15b	Fold	2,77	2,15	1,81	0,08	0,44	0,20
	p-value	**0,00**	**0,00**	**0'00**	**0,01**	**0,00**	**0,00**
miR-142	Fold	0,59	2,62	1,25			
	p-value	**0,00**	**0,04**	**0,00**			
miR-182	Fold	0,46	2,02	1,01	0,48	0,73	0,76
	p-value	**0,00**	**0,01**	0,85	0,07	0,08	0,25
miR-21	Fold	1,26	1,51	2,92	0,07	0,00	0,23
	p-value	0,50	0,57	**0,01**	**0,00**	**0,00**	**0,00**
miR-221	Fold	0,22	0,62	0,66			
	p-value	0,20	0,05	**0,03**			
miR-210	Fold	0,32	0,61	1,16	0,31	0,19	0,31
	p-value	**0,00**	0,31	0,30	**0,00**	**0,00**	**0,00**

Table 14: *p-values* comparing monolayer and ALDH1+ mammospsheres fold changes in SKBR3.

	SKBR3		
	2 Gy	**4 Gy**	**6 Gy**
miR-93	0,81	0,57	**0,00**
miR-10b			
miR-15b	**0,00**	**0,00**	**0,00**
miR-142			
miR-182	0,81	**0,00**	**0,02**
miR-21	**0,00**	**0,00**	**0,00**
miR-221			
miR-210	0,97	**0,02**	**0,00**

7. EXPRESSION OF SELECTED miRNAS IN BREAST CANCER PATIENTS TREATED WITH RADIOTHERAPY.

To examine the modulation of miRNAs in patient's serum, we determine the differential expression of miRNAs before-, during and post-RT (Figure 46). We observed that in all cases miRNA expression significantly increased during RT (**$p<0.01$) except for miR-93. In addition, in comparison to pre-RT, miR-21 and miR-10b expression significantly increased in post-RT (*$p<0.05$); and very significantly (**$p<0.01$) for miR-221, miR-210 and miR-142. When compared, during-RT and post-RT groups significant differences were found, with a decrease of expression of miR-21, mir-15b and miR-182; and an increased expression of miR-221 (Figure 46).
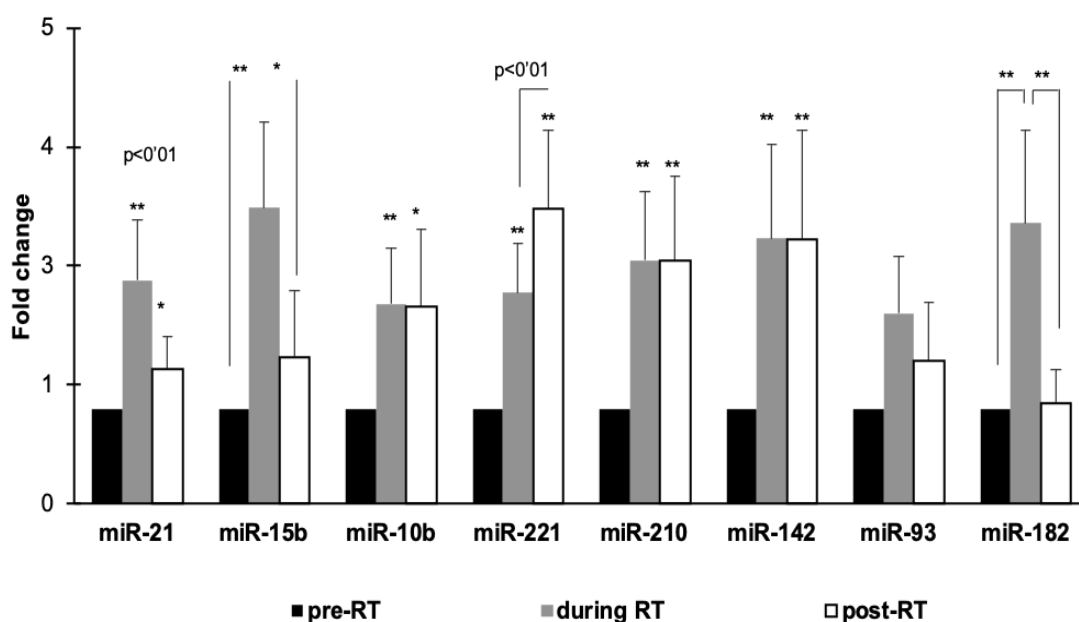
Figure 46: Relative gene expression of selected miRNAs differentially expressed by qRT-PCR Analysis was done in BC patients treated with radiotherapy *versus* pre-treatment samples. (A) miRNA expression levels pre-RT (control), during-RT and post-RT.

Also, when we selected only the three patients with TNBC, and also with expression of p53 we observed that miR-221 was up-regulated during radiotherapy and post radiotherapy TNBC patient p53+ (Figure 47).
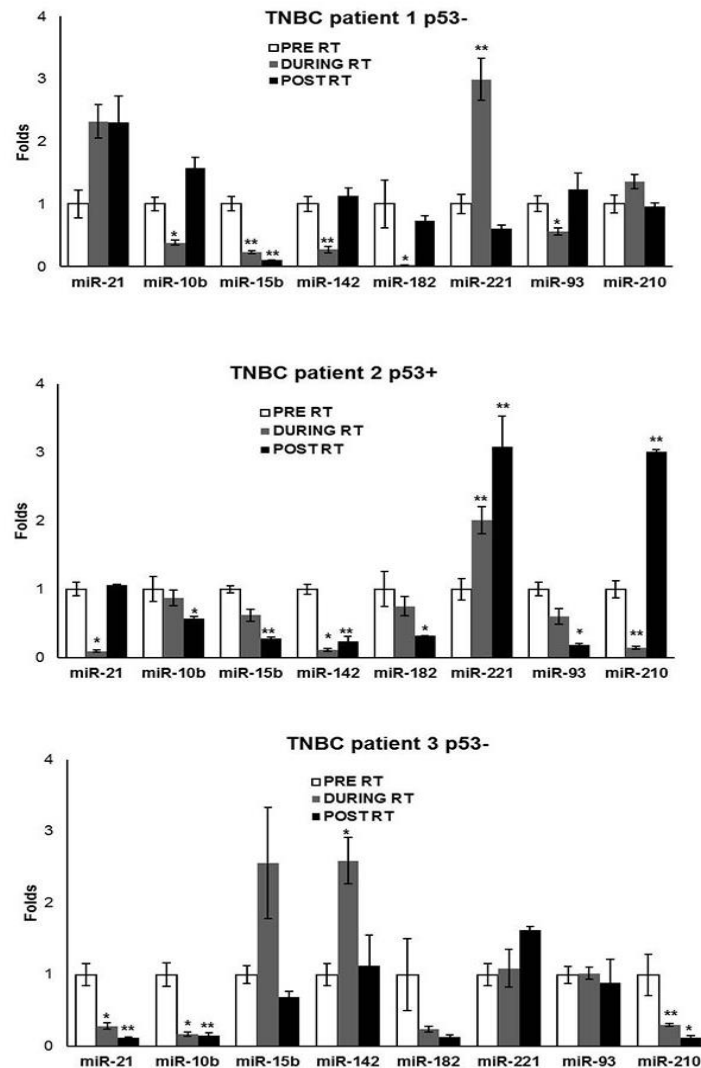
Figure 47. miRNA expression levels pre-RT, during-RT and post-RT of triple-negative breast cancer patients. Data are mean value $\pm$ SEM. *$p<0.05$ and **$p<0.01$.

When grouped by the clinicopathological characteristics of the patients (age, menopausal status, tumour classification, Ki67, etc.), we found significative differences in determined miRNAs expression (Table 15).

Table 15. Clinicopathological features of the BC patients studied.

Variables		N= 20	Recurrence	
Age	<50	10	9	1
	>50	10	8	2
Menopausal status	pre-menopausal	10	9	1
	menopausal	6	5	1
	post-menopausal	4	3	1
Tumour classification	Triple negative	3	2	1
	ER+/PR+	17	15	2
Differentiation grade	G I	9	8	1
	G II	7	6	1
	G III	4	3	1
Histological type	Ductal	17	15	2
	Other	3	2	1
E-cadherin	positive	16	14	2
	negative	4	3	1
P53	positive	3	2	1
	negative	17	15	2
Ki67	< 20%	14	13	1
	≥ 20 %	6	4	2
Chemotherapy	No QT	9	8	1
	Yes QT	11	9	2
Radiation Doses	2 Gy	7	6	1
	2,65 Gy	13	11	2
RT Toxicity	yes	18	15	3
	no	2	2	0
Recurrence (end of trial)	yes	3		
	no	17		

We observed that miR-21 was significant (*$p<0.05$) for age and the histological type in post-RT and for Ki67 during RT (*$p<0.05$) (Figure 48; Table 16).
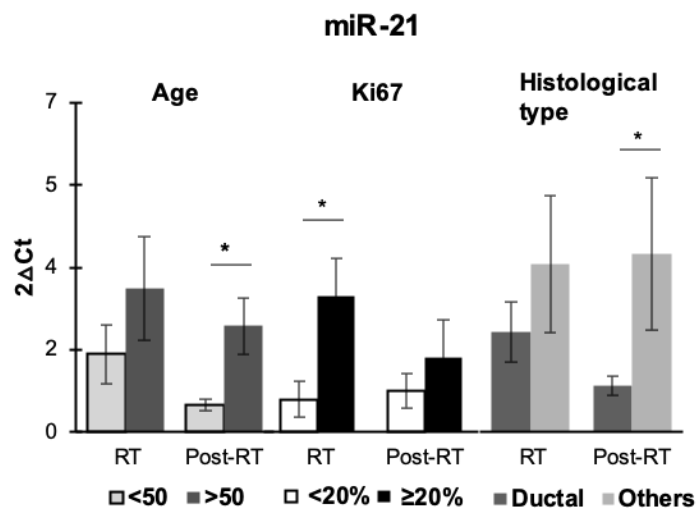
Figure 48: miR-21 expression changes when aggregated by clinicopathological features. Data are mean values ± SEM. * p < 0.05 shows the significant values calculated using Kruskal-Walls test.

In the Figure 49 and Table 16, we observed that miR-10b expression was significant during RT for Ki67 and E-cadherin, but in post-RT when grouped by treatment with chemotherapy.
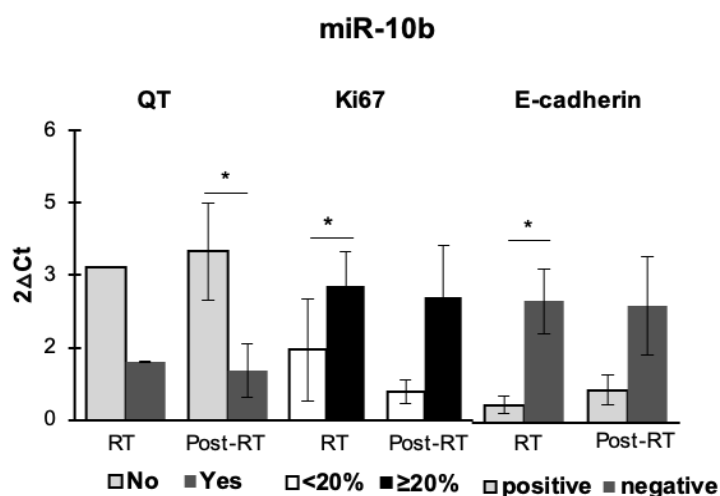
Figure 49: miR-10b expression changes when aggregated by clinicopathological features. Data are mean values ± SEM. * p < 0.05 shows the significant values calculated and Kruskal-Walls test.

miR-142 showed significant expression for differentiation grade (GII *vs* GIII) and marker p53 in treatment. Moreover, mir-142 expression in p53 positive patients during RT and post-RT was also significant (Figure 50; Table 16).
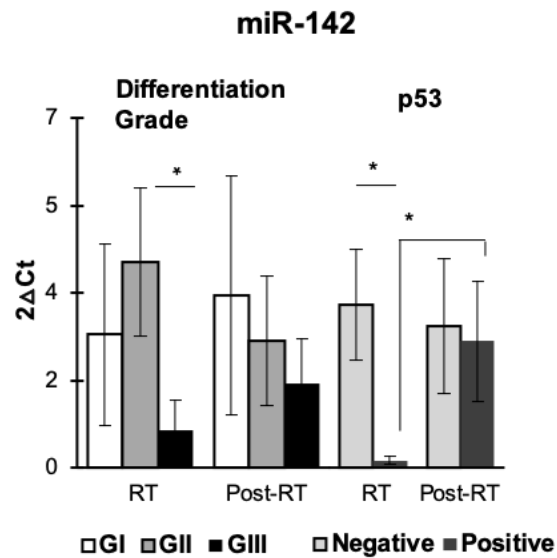
Figure 50. miR-142 expression changes when aggregated by clinicopathological features. Data are mean values ± SEM. * p < 0.05 shows the significant values calculated Kruskal-Walls test.

Also, for miR-182 expression significant differences were found for Ki67 and E-cadherin during RT. The expression was greater for patients Ki67 >20% and E-cadherin negative (Figure 51; Table 16).
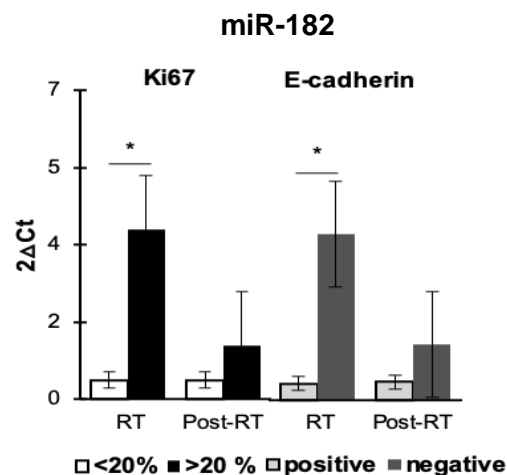

Figure 51. miR-182 expression changes when aggregated by clinicopathological features. Data are mean values ± SEM. * p < 0.05 shows the significant values calculated Kruskal-Walls test.

Finally, miR-210 showed significant differences related to recurrence and toxicity after RT. However, in patients with recurrence miR-210 expression significantly increased after RT and also in patients that had not RT toxicity (Figure 52; Table 16).
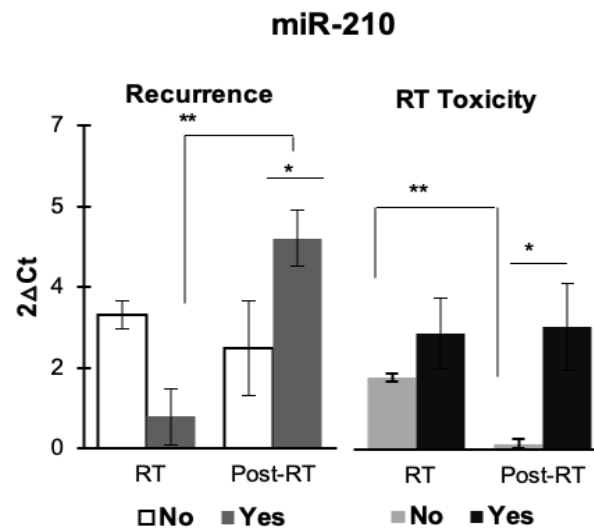

Figure 52: miR-210 expression changes when aggregated by clinicopathological features. Data are mean values ± SEM. * p < 0.05 shows the significant values calculated Kruskal-Walls test.

Table 16: Statistical data of p-values corresponding to Figures 47-51.

Groups		RT	Post- RT
		p-value	p-value
miR-21			
Age	**< 50**	0,43	**0,04**
	> 50		
Histological type	**Ductal**	0,31	**0,02**
	Others		
Ki67	**< 20%**	**0,05**	0,275
	≥ 20%		
miR-10b			
Chemotherapy	**no**	**0,04**	0,09
	yes		
Ki67	**< 20%**	**0,05**	0,266
	≥ 20%		
E-cadherin	**positive**	**0,038**	0,549
	negative		
miR-142			
p53	**positive**	**0,04**	0,74
	negative		
Histological grade	**GI vs GII**	0,053	0,72
	GI vs GIII	0,28	0,22
	GII vs GIII	**0,019**	0,34
miR-182			
Ki67	**< 20%**	**0,04**	0,57
	≥ 20%		
E-cadherin	**positive**	**0,046**	0,277
	negative		
miR-210			
Recurrence	**no**	0,35	**0,03**
	yes		
Toxicity	**No**	0,69	**0,046**
	yes		

DISCUSSION

The concept of cancer has been changing and evolving over the years since tumours are composed of various cell types such as differentiated, post-mitotic, some with tumour-initiating potential, etc…, but the CSC model argues that a little subpopulation within the tumour has stem cell-like properties with higher tumorigenic potential among other (Ghaffari, 2011). Their existence has been known for a long time. Their presence within the tumour was first described in leukaemia cells, where they were identified with different surface markers not present in non-cancerous cells (Cojoc *et al.*, 2015a). This subpopulation presents inside tumour has unlimited proliferation potential, ability to self-renew, capacity to generate a differentiated lineage that form the major tumour population, they are relatively quiescent and have a slow cycling rate (Ablett *et al.*, 2012; Batlle and Clevers, 2017; Rich, 2007).

Moreover, CSCs are able to give rise to all the cells within tumours, among them those resistant to radiotherapy and responsible for recurrence of the disease. They used different mechanisms of genetic and cellular adaptations that confer resistance to RT. Thus, CSC have more efficiency in DNA repair mainly attributed to the activation of the ATR-Chk1 and ATM-Chk2 signalling pathways (Krause *et al.*, 2017). Alike CSCs, TME and hypoxia play an essential role in radioresistance. Oxygen is a well-known radio-sensitizing agent due to its ability to form radiation-induced reactive oxygen species that can indirectly damage DNA (Brunner *et al.*, 2012; Krause *et al.*, 2017).

Apoptosis resistance to therapy might also be conferred to CSCs through the activation of the Akt pathway and the over-amplification of apoptosis inhibitor proteins (Morrison *et al.*, 2011). In addition, cells than often acquire RT resistance after non-lethal exposure, repair sublethal damage between irradiation fractions. Therefore, a failure of radiation treatment might be attributed to the incomplete eradication of CSCs subpopulation (Krause *et al.*, 2011; Pawlik and Keyomarsi, 2004). Since the CSCs

model is highly relevant for recurrence of cancer, a treatment based on targeting CScs may be more effective in preventing metastasis and future relapses.

In this sense, several studies have demonstrated that IR enhances BCSC-like phenotype (Gao *et al.*, 2016; Gomez-Casal *et al.*, 2013; Kim *et al.*, 2015). Controlling the phenotypical and functional properties of CSCs during RT could be useful for the optimization and individualization of treatment strategy. How to use CSCs model with genomics, proteomics and high-throughput studies validated by functional radiobiological assays and clinical observations are expected to provide more information about new CSC-associated biomarkers and CSC-targeted therapies in order to enhance the efficacy of radiation treatment and in improving the lives of cancer patients (Ghaffari, 2011; Peitzsch *et al.*, 2013; Thomas B. Brunner *et al.*, 2012).

In our study, we found how different doses of IR induce the selection of BC cells with stemness properties (mammospheres) and determined molecular profile (cells ER + cells-MCF7-, HER2 positive-SKBR3- and triple negative-MDA-MB-231-). Moreover, we determined how different doses modify the expression levels of miRNAs related to important oncogenic processes in BC. At difference with previous works we analyse the effect of IR on the three most common BC molecular subtypes (luminal, HER2+ and TNBC). We isolated CSCs by sorting in basis to the ALDH1 activity, a widely normalized method in BC (Ginestier *et al.*, 2007; Owens and Naylor, 2013). After isolation these BCSCs were able to form mammospheres *in vitro* in serum-free suspension cultures and were enriched in stem cell properties after using a specific culture medium.

Firstly, we proved that in MDA-MB-231 TNBC cells irradiated at 2 Gy, stemness properties were promoted in monolayer cultures, as showed the enrichment and maintenance of CSCs phenotype supported by the higher ALDH1 activity found for the different IR doses and also the incremented expression in CD44$^+$/CD24$^{-/low}$ surface markers, which has been related to radioresistance and poor prognosis in BC patients (Kim *et al.*, 2016; Phillips *et al.*, 2006; Wang *et al.*, 2017). Interestingly, our results showed that, in both MCF7 and SKBR3 mammospheres, all IR doses decreased ALDH1 activity and CD44$^+$/CD24$^{-/low}$ expression. However, in ER+ and HER2+ cells IR decreased stemness markers in a dose-dependent manner. Remarkably, our results showed that in mammospheres all IR doses decreased ALDHI1 activity and this fact was similar for CD44$^+$/CD24$^{-/low}$ surface markers except for the TNBC cell line where all IR doses significantly increased this expression, and also 4 Gy increased 2nd generation spheres number. MDA-MB-231 cell line is classified as TNBC B type basal (claudin-low, mesenchymal-like, metaplastic BC cells) featured by the CSC pattern such as CD44$^+$CD24$^-$ and migration markers such as *VIMENTIN* (Dai *et al.*, 2017). Moreover, it is known that IR induces EMT and CSC phenotypes by regulating cellular metabolism, which are associated with resistance to RT and chemotherapy (Chumsri and Shah, 2013; Ginestier *et al.*, 2007; Lee *et al.*, 2017). Specific IR doses promoted BCSCs growth and the increased CD44$^+$CD24$^-$ expression, which has been related to radioresistance mediated by STAT1 signalling (Phillips *et al.*, 2006; Zhan *et al.*, 2011). However, the proliferation rates in mammospheres in all IR doses and in the three BC cell lines were lower, without significant growth respect to sham-irradiated control. These results could be explained with one of the CSCs features, the quiescence, that keep cells in a stage where they are not actively dividing to create new cells, but can re-

enter in the cell cycle division and proliferate at some later time (Batlle and Clevers, 2017; Chumsri and Shah, 2013).

Apoptosis is the natural mechanism for programmed cell death and it plays a critical role in development as well as homeostasis. It serves to eliminate any unnecessary cells and is a highly regulated process. Thera are a variety of conditions that can induce the apoptotic pathway, such as DNA-damaging agents, anticancer drugs, ROS, UV irradiation, TNF-α, and bacterial toxins (Evan and Vousden, 2001; Pfeffer and Singh, 2018). After IR, surviving CSCs have the capacity to repopulate the tumour due the activation of the DNA damage checkpoints to a greater degree than the non–CSCs. The outcome of radiation-induced DNA damage is skewed toward survival and repair in CSCs, whereas non–stem cancer cells are more likely to undergo apoptosis (Rich, 2007). The analysis of apoptosis after IR at different doses showed the radioresistance of both MDA-MB-231 and MCF7 mammospheres (BCSCs) while monolayer cultures of these BC molecular subtypes were more radiosensitive to 4 and 6 Gy. In contrast, SKBR3 cell line was more radioresintant in monolayer cultures, due to the overexpression of the HER-2 growth factor receptor, which is related with poor clinical outcome, including earlier local relapse after conservative surgery and RT (Pietras *et al.*, 1999).

Also, our study showed that IR doses modulated the expression of *NANOG*, *SOX2* and *OCT4* pluripotency genes that contribute to CSCs phenotype (Kim *et al.*, 2018; K. Takahashi and Yamanaka, 2006; Yu *et al.*, 2007) and EMT-related genes (Theys *et al.*, 2016; Zhou *et al.*, 2011) in cells grown in monolayer or mammospheres

depending on the BC molecular subtype that can be explained by the different sensitivity of BC molecular subtypes to IR (Kim *et al.*, 2015).

So, in MDA-MB-231 cell line *NANOG* expression was the only gene that increased at 4 Gy in monolayer; however, in mammospheres 6 Gy was able to induce overexpression of *SOX2* and *OCT4* accompanied by a decreased of *E-CADHERIN* gene in all doses (Shen *et al.*, 2014; Theys *et al.*, 2016). In HR+ MCF7 cells grown in monolayer IR significantly increased *NANOG* expression at 6 Gy and *OCT4, E-CADHERIN* and *N-CADHERIN* at 4 Gy and 6 Gy, whereas *VIMENTIN* was downregulated after treatment with 6 Gy. These heterogenous modifications depending of the IR could be due to the selection of subpopulations with different stemness characteristics (Zhou *et al.*, 2011). In contrast, the main change induced by radiation in mammospheres was the increased expression of *OCT4* after treatment with 2 Gy. Curiously increased expression levels of *N-CADHERIN, VIMENTIN* and a lower expression of *E-CADHERIN* was related to an overexpression of *OCT4* and *NANOG* in CSCs (Theys *et al.*, 2016; D. Wang *et al.*, 2014; J. M. Zhang *et al.*, 2018). Finally, in HER2+ cells grown in monolayer *NANOG* and *SOX2* significantly increased at 4 Gy and *OCT4* for all doses assessed with an increase of *VIMENTIN* expression after treatment with 6 Gy. Differences observed for each cell line after treatment can be explained by the different sensitivity of BC molecular subtypes to IR. Moreover, several studies demonstrated that IR promote EMT-related gene expression and enhances the migration and invasiveness capacity (Artacho-Cordón *et al.*, 2012; Kim *et al.*, 2015; Zhou *et al.*, 2011).

To analyse the *in vivo* tumorigenic capacity after treatment of cells with IR, MDA-MB-231 TNBC cell line was chosen due to its most stemness properties and their potent migratory response and aggressiveness in mice (Price *et al.*, 1999). Our results support that IR affects negatively tumour growth when increased doses in cells cultured as monolayer; however, in mammospheres injected in the mice, and according to the *in vitro* results, we observed a similar growth rate in sham-irradiated controls and the 4 Gy group. This result would suggest that 4 Gy selected the more resistant triple negative BCSCs *in vitro*, which had more aggressive behaviour *in vivo* (Ghisolfi *et al.*, 2012; Phillips *et al.*, 2006). In fact, the great heterogeneity of BCSC (Da Cruz Paula and Lopes, 2017; Hernández-Camarero *et al.*, 2018) has been reported. CSC plasticity may be a common response to IR with the generation of new induced BCSCs resistant to specific IR doses. Specifically, it has been documented that SUM159PT ALDH- triple negative BCSCs tumours irradiated with 4Gy, induce more aggressive BCSC subpopulations (Lagadec *et al.*, 2012).

Nonetheless, high levels of *VIMENTIN,* an indicator of BC progression (Calaf *et al.*, 2014) were found in tumours derived from monolayer cultures treated with 2 Gy. Local recurrence and distant metastases, despite therapy, indicate that BCSCs are able to evade the effects of chemotherapy and radiotherapy and thereby repopulate the tumour following treatment (Ablett, 2014). Our results could have a translation to TNBC patients and encourage to selectively irradiate tumour zones rich in CSCs subpopulations with higher doses of IR (Evers *et al.*, 2010).

Gene analysis studies have demonstrated aberrant miRNA expression in tumours compared to normal tissues and that miRNAs are deregulated in an array of solid

cancers as well as haematological malignancies. The findings about the role of miRNAs in cancer is supported by the fact that about 50% of miRNA genes are located in cancer associated genomic regions, or in fragile sites, further strengthening the evidence that miRNAs play a crucial role in cancer. As a result, human miRNAs are likely to be highly useful as biomarkers, especially for future cancer diagnostics, and are emerging as attractive targets for disease intervention (Abba et al, 2014).

miRNAs have an important relevance in all the process of resistance to RT. The essential role of miRNAs in an effective cellular response to radiation exposure have been described in different studies (Kraemer *et al.*, 2011; Surova *et al.*, 2012). It has also been shown that IR changes the expression of specific subsets or of individual miRNAs, that have an impact on radiosensitivity (Czochor and Glazer, 2014; Metheetrairut and Slack, 2013a). Overall, radiation-induced changes in miRNA expression are transient, dependent upon dose, and are cell type specific. For some miRNAs, the repression in their levels after exposure has been described. Although a mechanistic basis is not yet available reduced levels can be assumed to promote translation of specific miRNA target proteins. Mechanisms proposed to link a radiation response to increased miRNA biogenesis, however, include increased processing of pri-miRNAs through KSPR after phosphorylation by the DNA damage sensor protein ATM or the induction of pri-miRNA transcription by the DNA damage stabilized transcription factor p53 (e.g., miR- 34 family) (He *et al.*, 2007; Zhang *et al.*, 2011). Functionally, miRNAs affect many aspects of tumour radiation sensitivity by regulating cellular key components in cell cycle arrest, DNA damage repair, cell death and radiation related signal transduction (Zhao *et al.*, 2012). On the one hand, miRNAs can impair production of proteins essential for DNA damage recognition, signalling, and

cell cycle arrest indispensable to initiate repair. This may lead to lower DNA repair capacity and radiosensitivity (Hu *et al.*, 2010; Lal *et al.*, 2009). Together all these findings point to miRNAs as potential key players in determining the response to IR and, by inference, to RT.

The main purpose of our work was to analyse the role of determined key miRNAs (Summerer *et al.*, 2013) in response to IR in both CSC-like cells and BC patients that could be useful at the clinical level. It has been stablished in several tumoral cell types the involvement of specific miRNAs in the radio-response and how some miRNAs could be useful in modulating radio-response at the clinical level (Metheetrairut and Slack, 2013b). We analysed expression levels of selected miRNAs in three BC cell lines *versus* a sham-irradiated control and in serum from BC patients treated with RT (pre, during and post-RT).

We studied miR-21 and miR-182, two very well-known miRNAs overexpressed in a variety of human cancers, recognized as oncogenic miRNAs that promote cell proliferation, metastasis and both are valuable markers of prognosis in BC (Shah and Chen, 2014). We observed a different behaviour in both miRNAs in their response to IR, according to the cell line and IR doses. Thereby, in MDA-MB-231 and MCF7 mammospheres these miRNAs were highly expressed after treatment with 4 Gy and 6 Gy, in contrast to HER2+ SKBR3 cells where both miRNAs decreased their expression. It has been demonstrated that miR-21 is up-regulated and contributes to IR resistance upon high doses of irradiation (5Gy) in BC cells, since this miRNA influences cell cycle progression *via* the DNA damage-G2 checkpoint induction (Anastasov *et al.*,

2012). Equally, the over-expression of miR-182 confers radioresistance in non- small cell lung cancer (Chen *et al.*, 2019).

In our analysis, miRNAs related to metastasis, invasion and CSCs, such as miR-221, miR-10b and miR-93 were analysed. miR-221 plays an important role in CSCs homeostasis, being up-regulated in these cells and promoting tumorigenesis through the induction of EMT in TNBC (Metheetrairut and Slack, 2013a). In our study, miR-221 showed low expression in all the three cell lines cultured in monolayer after treatment with IR; however, only in MDA-MB-231 mammospheres increased after treatment with higher doses (4 Gy and 6 Gy) and no expression was found in HER2+ CSCs for any doses. It is known that miR-221 induces expression of pluripotency-associated genes, enforcing stemness phenotype, mammospheres formation and radioresistance processes (Roscigno *et al.*, 2016; C. Zhang *et al.*, 2011). Then, our results suggest that this miRNA could be a marker of resistance to IR in triple negative BCSCs and that high doses of IR could be effective in resistant HER2+ CSCs.

On the other hand, miR-93 and miR-10b overexpression are related to cancer development and metastatic BC progression (Korpela *et al.*, 2015; Li *et al.*, 2017; Ma, 2010). In fact, we observed an increased expression of miR-93 in SKBR3 mammospheres at 4 Gy and 6 Gy, and in MDA-MB-231 mammospheres at 2 Gy; however, MCF7 mammospheres treated with high doses of radiation showed a downregulated miR-93 expression. Moreover, miR-10b was mainly overexpressed for all doses in MDA-MB-231 cell line that together the increased expression shown in EMT makers (*VIMENTIN* and *N-CADHERIN*) after treatment with 2 Gy, suggest that this dose could promote the expansion of CSCs subpopulations in this molecular subtype. All these data collected in the three cell lines, suggest that BCSC

subpopulations with a more aggressive behaviour were selected after high IR for HER2+CSCs and TNBCSCs, in contrast to HR+BCSCs, where high doses significantly decreased the expression of those miRNAs. Therefore, these findings indicate that IR was effective against ER+BCSCs and that miR221, miR-93 and miR-10b could be useful markers for IR response in BC patients.

Hypoxic intratumoral niches can protect cancer cells from irradiation through activation of the hypoxia-inducible factor-1 (HIF-1) pathway and transcription of HIF-1-responsive genes. One of hypoxia-induced miRNAs is miR-210 that can stabilize the HIF-1 complex and to enhance radioresistance *in vitro* (Wilson and Hay, 2011). In this sense, in our analysis miR-210 was overexpressed in MDA-MB 231 mammospheres and mainly in MCF7 mammospheres at high doses of radiation, but not in SKBR3 that decreased after treatment. In fact, a recent study showed that the hypoxic TME maintains CSC phenotype, which may influence their intrinsic resistance to radiation (Korpela *et al.*, 2015).

We also studied miRNAs that are tumour suppressors and they are related to radiosensitivity such as miR-15b and miR-142 (Isobe *et al.*, 2014; Pajic *et al.*, 2018). Specifically, miR-142 downregulates BCSC phenotype and decreases radioresistance *in vitro* (Troschel *et al.*, 2018) and miR-15b belongs to the miR-15 family related to BC cell radiosensitivity by influencing G_2/M checkpoint proteins (Mei *et al.*, 2015). In agreement with the previous results, a high expression of both miR-142 and miR-15b in MCF7-BCSCs was found at 6 Gy. These results could support the radiosensitivity of BCSCs to these IR doses.

The final step of this work was to analyse the eight miRNAs tested in our basic research in serum from BC patients treated with RT. Interestingly, all miRNAs analysed were up-regulated during RT. In fact, there are specific miRNAs associated with cellular responses to IR and some of them change significantly upon irradiation, doing so reproducibly across various tumour cell types (Calaf *et al.*, 2014).

We observed that during and after RT high amounts of circulating miRNAs were mobilized, which could be used as prognostic and predictive markers in combination with classical markers in the clinic. For this reason, we grouped the patients by their clinicopathological characteristic and compared them with miRNA expression after RT. Ki67 marker is used for early BC arrest and is an indicator of proliferation whose high expression has been related to worse prognosis, recurrence and death in BC (Yerushalmi *et al.*, 2010). Our results displayed that miR-21, miR-182 and miR-10b were significantly increased in patients who were positive for Ki67 during RT period. In addition, miR-21 elevated expression correlates with poor survival of patients (Anastasov *et al.*, 2012). miR-10b and miR-182 were also overexpressed in patients negative for E-Cadherin during RT, and their positive expression is correlated to a better prognosis and survival (Yang *et al.*, 2018). Moreover, miR-10b decreased during and after treatment with chemotherapy, which agrees with the low recurrence in the most of BC patients. miR-142 that is related to radiosensitivity and acts as a tumour suppressor in HR+BC (Mansoori *et al.*, 2019) was downregulated in our patients with Grade III of differentiation and p53 positive. Finally, miR-210 is related to poor prognosis and metastasis (Hong *et al.*, 2012) and in our study was overexpressed in patients with relapse after treatment, and was also overexpressed in patients showing toxicity after RT. These results are in concordance with those found in BCSCs after treatment in TNBC and ER+ cells lines and indicate the close relationship between this

miRNA, the clinical response to IR and stemness properties. In addition, there was also an association between the increased expression of both miR-210 and miR-221 in TNBC mammospheres and the levels found in the only TNBC patient p53+ that had recurrence after RT (Friedrichs *et al.*, 1993).

All our data together suggest that several doses of IR affect very differently depending on both the BCSCs subpopulation in comparison with more differentiated cells and the molecular subtype of BC. Certain doses select favourably stemness properties, which are related to metastasis, relapse and resistance to RT. In the same way, the expression levels of miRNAs were very different, corroborating that some doses increase their expression and others do the opposite effect. Despite their rapid expansion as biomarkers, there are not many clinical studies of miRNAs with clinical utility in RT. In this sense our study supports how miRNAs related to BCSC subpopulations could provide a useful method to predict and monitor tumour radio-response depending on the molecular BC subtype. A future clinical implementation of miRNA signature determination as a liquid biopsy, for personalized and precision RT dosage regimes, is necessary to improve prognosis, treatments and survival of BC patients.

CONCLUSIONS

1. The expression of BCSCs markers such as ALDH1+, CD44$^{+/}$CD24$^{-/low}$, number of secondary spheres and colonies in soft agar varies with the dose of IR administered in each BC molecular subtype. Different IR doses select cells depending on BCSCs-like phenotype and behaviour.

2. Ionizing radiation modifies BCSCs-related miRNA expressions depending on BC molecular subtypes and the radiation dose (used 0, 2, 4 or 6 Gy) in monolayer and in mammospheres cultures.

3. In MDA-MB-231 and MCF7 mammospheres, miR-21, miR-182, and miR-142 were significantly overexpressed when compared to sham-irradiated control. Also, it was observed that miR-93 and miR-210 had lower expression levels in mammospheres than in monolayer and specifically for 4 and 6 Gy.

4. SKBR3 cell line mammospheres showed a low expression of most miRNAs in all irradiation doses. These results suggest that miRNAS in HER2+ mammospheres do not present enough modifications after IR.

5. *In vivo* tumour growth of irradiated ALDH1+ TNBCSCs with 4 Gy and monolayer with 2 Gy was similar to sham-irradiated control cells. This could suggest that these doses did not eradicated the totality of bulk cells.

6. Triple negative MDA-MB-231 BC tumour growth rate was low and slow in both cell subpopulations after treatment with IR. Moreover, at high doses of radiation (6 Gy) the tumour growth rate and the final volume of the tumour was most significantly reduced.

7. The eight miRNAS analysed in BC patients' serum showed a major expression during radiotherapy and also, after treatment. This fact indicates that RT induces modifications and alterations of miRNAs depending on the specific moment of treatment regimen.

8. In BC patients with Ki67 >20%, miR-21, miR-10b, and miR-182 showed an increased expression during treatment with RT. These miRNAs are related with radioresitance and poor prognosis, and could be useful as markers for RT response.

9. In patients that had recurrence or toxicity to RT, miR-210 expression was up-regulated during treatment. These results support other studies where this miRNA plays a crucial role as regulator of radioresistance.

10. Finally, ours results suggest that the determination of miRNAs related to BCSC subpopulations in BC patients could provide a useful method to predict and monitor tumour radio-response depending on the molecular BC subtype.

CONCLUSIONES

1. La expresión de los marcadores células madre cancerígenas de cáncer de mama, ALDH1+, CD44$^{+/}$CD24$^{-/low}$, el número de esferas secundarias y de colonias en agar blando varía con la dosis de RI administrada en cada subtipo molecular. Diferentes dosis de RI seleccionan células según el fenotipo y comportamiento similar a las células madre cancerígenas de cáncer de mama.

2. La RI modifica las expresiones de miARN relacionadas con BCSCs dependiendo de los subtipos moleculares BC y la dosis de radiación (utilizada 0, 2, 4 o 6 Gy) en cultivos de monocapa y de mamosferas.

3. En las mamosferas de MDA-MB-231 y MCF7, miR-21, miR-182 y miR-142 fueron significativamente sobreexpresadas cuando comparamos con el control no irradiado. Además, pudimos observar que miR-93 y miR-210 tuvieron menor expresión en mamosferas que en monocapa, concretamente, para 4 y 6 Gy.

4. Las mamosferas de la línea celular SKBR3 mostraron una baja expresión de la mayoría de los miARN en todas las dosis de irradiación. Estos resultados sugieren que miRNAS en las mamosferas HER2 + no presentan suficientes modificaciones después de IR.

5. El crecimiento tumoral *in vivo* de ALDH1 + TNBCSC irradiados con 4 Gy y monocapa con 2 Gy fue similar a las células control irradiadas. Esto podría sugerir que estas dosis no erradicaron la totalidad de las células del tumor.

6. La tasa de crecimiento tumoral MDA-MB-231 BC triple negativo fue baja y lenta en ambas subpoblaciones celulares después del tratamiento con IR. Además, a altas dosis de radiación (6 Gy), la tasa de crecimiento tumoral y el volumen final del tumor se redujeron de manera más significativa.

7. Los ocho miARNS analizados en el suero de pacientes con BC mostraron una expresión elevada durante la radioterapia y también, después del tratamiento. Este hecho indica que la RT induce modificaciones y alteraciones de los miARNs dependiendo del momento específico del régimen de tratamiento.

8. En pacientes con BC con Ki67> 20%, miR-21, miR-10b y miR-182 mostraron una mayor expresión durante el tratamiento con RT. Estos miARNs están relacionados con la radiorresitancia y el mal pronóstico, y podrían ser útiles como marcadores para la respuesta de RT.

9. En pacientes que tuvieron recurrencia o toxicidad a la RT, la expresión de miR-210 se reguló durante el tratamiento. Estos resultados respaldan otros estudios en los que este miARN juega un papel crucial como regulador de la radiorresistencia.

10. Finalmente, nuestros resultados sugieren que la determinación de miRNAs relacionados con las subpoblaciones de BCSC en pacientes con BC podría proporcionar un método útil para predecir y monitorear la radio-respuesta tumoral dependiendo del subtipo de BC molecular.

GLOSSARY

AJCC: American Joint Committee on Cancer

ALDH1: aldehyde dehydrogenase 1

ATCC: American Type Culture Collection

BAA: BODIPY-aminoacetato

BAAA: BODIPY-aminoacetaldehido

BC: breast cancer

BCSCs: Breast Cancer Stem Cells

BRCA1, BRCA2:

cDNA: complementary DNA

CT: Cycle Threshold

CSCs: Cancer Stem Cells

DAPI: 4',6-Diamidino-2-Phenylindole Dihydrochloride

DEAB: Dietilbenzaldehide

DMEM: Dulbecco's Modified Eagle's Medium

DMEM-F12 Dulbecco's Modified Eagle's Medium/Nutrient Mixture F-12 Ham

DMSO: Dimetilsulfoxi

DNA: Deoxyribonucleic Acid

EDTA: Ethylenediaminetetraacetic Acid

EGF: Epidermal Growth Factor

EGFR: Epidermal Growth Factor Receptor

EMT: epithelial-to-mesenchymal transition

ER: Estrogens Receptors

FACS: Fluorescence-activated Cell Sorting

FBS: Fetal Bovine Serum

FGF: Fibroblast Growth Factor

FITC: Fluorescein Isothiocyanate

GAPDH: glyceraldehyde 3- phosphate dehydrogenase

Gy: Gray

H&E: Haematoxylin and Eosin

HER2: Human Epidermal Growth Factor Receptor 2

Hh: Hedgehog

HIF-1: Hypoxia-Inducible Factor 1

IR: ionizing radiation

ITS: insulin transferrin selenium

IU: International Unit

MMPs: Matrix Metalloproteinases

mRNA: messenger RNA

miR: microRNA

miRNAS: microRNAs

MMP: Matrix Metalloproteinase

MTT: 3-[4,5-dimethylthiazol-2-yl]- 2,5-diphenyltetrazolium bromide

P53: gene tp53

PBS: Phosphate-Buffered Saline

PCR: Polymerase Chain Reaction

PFA: Paraformaldehyde

PI: Propidium Iodide

PTEN: The phosphatase and tensin homolog gene

P/S: penicillin/streptomycin

qPCR: Quantitative Polymerase Chain Reaction

RNA: Ribonucleic Acid

RT: Radiotherapy

RT: Room Temperature

ROS: Reactive Oxygen Species

Rpm: Revolutions per minute

RT-qPCR: Real-time Reverse-Transcription PCR

TME: tumour microenvironment

TNBC: triple negative breast cancer

UVA: Ultraviolet Radiation A

UVA: Ultraviolet Radiation B

WBI: Whole breast irradiation

WHO: World Health Organization

BIBLIOGRAPHY

Abba M, Patil N, and Allgayer H (2014) MicroRNAs in the regulation of MMPs and metastasis *Cancers (Basel)* **6**, 625–645.

Ablett MP, Singh JK, and Clarke RB (2012) Stem cells in breast tumours: Are they ready for the clinic? *Eur J Cancer* **48**, 2104–2116.

Ahmad A (2013) Pathways to Breast Cancer Recurrence *ISRN Oncol* **2013**, 1–16.

Al-Hajj M, and Clarke MF (2004) Self-renewal and solid tumor stem cells *Oncogene* **23**, 7274–7282.

Anastasov N, Höfig I, Vasconcellos IG, Rappl K, Braselmann H, Ludyga N, … Atkinson MJ (2012) Radiation resistance due to high expression of miR-21 and G2/M checkpoint arrest in breast cancer cells *Radiat Oncol* **7**, 1–12.

Anderson KN, Schwab RB, and Martinez ME (2014) Reproductive Risk Factors and Breast Cancer Subtypes: A Review of the Literature *Breast Cancer Res Treat* **144**, 1–10.

Artacho-Cordón F, Ríos-Arrabal S, Lara PC, Artacho-Cordón A, Calvente I, and Núñez MI (2012, September) Matrix metalloproteinases: Potential therapy to prevent the development of second malignancies after breast radiotherapy *Surg Oncol*.

Bao S, Wu Q, McLendon RE, Hao Y, Shi Q, Hjelmeland AB, … Rich JN (2006) Glioma stem cells promote radioresistance by preferential activation of the DNA damage response *Nature* **444**, 756–760.

Batlle E, and Clevers H (2017) Cancer stem cells revisited *Nat Med* **23**, 1124–1134.

Blackadar CB (2016) Historical review of the causes of cancer *World J Clin Oncol* **7**, 54–86.

Bower JJ, Vance LD, Psioda M, Smith-Roe SL, Simpson DA, Ibrahim JG, … Kaufmann WK (2017) Patterns of cell cycle checkpoint deregulation associated with intrinsic molecular subtypes of human breast cancer cells. *NPJ Breast Cancer*

3, 9.

Bray F, Ferlay J, Soerjomataram I, Siegel RL, Torre LA, and Jemal A (2018) Global cancer statistics 2018: GLOBOCAN estimates of incidence and mortality worldwide for 36 cancers in 185 countries *CA Cancer J Clin* **68**, 394–424.

Brunner TB, Kunz-Schughart LA, Grosse-Gehling P, and Baumann M (2012) Cancer Stem Cells as a Predictive Factor in Radiotherapy *Semin Radiat Oncol* **22**, 151–174.

Burkhart DL, and Sage J (2008) Cellular mechanisms of tumour suppression by the retinoblastoma gene *Nat Rev Cancer* **8**, 671–682.

Calaf GM, Balajee AS, Montalvo-Villagra MT, Leon M, Daniela Navarrete M, Alvarez RG, … Abarca-Quinones J (2014) Vimentin and Notch as biomarkers for breast cancer progression *Oncol Lett* **7**, 721–727.

Cantley TY and L (2008) PI3K pathway alterations in cancer: variations on a theme *Oncogene* **27**, 5497–5510.

Carbon S, Dietze H, Lewis SE, Mungall CJ, Munoz-Torres MC, Basu S, … Westerfield M (2017) Expansion of the gene ontology knowledgebase and resources: The gene ontology consortium *Nucleic Acids Res* **45**, D331–D338.

Cellini F, Morganti AG, Genovesi D, Silvestris N, and Valentini V (2014) Role of microRNA in response to ionizing radiations: Evidences and potential impact on clinical practice for radiotherapy *Molecules* **19**, 5379–5401.

Chao HX, Poovey CE, Privette AA, Grant GD, Chao HY, Cook JG, and Purvis JE (2017) Orchestration of DNA Damage Checkpoint Dynamics across the Human Cell Cycle. *Cell Syst* **5**, 445-459.e5.

Chen G, Yu L, Dong H, Liu Z, and Sun Y (2019) MiR-182 enhances radioresistance in non-small cell lung cancer cells by regulating FOXO3 *Clin Exp Pharmacol*

Physiol **46**, 137–143.

Chumsri S, and Shah P (2013) Radiation resistance of cancer stem cells as an obstacle in cancer therapy *Mol Cell Pharmacol* **5**, 39–49.

Cojoc M, Mäbert K, Muders MH, and Dubrovska A (2015a) A role for cancer stem cells in therapy resistance: Cellular and molecular mechanisms *Semin Cancer Biol* **31**, 16–27.

Cojoc M, Mäbert K, Muders MH, and Dubrovska A (2015b) A role for cancer stem cells in therapy resistance: Cellular and molecular mechanisms *Semin Cancer Biol* **31**, 16–27.

Croker AK, and Allan AL (2012) Inhibition of aldehyde dehydrogenase (ALDH) activity reduces chemotherapy and radiation resistance of stem-like ALDH hiCD44 + human breast cancer cells *Breast Cancer Res Treat* **133**, 75–87.

Czochor JR, and Glazer PM (2014) MicroRNAs in cancer cell response to ionizing radiation *Antioxidants Redox Signal* **21**, 293–312.

Da Cruz Paula A, and Lopes C (2017) Implications of different cancer stem cell phenotypes in breast cancer *Anticancer Res* **37**, 2173–2183.

Dai X, Cheng H, Bai Z, and Li J (2017) Breast cancer cell line classification and Its relevance with breast tumor subtyping *J Cancer* **8**, 3131–3141.

Davies M, and Samuels Y (2010) Analysis of the genome to personalize therapy for melanoma *Oncogene* **29**, 5545–5555.

Delaney G, Jacob S, Featherstone C, and Barton M (2005) The role of radiotherapy in cancer treatment: estimating optimal utilization from a review of evidence-based clinical guidelines. *Cancer* **104**, 1129–37.

Dixit IW and V (2010) Regulation of death receptor signaling by the ubiquitin system. *Cell Death Differ* **17**, 14–24.

Ejtehadifar M, Shamsasenjan K, Movassaghpour A, Akbarzadehlaleh P, Dehdilani N, Abbasi P, … Saleh M (2015) The effect of hypoxia on mesenchymal stem cell biology *Adv Pharm Bull* **5**, 141–149.

Evan G, and Vousden K (2001) Proliferation, cell cycle and apoptosis in cancer *Nature* **411**, 342–348.

Evers P, Lee PP, DeMarco J, Agazaryan N, Sayre JW, Selch M, and Pajonk F (2010) Irradiation of the potential cancer stem cell niches in the adult brain improves progression-free survival of patients with malignant glioma *BMC Cancer* **10**, 0–6.

Fabregat A, Sidiropoulos K, Viteri G, Forner O, Marin-Garcia P, Arnau V, … Hermjakob H (2017) Reactome pathway analysis: A high-performance in-memory approach *BMC Bioinformatics* **18**, 1–9.

Falck J, Coates J, and Jackson SP (2005) Conserved modes of recruitment of ATM, ATR and DNA-PKcs to sites of DNA damage. *Nature* **434**, 605–11.

Feinbaum R, Ambros V, and Lee R (2004) The C. elegans Heterochronic Gene lin-4 Encodes Small RNAs with Antisense Complementarity to lin-14 *Cell* **116**, 843–854.

Friedrichs K, Gluba S, Eidtmann H, and Jonat W (1993) Overexpression of p53 and prognosis in breast cancer *Cancer* **72**, 3641–3647.

Gangopadhyay S, Nandy A, and Pooja Hor AM (2013) Breast Cancer Stem Cells: A Novel Therapeutic Target *Clin Breast Cancer* **13**, 7–15.

Gao X, Sishc BJ, Nelson CB, Hahnfeldt P, Bailey SM, and Hlatky L (2016) Radiation-induced reprogramming of pre-senescent mammary epithelial cells enriches putative CD44+/CD24-/low stem cell phenotype *Front Oncol* **6**, 1–9.

Garofalo M, and Croce CM (2015) Role of microRNAs in maintaining cancer stem cells *Adv Drug Deliv Rev* **81**, 53–61.

Garvalov BK, and Acker T (2011, February) Cancer stem cells: A new framework for the design of tumor therapies *J Mol Med*.

Ghaffari S (2011) Cancer, stem cells and cancer stem cells: Old ideas, new developments *F1000 Med Rep* **3**, 4–7.

Ghisolfi L, Keates AC, Hu X, Lee D ki, and Li CJ (2012) Ionizing radiation induces stemness in cancer cells *PLoS One* **7**, 1–11.

Ginestier C, Hur MH, Charafe-Jauffret E, Monville F, Dutcher J, Brown M, … Dontu G (2007) ALDH1 Is a Marker of Normal and Malignant Human Mammary Stem Cells and a Predictor of Poor Clinical Outcome *Cell Stem Cell* **1**, 555–567.

Giuliano AE, Connolly JL, Edge SB, Mittendorf EA, Rugo HS, Solin LJ, … Hortobagyi GN (2017) Breast Cancer-Major changes in the American Joint Committee on Cancer eighth edition cancer staging manual *CA Cancer J Clin* **67**, 290–303.

Gomez-Casal R, Bhattacharya C, Ganesh N, Bailey L, Basse P, Gibson M, … Levina V (2013) Non-small cell lung cancer cells survived ionizing radiation treatment display cancer stem cell and epithelial-mesenchymal transition phenotypes *Mol Cancer* **12**, 1.

Halimi M, Asghari SM, Sariri R, Moslemi D, and Parsian H (2012) Cellular Response to Ionizing Radiation: A MicroRNA Story. *Int J Mol Cell Med* **1**, 178–17884.

Hanahan D, and Weinberg RA (2011) Hallmarks of cancer: The next generation *Cell* **144**, 646–674.

He X, He L, and Hannon GJ (2007, December 1) The guardian's little helper: MicroRNAs in the p53 tumor suppressor network *Cancer Res*.

Hernández-Camarero P, Jiménez G, López-Ruiz E, Barungi S, Marchal JA, and Perán M (2018) Revisiting the dynamic cancer stem cell model: Importance of tumour edges *Crit Rev Oncol Hematol* **131**, 35–45.

Hong L, Yang J, Han Y, Lu Q, Cao J, and Syed L (2012) High expression of miR-210 predicts poor survival in patients with breast cancer: A meta-analysis *Gene* **507**, 135–138.

Hu H, Du L, Nagabayashi G, Seeger RC, and Gatti RA (2010) ATM is down-regulated by N-Myc-regulated microRNA-421. *Proc Natl Acad Sci U S A* **107**, 1506–11.

Isobe T, Hisamori S, Hogan DJ, Zabala M, Hendrickson DG, Dalerba P, … Shimono Y (2014) miR-142 regulates the tumorigenicity of human breast cancer stem cells through the canonical WNT signaling pathway *Elife* **3**, 1–23.

Kans J (2010) Entrez Programming Utilities Help [Internet]. Bethesda (MD): National Center for Biotechnology Information (US); Retrieved November 6, 2019, from https://www.ncbi.nlm.nih.gov/books/NBK25501/

Kaufmann M, Karn T, and Ruckhäberle E (2012) Controversies concerning the use of neoadjuvant systemic therapy for primary breast cancer. *World J Surg* **36**, 1480–5.

Kim JY, Kim JC, Lee JY, and Park MJ (2018) Oct4 suppresses IR-induced premature senescence in breast cancer cells through STAT3- and NF-κB-mediated IL-24 production *Int J Oncol* **53**, 47–58.

Kim MH, Kim MH, Kim KS, Park MJ, Jeong JH, Park SW, … Lee YJ (2016) In vivo monitoring of CD44+ cancer stem-like cells by γ-irradiation in breast cancer *Int J Oncol* **48**, 2277–2286.

Kim R, Cui Y, Yoo K, Kim IG, Lee M, Choi YH, … Lee SJ (2015) Radiation promotes malignant phenotypes through SRC in breast cancer cells *Cancer Sci* **106**, 78–85.

Kim RK, Cui YH, Yoo KC, Kim IG, Lee M, Choi YH, … Lee SJ (2015) Radiation promotes malignant phenotypes through SRC in breast cancer cells *Cancer Sci* **106**, 78–85.

Kim SY, Rhee JG, Song X, Prochownik E V., Spitz DR, and Lee YJ (2012) Breast

Cancer Stem Cell-Like Cells Are More Sensitive to Ionizing Radiation than Non-Stem Cells: Role of ATM *PLoS One* **7**, 1–13.

Korpela E, Vesprini D, and Liu SK (2015) MicroRNA in radiotherapy: MiRage or miRador? *Br J Cancer* **112**, 777–782.

Kraemer A, Anastasov N, Angermeier M, Winkler K, Atkinson MJ, and Moertl S (2011) MicroRNA-mediated processes are essential for the cellular radiation response. *Radiat Res* **176**, 575–86.

Krause M, Dubrovska A, Linge A, and Baumann M (2017) Cancer stem cells: Radioresistance, prediction of radiotherapy outcome and specific targets for combined treatments *Adv Drug Deliv Rev* **109**, 63–73.

Krause M, Yaromina A, Eicheler W, Koch U, and Baumann M (2011) Cancer stem cells: Targets and potential biomarkers for radiotherapy *Clin Cancer Res* **17**, 7224–7229.

Lagadec C, Vlashi E, Alhiyari Y, Phillips TM, Bochkur Dratver M, and Pajonk F (2013) Radiation-induced notch signaling in breast cancer stem cells *Int J Radiat Oncol Biol Phys* **87**, 609–618.

Lagadec C, Vlashi E, Della Donna L, Dekmezian C, and Pajonk F (2012) Radiation-induced reprogramming of breast cancer cells *Stem Cells* **30**, 833–844.

Lal A, Pan Y, Navarro F, Dykxhoorn DM, Moreau L, Meire E, … Chowdhury D (2009) MiR-24-mediated downregulation of H2AX suppresses DNA repair in terminally differentiated blood cells *Nat Struct Mol Biol* **16**, 492–498.

Lee SY, Jeong EK, Ju MK, Jeon HM, Kim MY, Kim CH, … Kang HS (2017) Induction of metastasis, cancer stem cell phenotype, and oncogenic metabolism in cancer cells by ionizing radiation *Mol Cancer* **16**, 1–25.

Li N, Miao Y, Shan Y, Liu B, Li Y, Zhao L, and Jia L (2017) MiR-106b and miR-93

regulate cell progression by suppression of PTEN via PI3K/Akt pathway in breast cancer *Cell Death Dis* **8**, e2796.

Ling Y, Zhao X LX (2015) ovel FTS-diamine/cinnamic acid hybrids inhibit tumor cell proliferation and migration and promote apoptosis via blocking Ras-related signaling in vitro. *Cancer Chemother Pharmacol* **75**, 381–392.

Liu J, and Wang Z (2015) Increased oxidative stress as a selective anticancer therapy *Oxid Med Cell Longev* **2015**.

Lomax ME, Folkes LK, and O'Neill P (2013) Biological consequences of radiation-induced DNA damage: Relevance to radiotherapy *Clin Oncol* **25**, 578–585.

Ma L (2010) Role of miR-10b in breast cancer metastasis *Breast Cancer Res* **12**, 8–12.

Maechler M, Rousseeuw P, Struyf A, Hubert M HK (2018) cluster: Cluster Analysis Basics and Extensions.

Mansoori B, Mohammadi A, Gjerstorff MF, Shirjang S, Asadzadeh Z, Khaze V, … Baradaran B (2019) miR-142-3p is a tumor suppressor that inhibits estrogen receptor expression in ER-positive breast cancer *J Cell Physiol* **234**, 16043–16053.

Marie-Egyptienne DT, Lohse I, and Hill RP (2013) Cancer stem cells, the epithelial to mesenchymal transition (EMT) and radioresistance: Potential role of hypoxia *Cancer Lett* **341**, 63–72.

Matsuoka S, Ballif BA, Smogorzewska A, III ERM, Hurov KE, Luo J, … Elledge SJ (2007) Responsive to DNA Damage *Science (80-)* **1160**, 1160–1166.

McGuire S (2016) World Cancer Report 2014. Geneva, Switzerland: World Health Organization, International Agency for Research on Cancer, WHO Press, 2015 *Adv Nutr* **7**, 418–419.

Mcpherson K, Steel CM, and Dixon JM (2000) ABC of breast diseases: Breast cancer???epidemiology, risk factors, and genetics *Bmj* **321**, 1198.

Mei Z, Su T, Ye J, Yang C, Zhang S, and Xie C (2015) The miR-15 Family Enhances the Radiosensitivity of Breast Cancer Cells by Targeting G 2 Checkpoints *Radiat Res* **183**, 196–207.

Metheetrairut C, and Slack FJ (2013a) MicroRNAs in the ionizing radiation response and in radiotherapy *Curr Opin Genet Dev* **23**, 12–19.

Metheetrairut C, and Slack FJ (2013b) MicroRNAs in the ionizing radiation response and in radiotherapy *Curr Opin Genet Dev* **23**, 12–19.

Minoru Kanehisa and Susumu Goto (2000) KEGG: Kyoto Encyclopedia of Genes and Genomes *Nucleic Acids Res* **28**, 27–30.

Mladenov E, Fan X, Dueva R, Soni A, and Iliakis G (2019) Radiation-dose-dependent functional synergisms between ATM, ATR and DNA-PKcs in checkpoint control and resection in G2-phase. *Sci Rep* **9**, 8255.

Morrison R, Schleicher SM, Sun Y, Niermann KJ, Kim S, Spratt DE, … 1 (2011) Targeting the mechanisms of resistance to chemotherapy and radiotherapy with the cancer stem cell hypothesis *J Oncol* 13.

Ohri N, and Haffty BG (2020) The evolution of adjuvant radiation therapy for early-stage and locally advanced breast cancer. *Breast J* **26**, 59–64.

Owens TW, and Naylor MJ (2013) Breast cancer stem cells *Front Physiol* **4**, 225.

Pajic M, Froio D, Daly S, Doculara L, Millar E, Graham PH, … Molloy TJ (2018) miR-139-5p modulates radiotherapy resistance in breast cancer by repressing multiple gene networks of DNA repair and ROS defense *Cancer Res* **78**, 501–515.

Paull TT (2015) Mechanisms of ATM Activation *Annu Rev Biochem* **84**, 711–738.

Pawlik TM, and Keyomarsi K (2004) Role of cell cycle in mediating sensitivity to radiotherapy *Int J Radiat Oncol Biol Phys* **59**, 928–942.

Peitzsch C, Kurth I, Kunz-Schughart L, Baumann M, and Dubrovska A (2013)

Discovery of the cancer stem cell related determinants of radioresistance *Radiother Oncol* **108**, 378–387.

Pfeffer CM, and Singh ATK (2018) Apoptosis: A target for anticancer therapy *Int J Mol Sci* **19**.

Phillips TM, McBride WH, and Pajonk F (2006) The response of CD24-/low/CD44+ breast cancer-initiating cells to radiation *J Natl Cancer Inst* **98**, 1777–1785.

Pietras RJ, Poen JC, Gallardo D, Wongvipat PN, Lee HJ, and Slamon DJ (1999) Monoclonal antibody to HER-2/neu receptor modulates repair of radiation-induced DNA damage and enhances radiosensitivity of human breast cancer cells overexpressing this oncogene *Cancer Res* **59**, 1347–1355.

Price JT, Tiganis T, Agarwal A, Djakiew D, and Thompson EW (1999) Epidermal growth factor promotes MDA-MB-231 breast cancer cell migration through a phosphatidylinositol 3'-kinase and phospholipase C-dependent mechanism *Cancer Res* **59**, 5475–5478.

Rabinovich I, Sebastião APM, Lima RS, Urban C de A, Schunemann E, Anselmi KF, … Moreno-Amaral AN (2018) Cancer stem cell markers ALDH1 and CD44+/CD24– phenotype and their prognosis impact in invasive ductal carcinoma *Eur J Histochem* **62**, 231–237.

Reya T, Morrison SJ, Clarke MF, and Weissman IL (2001) Stem cells and cancer stem cells *Nature* **414**, 105–11.

Rich JN (2007) Cancer stem cells in radiation resistance *Cancer Res* **67**, 8980–8984.

Rojas K, and Stuckey A (2016) Breast Cancer Epidemiology and Risk Factors *Clin Obstet Gynecol* **59**, 651–672.

Rosalind C. Lee RLF, and Ambrost and V (1993) The C. elegans Heterochronic Gene lin-4 Encodes Small RNAs with Antisense Complementarity to &II-14 *Cell* **75**,

843–854.

Roscigno G, Quintavalle C, Donnarumma E, Puoti I, Diaz-Lagares A, Iaboni M, … Condorelli G (2016) MiR-221 promotes stemness of breast cancer cells by targeting DNMT3b *Oncotarget* **7**, 580–592.

Schnitt SJ (2010) Classification and prognosis of invasive breast cancer: From morphology to molecular taxonomy *Mod Pathol* **23**, 60–64.

Schwarzenbacher D, Balic M, and Pichler M (2013) The role of microRNAs in breast cancer stem cells *Int J Mol Sci* **14**, 14712–14723.

Shah NR, and Chen H (2014) MicroRNAs in pathogenesis of breast cancer: Implications in diagnosis and treatment *World J Clin Oncol* **5**, 48–60.

Shen L, Huang X, Xie X, Su J, Yuan J, and Chen X (2014) High Expression of SOX2 and OCT4 Indicates Radiation Resistance and an Independent Negative Prognosis in Cervical Squamous Cell Carcinoma *J Histochem Cytochem* **62**, 499–509.

Shigdar S, Li Y, Bhattacharya S, O'Connor M, Pu C, Lin J, … Duan W (2014) Inflammation and cancer stem cells *Cancer Lett* **345**, 271–278.

Shiloh Y, and Ziv Y (2013, April) The ATM protein kinase: Regulating the cellular response to genotoxic stress, and more *Nat Rev Mol Cell Biol*.

Shimono Y, Mukohyama J, Nakamura S, and Minami H (2015) MicroRNA Regulation of Human Breast Cancer Stem Cells *J Clin Med* **5**, 2.

Steer A, Cordes N, Jendrossek V, and Klein D (2019) Impact of Cancer-Associated Fibroblast on the Radiation-Response of Solid Xenograft Tumors *Front Mol Biosci* **6**.

Summerer I, Niyazi M, Unger K, Pitea A, Zangen V, Hess J, … Zitzelsberger H (2013) Changes in circulating microRNAs after radiochemotherapy in head and neck cancer patients *Radiat Oncol* **8**, 1–9.

Surova O, Akbar NS, and Zhivotovsky B (2012) Knock-down of core proteins regulating microRNA biogenesis has no effect on sensitivity of lung cancer cells to ionizing radiation. *PLoS One* **7**, e33134.

Takahashi K, and Yamanaka S (2006) Induction of Pluripotent Stem Cells from Mouse Embryonic and Adult Fibroblast Cultures by Defined Factors *Cell* **126**, 663–676.

Takahashi R u, Miyazaki H, and Ochiya T (2013) The role of microRNAs in the regulation of cancer stem cells *Front Genet* **4**, 1–11.

Tessitore A, Cicciarelli G, Del Vecchio F, Gaggiano A, Verzella D, Fischietti M, … Alesse E (2014) MicroRNAs in the DNA damage/repair network and cancer *Int J Genomics* **2014**.

Theys J, Jutten B, Habets R, Paesmans K, and Groot AJ (2016) Europe PMC Funders Group E-Cadherin loss associated with EMT promotes radioresistance in human tumor cells **99**, 392–397.

Thomas B. Brunner, Kunz-Schughart LA, Grosse-Gehling P, and Michael Baumann (2012) Cancer Stem Cells as a Predictive Factor in Radiotherapy *Semin Radiat Oncol* **22**, 151–174.

Troschel FM, Böhly N, Borrmann K, Braun T, Schwickert A, Kiesel L, … Greve B (2018) miR-142-3p attenuates breast cancer stem cell characteristics and decreases radioresistance in vitro *Tumor Biol* **40**, 1–10.

Vermeulen L, de Sousa e Melo F, Richel DJ, and Medema JP (2012) The developing cancer stem-cell model: Clinical challenges and opportunities *Lancet Oncol* **13**, e83–e89.

Virginie O, Qijing L, and He L (2013) mir-17-92, a polycistronic oncomir with pleiotropic functions Virginie *Immunol Rev* **253**, 158–166.

Vlashi E, and Pajonk F (2015) Cancer stem cells, cancer cell plasticity and radiation

therapy *Semin Cancer Biol* **31**, 28–35.

Wang D, Lu P, Zhang H, Luo M, Zhang X, Wei X, … Liu C (2014) Oct-4 and Nanog promote the epithelial-mesenchymal transition of breast cancer stem cells and are associated with poor prognosis in breast cancer patients *Oncotarget* **5**, 10803–10815.

Wang H, Wang L, Song Y, Wang S, Huang X, Xuan Q, … Zhang Q (2017) CD44+/CD24- phenotype predicts a poor prognosis in triple-negative breast cancer *Oncol Lett* **14**, 5890–5898.

Wilson WR, and Hay MP (2011) Targeting hypoxia in cancer therapy *Nat Rev Cancer* **11**, 393–410.

Yang L, Wang XW, Zhu LP, Wang HL, Wang B, Zhao Q, and Wang XY (2018) Significance and prognosis of epithelial-cadherin expression in invasive breast carcinoma *Oncol Lett* **16**, 1659–1665.

Yerushalmi R, Woods R, Ravdin PM, Hayes MM, and Gelmon KA (2010) Ki67 in breast cancer: prognostic and predictive potential *Lancet Oncol* **11**, 174–183.

Yu J, Vodyanik MA, Smuga-Otto K, Antosiewicz-Bourget J, Frane JL, Tian S, … Thomson JA (2007) Induced pluripotent stem cell lines derived from human somatic cells *Science (80-)* **318**, 1917–1920.

Zhan J, Chen L, Yuan Y, Xie G, Sun A, Liu Y, and Chen Z (2011) STAT1 promotes radioresistance of CD44(+)/CD24(-/low) cells in breast cancer. *Exp Biol Med* **236**, 418–422.

Zhang C, Kang C, Wang P, Cao Y, Lv Z, Yu S, … Pu P (2011) MICRORNA-221 and -222 regulate radiation sensitivity by targeting the PTEN pathway *Int J Radiat Oncol Biol Phys* **80**, 240–248.

Zhang JM, Wei K, and Jiang M (2018) OCT4 but not SOX2 expression correlates with

worse prognosis in surgical patients with triple-negative breast cancer *Breast Cancer* **25**, 447–455.

Zhang X, Wan G, Berger FG, He X, and Lu X (2011) The ATM kinase induces microRNA biogenesis in the DNA damage response. *Mol Cell* **41**, 371–83.

Zhao L, Bode AM, Cao Y, and Dong Z (2012) Regulatory mechanisms and clinical perspectives of miRNA in tumor radiosensitivity *Carcinogenesis* **33**, 2220–2227.

Zhou YC, Liu JY, Li J, Zhang J, Xu YQ, Zhang HW, … Guo GZ (2011) Ionizing radiation promotes migration and invasion of cancer cells through transforming growth factor-beta-mediated epithelial-mesenchymal transition *Int J Radiat Oncol Biol Phys* **81**, 1530–1537.

ANNEXES

CURRICULUM

ACADEMIC ACHIEVEMENTS:

Master's Degree in Advances in Diagnostic and Therapeutic Radiology and Medical Physic.

Department of Radiology and Physical Medicine, Faculty of Medicine, University of Granada, Spain. 2014.

Graduate in Biology

Faculty of Sciences, University of Granada, Spain. 2004-2011

PUBLICATIONS:

Griñán-Lisón C, Olivares-Urbano MA, Jiménez G, López-Ruiz E, Del Val C, Morata-Tarifa C, Entrena JM, González-Ramírez AR, Boulaiz H, Zurita Herrera M, Núñez MI, Marchal JA. **miRNAs as radio-response biomarkers for breast cancer stem cells.** *Mol Oncol.* 2020 Jan 13. Impact factor (JCR): 5.962. Quartile: Q1.

Olivares-Urbano MA, **Griñán-Lisón C**, Ríos-Arrabal S, Artacho-Cordón F, Torralbo AI, López-Ruiz E, Marchal JA, Núñez MI. **Radiation and Stemness Phenotype May Influence Individual Breast Cancer Outcomes: The Crucial Role of MMPs and Microenvironment.** *Cancers (Basel).* 2019 Nov 12;11(11). pii: E1781. Impact factor (JCR): 6.162. Quartile: Q1.

Lamolda M, Montes R, Simón I, Perales S, Martínez-Navajas G, Lopez-Onieva L, Ríos-Pelegrina R, Del Moral RG, **Griñan-Lison C**, Marchal JA, Lozano ML, Ramos-Mejia V, Rivera J, Bastida JM, Real PJ**. GENYOi005-A: An induced pluripotent stem cells (iPSCs) line generated from a patient with Familial Platelet Disorder with associated Myeloid Malignancy (FPDMM) carrying a p.Thr196Ala variant.** *Stem Cell Res.* 2019 Dec. Impact factor (JCR): 3.929. Quartile: Q1.

Olivares-Urbano MA, **Griñán-Lisón C**, Zurita M, Del Moral R, Ríos-Arrabal S, Artacho-Cordón F, Arrebola JP, González AR, León J, Marchal JA, Núñez MI. **Matrix metalloproteases and TIMPs as prognostic biomarkers in breast cancer patients treated**

with radiotherapy: A pilot study. *J Cell Mol Med*. 2020 Jan;24(1):139-148. Impact factor (JCR): 4,302 Quartile: Q1.

Hernández-Camarero P, López-Ruiz E, **Griñán-Lisón C**, García MÁ, Chocarro-Wrona C, Marchal JA, Kenyon J, Perán M. **Pancreatic (pro)enzymes treatment suppresses BXPC-3 pancreatic Cancer Stem Cell subpopulation and impairs tumour engrafting.** *Sci Rep.* 2019 Aug 6;9(1):11359. Impact factor (JCR): 4.122. Quartile: Q1.

Jiménez-Martínez Y, **Griñán-Lisón C**, Khaldy H, Martín A, Cambrils A, Ibáñez Grau A, Jiménez G, Marchal JA, Boulaiz H. **LdrB Toxin with In Vitro and In Vivo Antitumor Activity as a Potential Tool for Cancer Gene Therapy.** *Cancers (Basel).* 2019 Jul 20;11(7). pii: E1016. Impact factor (JCR): 6.162. Quartile: Q1.

Cáceres B, Ramirez A, Carrillo E, Jimenez G, **Griñán-Lisón C**, López-Ruiz E, Jiménez-Martínez Y, Marchal JA, Boulaiz H. **Deciphering the Mechanism of Action Involved in Enhanced Suicide Gene Colon Cancer Cell Killer Effect Mediated by Gef and Apoptin.** *Cancers (Basel)*. 2019 Feb 23;11(2):264. Impact factor (JCR): 6.162. Quartile: Q1.

Baena, J., Jiménez, G., López-Ruiz, E., Antich, C., **Griñán-Lisón, C**., Perán, M., … Marchal, J. **Volume-by-volume bioprinting of chondrocytes-alginate bioinks in high temperature thermoplastic scaffolds for cartilage regeneration**. *Experimental Biology and Medicine*, 2019; *244*(1), 13–21. Impact factor (JCR): 3.005. Quartile: Q2.

Ramírez A, Conejo-García A, **Griñán-Lisón C**, López-Cara LC, Jiménez G, Campos JM, Marchal JA, Boulaiz H. **Enhancement of Tumour Cell Death by Combining *gef* Gene Mediated Therapy and New 1,4-Benzoxazepin-2,6-Dichloropurine Derivatives in Breast Cancer Cells.** *Front Pharmacol*. 2018 Jul 26; 9:798. Impact factor (JCR): 4.418. Quartile: Q1.

Gema Jiménez, Michael Hackenberg, Purificación Catalina, Houria Boulaiz, **Carmen Griñán-Lisón**, María Ángel García, Macarena Perán, Elena López-Ruiz, Alberto Ramírez, Cynthia Morata-Tarifa, Esther Carrasco, Margarita Aguilera, Juan Antonio Marchal.2018. **Mesenchymal stem cell's secretome promotes selective enrichment of**

cancer stem-like cells with specific cytogenetic profile. *Cancer Letter. Elsevier.* 429, pp.78-88. Impact factor (JCR): 6.491. Quartile: Q1.

Morata-Tarifa C, Picon-Ruiz M, **Griñan-Lison C**, Boulaiz H, Perán M, Garcia MA, Marchal JA. **Validation of suitable normalizers for miR expression patterns analysis covering tumour heterogeneity.** *Sci Rep.* 2017 Jan 4;7:39782. Impact factor (JCR): 4.259. Quartile: Q1.

Houria Boulaiz, Carmen Ramos Marin, **Carmen Griñan Lison**, Juan Antonio Marchal; Francisca Vicente. **What's new in the diagnosis of pancreatic cancer: a patent review (2011-present).** *Expert Opin Ther Pat.* 1319 -1328. 13/12/2017. Impact factor (JCR): 3.041. Quartile: Q2

Carmen Ramos Marin; Houria Boulaiz; **Carmen Griñan Lison**; Juan Antonio Marchal; Francisca Vicente. **What's new in treatment of pancreatic cancer: a patent review (2010-2017)**. *Expert Opin Ther Pat.* 2017. Impact factor (JCR): 3.041. Quartile: Q2.

Jiménez G, López-Ruiz E, Griñán-Lisón C, Antich C, Marchal JA. **Chapter: Brown adipose tissue and obesity.** Libro Obesity, A practical guide. (Ed. Springer) 2015. pp 13-28. ISBN 978-3-319-19821-7.

Navarro SA, Carrillo E, **Griñán-Lisón C**, Martín A, Perán M, Marchal JA, Boulaiz H. **Cancer suicide gene therapy: a patent review.** *Expert Opin Ther Pat.* 2016 Sep; 26(9):1095-104. Impact factor (JCR): 4.626. Quartile: Q1.

Morata-Tarifa C, Jiménez G, García MA, Entrena JM, **Griñán-Lisón C**, Aguilera M, Picon-Ruiz M, Marchal JA. **Low adherent cancer cell subpopulations are enriched in tumorigenic and metastatic epithelial-to-mesenchymal transition-induced cancer stem-like cells.** *Sci Rep.* 2016 Jan 11; 6:18772. Impact factor (JCR): 5.228. Quartile: Q1.

Carrillo E, Navarro SA, Ramírez A, García MÁ, **Griñán-Lisón C**, Perán M, Marchal JA. **5-Fluorouracil derivatives: a patent review (2012 - 2014).** *Expert Opinion Therapy Pat.* 2015 Oct; 25(10):1131-44. Impact factor (JCR): 4.626. Quartile: Q1.

INTELLECTUAL PROPERTY PATENT:

Nuria de Pedro Montejo; Victor Manuel Gonzalez Menendez; Gloria Crespo Suerio; Ignacioperez-Victoria Moreno de Barreda; Bastien Cautain; Maria Francisca Vicente Perez; Jose Fernando Reyes Benitez; Olga Genilloud; **Carmen Griñan Lison**; Juan Antonio Marchal Corrales. **PCT/EP2016/059650. Phenol Derivatives to Treat Cancer** Fundación: Centro de Excelencia en Investigación de Medicamentos Innovadores en Andalucía (MEDINA).

CONTRIBUIONS TO CONGRESS:

- Sociedad Andaluza de Cancerología (SAC). Granada 2014.

Poster: Células madre tumorales y respuesta a radiación ionizante.

- 8th European Scientific Oncology Conference (ESOC-8). Marbella, Spain, 2014.

Poster: Importance of cancer stem cells in determining ionizing radiation response.

- I Jornadas Científicas Centro de Investigación Biomédica (CIBM). Granada, Spain, 2017

Poster: Desarrollo de un nuevo sistema de bioimpresión 3D para la regeneración de tejidos y órganos

- I Jornadas Científicas Centro de Investigación Biomédica (CIBM). Granada, Spain, 2017

Poster: Importancia de la validación de normalizadores para el análisis de los patrones de expresión de miRs en la heterogeneidad tumoral

- I Jornada de Neurocientíficas. Instituto de Neurociencias de Granada. Gramada, Spain, 2018.

Poster: Enhancement of tumour cell death by combining gef gene mediated therapy and new 1,4-benzoxazepin-2,6-dichloropurine derivatives in breast cancer cells

- I Jornada de Neurocientíficas. Instituto de Neurociencias de Granada. Gramada, Spain, 2018.

Poster: Importancia de la validación de normalizadores para el análisis de los patrones de expresión de miRs en la heterogeneidad tumoral

- I Jornadas de jóvenes investigadores. Facultad de Farmacia. Granada, Spain, 2018.

Poster: Importancia de la validación de normalizadores para el análisis de los patrones de expresión de miRs en la heterogeneidad tumoral.

- I congreso PTS. CIBM, de la Universidad de Granada. Granada, Spain, 2019.

Poster: Determination of characteristic cancer stem cells miRNAs with prognostic and predictive value in patients with colorectal cancer

PUBLICATION